UNCLASSIFIED

DTIC FILE COPY

(1)

SECURITY CLASSIFICATION OF THIS PAGE (When Data Entered)

AD-A196 385

REPORT DOCUMENTATION PAGE		READ INSTRUCTIONS BEFORE COMPLETING FORM
1. REPORT NUMBER AFIT/CI/NR 88-102	2. GOVT ACCESSION NO.	3. RECIPIENT'S CATALOG NUMBER
4. TITLE (and Subtitle) DAMAGE EFFECTS ON THIN ACRYLIC TARGETS CAUSED BY INFRARED RADIATION FROM A PULSED CARBON DIOXIDE LASER		5. TYPE OF REPORT & PERIOD COVERED MS THESIS 6. PERFORMING ORG. REPORT NUMBER
7. AUTHOR(s) THEODORE L. KREIFELS		8. CONTRACT OR GRANT NUMBER(s)
9. PERFORMING ORGANIZATION NAME AND ADDRESS AFIT STUDENT AT: CREIGHTON UNIVERSITY		10. PROGRAM ELEMENT, PROJECT, TASK AREA & WORK UNIT NUMBERS
11. CONTROLLING OFFICE NAME AND ADDRESS		12. REPORT DATE 1988 13. NUMBER OF PAGES 137
14. MONITORING AGENCY NAME & ADDRESS (if different from Controlling Office) AFIT/NR Wright-Patterson AFB OH 45433-6583		15. SECURITY CLASS. (of this report) UNCLASSIFIED 15a. DECLASSIFICATION/DOWNGRADING SCHEDULE

16. DISTRIBUTION STATEMENT (of this Report)

DISTRIBUTED UNLIMITED: APPROVED FOR PUBLIC RELEASE

DTIC ELECTE AUG 0 4 1988 S D H

17. DISTRIBUTION STATEMENT (of the abstract entered in Block 20, if different from Report)

SAME AS REPORT

18. SUPPLEMENTARY NOTES

Approved for Public Release: IAW AFR 190-1
LYNN E. WOLAVER 20 July 88
Dean for Research and Professional Development
Air Force Institute of Technology
Wright-Patterson AFB OH 45433-6583

19. KEY WORDS (Continue on reverse side if necessary and identify by block number)

20. ABSTRACT (Continue on reverse side if necessary and identify by block number)

ATTACHED

1

DD FORM 1 JAN 73 1473 EDITION OF 1 NOV 65 IS OBSOLETE

UNCLASSIFIED

SECURITY CLASSIFICATION OF THIS PAGE (When Data Entered)

ABSTRACT

The damage on thin acrylic targets caused by focused radiation from a 10 megawatt pulsed carbon dioxide laser was measured as a function of air pressure and target distance from the focal point of the radiation. The laser was fired at targets placed in a test chamber. Target damage and the effects of optical detonations near the target were studied as chamber pressure was reduced from one to 0.01 atmosphere. The first chapter of this major report introduces the fundamental concepts of laser physics. The second chapter discusses the specific characteristics of a carbon dioxide laser. The final chapter presents the equipment, procedures, results, and conclusions of this research. All data is summarized in easy-to-read tables and graphs. Evidence was gathered to conclude that target damage increases as pressure decreases while optical detonations absorb and reflect beam energy.

DAMAGE EFFECTS ON THIN ACRYLIC TARGETS CAUSED BY INFRARED RADIATION FROM A PULSED CARBON DIOXIDE LASER

BY

First Lieutenant THEODORE L. KREIFELS, USAF

A MAJOR REPORT

Submitted to

Dr. Thomas H. Zepf
Chairperson, Department of Physics
Creighton University

May 7th, 1988

ABSTRACT

The damage on thin acrylic targets caused by focused radiation from a 10 megawatt pulsed carbon dioxide laser was measured as a function of air pressure and target distance from the focal point of the radiation. The laser was fired at targets placed in a test chamber. Target damage and the effects of optical detonations near the target were studied as chamber pressure was reduced from one to 0.01 atmosphere. The first chapter of this major report introduces the fundamental concepts of laser physics. The second chapter discusses the specific characteristics of a carbon dioxide laser. The final chapter presents the equipment, procedures, results, and conclusions of this research. All data is summarized in easy-to-read tables and graphs. Evidence was gathered to conclude that target damage increases as pressure decreases while optical detonations absorb and reflect beam energy.

PREFACE

This document is divided into three main sections. In the first section, I answer the question "What is a laser?" in the most general case. I go on to specify the characteristics that all lasers share. Lasers are made from so many types of materials and operate by such a variety of techniques--I never appreciated just how many types of lasers existed until now!

The second section of this report focuses on how a carbon dioxide laser operates. The CO_2 laser in the Physics Department of Creighton University is a pulsed, molecular gas, Transversely Excited Atmospheric (TEA) laser that emits infrared radiation with a 10.6 micron wavelength. Specific information for the Lumonics Lasermark 901 CO_2 laser may be found in technical manuals listed in the REFERENCE section.

The third section explains my experimental research in detail. You'll find drawings of equipment, tables and graphs of data, an explanation of my procedure, my final results, and recommendations for future work. Hoping the next fellow may benefit from my experience, I end the report by sharing some lessons I've learned in the past six months.

I wish to thank a few very important people. To Chris Stoffel for his skill in making my crude equipment drawings a reality. To Captain Tom Reebe from the Air Force Manpower and Resource Center for pushing "the system" hard to send me back to school with financial support that is unequalled.

To Dr. Zepf for his patient guidance and support. To my parents, Gerald and Nettie, who inspired me to set my goals high. Finally, I dedicate this report to my favorite proofreader and loving wife, Susan--her encouragement, patience, intelligence, and humor will always be my greatest source of joy.

Ted Kreifels
May 1st, 1988

TABLE OF CONTENTS

Chapter III : Damage Effects On Thin Acrylic Targets

Appendices

List of Tables

List of Figures

INTRODUCTION

In 212 B.C. the great mathematician Archimedes was faced with an awesome dilemma. How could the small Sicilian army defend his native island from an imminent Roman attack from the sea? Archimedes instructed the battle commander to arrange his legions along the harbor and surrounding hills in the outline of a parabola. From these positions, the men were to use their shields to reflect the sun's rays on each ship at sea. Legend claims that when this enormous collection of solar energy was directed toward the attacking vessels, their sails burst into flames, sailors were instantly blinded, and the attack driven off. Since Archimedes' time, man has harnessed solar power with varying degrees of success and moved the incandescent light from the cave to our homes and factories. But not until the mid 20th century has man discovered a new type of light--the special light emitted by the laser.

A laser is a device that generates and amplifies light, just as a transistor amplifies an electronic signal. Specifically, a laser amplifies coherent optical radiation from the infrared to the ultraviolet wavelengths in the electromagnetic spectrum shown in Figure 1. The transistor, in contrast, amplifies signals with much longer wavelengths in the audio, radio, and microwave range.

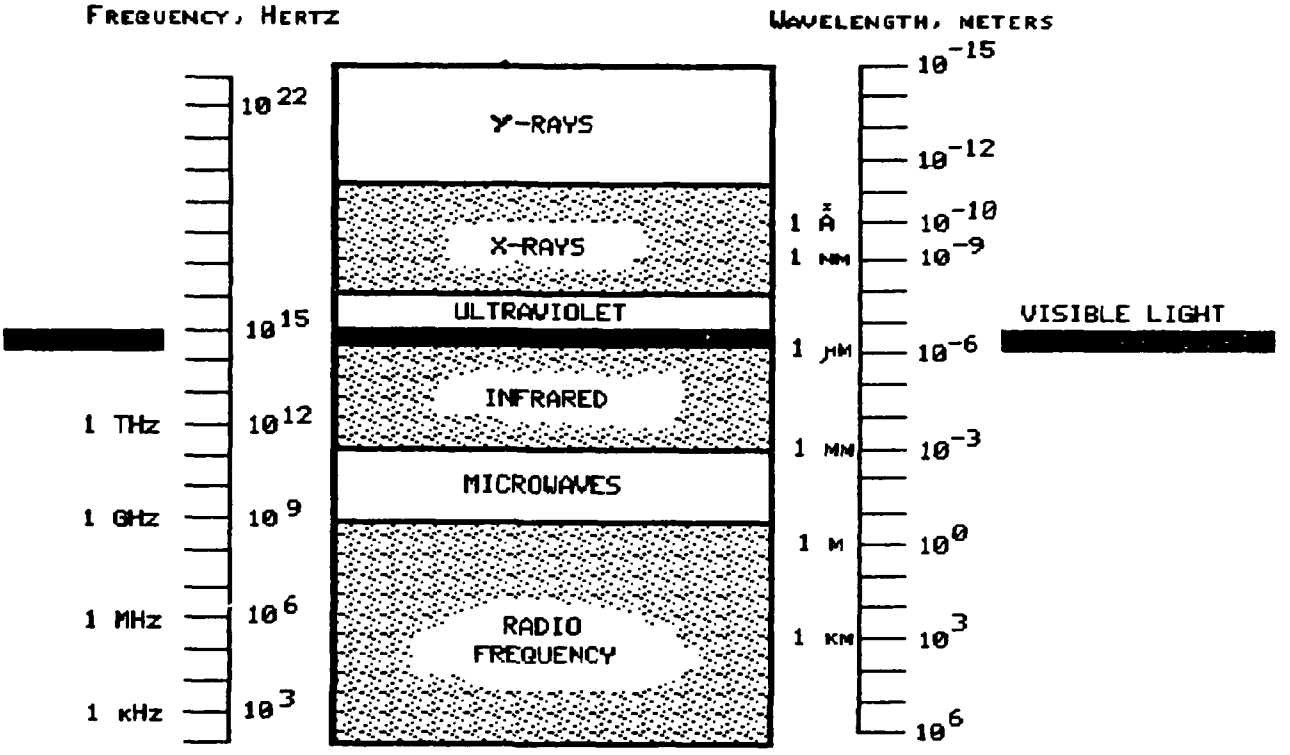

Figure 1. The electromagnetic spectrum.

Lasers have been made from unbelievably diverse materials and operate by many different methods. There are nearly one thousand different types of lasers today [1], and while not all lasers are practical, many have been used in an enormous variety of medical, scientific, military, and commercial applications. Lasers are used in delicate eye surgery, experimental fusion reactors, weapon guidance systems, electro-optical computers, and grocery checkout

registers. These are just a few examples of the hundreds of ways lasers are becoming a growing part of our lives.

Despite their diversity, all laser designs require the following three essential elements which are illustrated in the figure below: a laser medium, a pumping process, and optical feedback components. The laser medium is a carefully chosen collection of particles, such as atoms, molecules, or ions. This collection might be in any state of matter--gas, liquid, or solid.

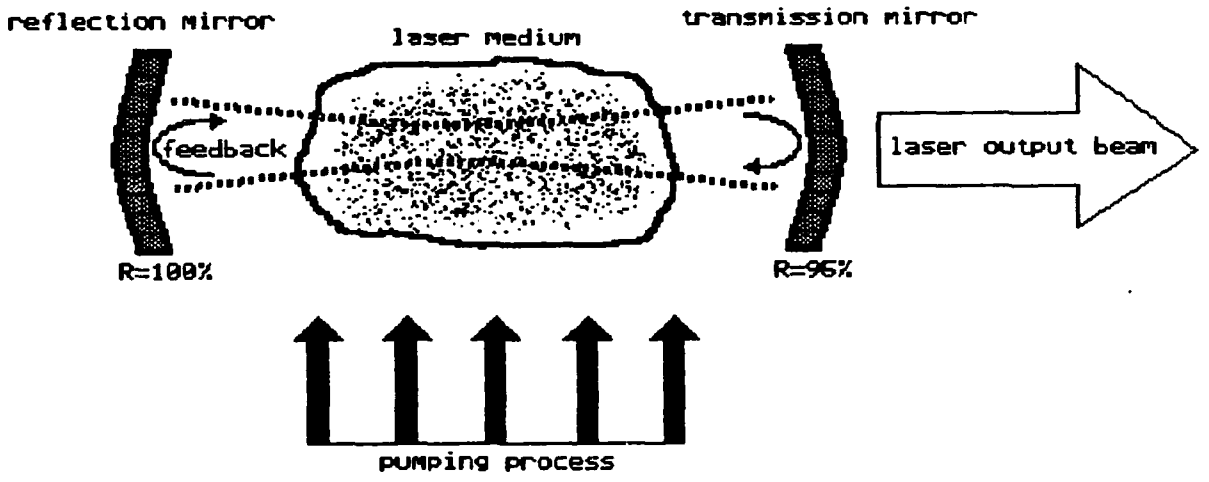

Figure 2. Essential components of a laser oscillator.

This collection of particles, let's say atoms, have various individual quantum energies. The majority of the atoms in the laser medium will normally have the lowest

possible individual energy. Together, they form a population of atoms at the lowest energy level, or ground state, of the laser medium. The remaining atoms, however, have greater individual energies and populate higher energy levels. The only requirement of the laser medium is that it consist of a low-energy population of atoms that can be excited to a higher energy level, and momentarily remain at the higher energy level to create a population inversion, see Figure 3.

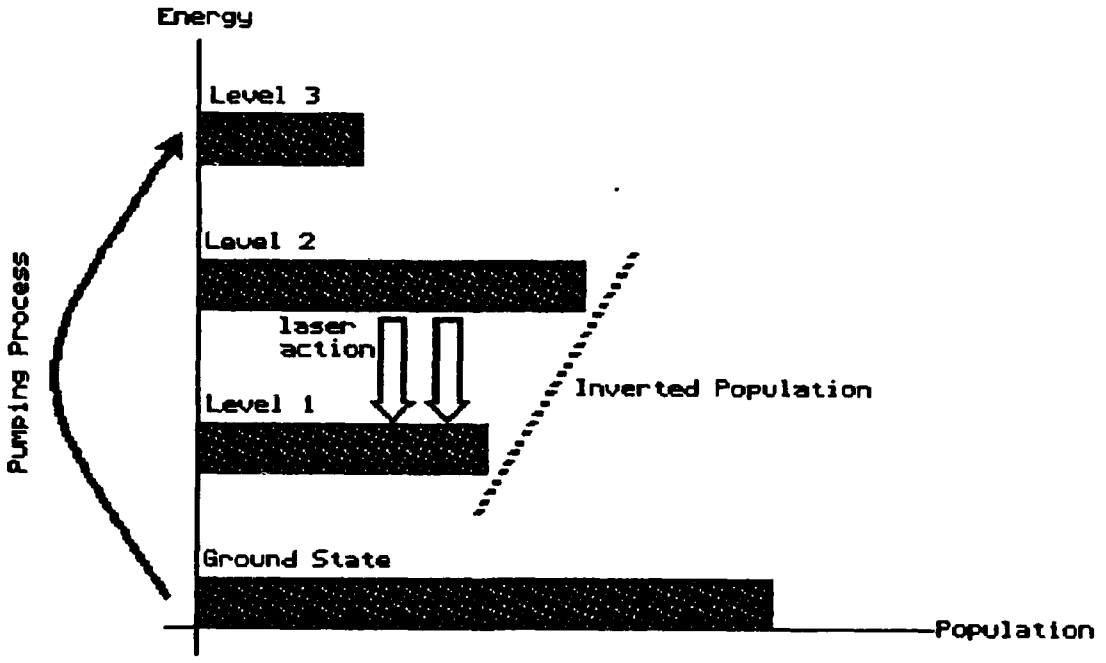

Figure 3. Population inversion between two energy levels.

As individual atoms lose their energy, the population of atoms at the high energy level decreases while the populations of lower energy levels increase. If an optical

signal is applied to the laser medium, and the signal frequency is proportional to the energy difference between the inverted populations, the atoms cascade from the higher energy level to the lower level releasing their energy in a process called stimulated emission. Thus we have light amplification by stimulated emission of radiation or the acronym laser.

The pumping process is the means by which the laser medium is excited to the higher energy level. Energy pumping has been accomplished using many different techniques and serves as another category in which lasers are classified. Lasers have been successfully pumped by mechanical, electrical, chemical, optical, and nuclear methods which will be discussed later.

Optical feedback elements are the lenses and mirrors that surround the laser medium and guide the beam of radiation created by the laser action. In a simple laser amplifier, lenses are used to pass the beam through the laser medium once in a specific direction to be coherently amplified. In this context, coherent amplification means the output signal is exactly like the input signal except for a substantial increase in amplitude. Effects that may degrade the output signal, such as phase shift, distortion, and noise are negligible. The low-intensity input beam is coherently amplified to a higher intensity or "brighter" output beam.

A laser oscillator, however, uses special mirrors to reflect the beam back and forth through the medium many times to create optical feedback. This oscillation is similar to the loud squeal of noise you hear (created by audio feedback) when someone places a speaker too close to a microphone and turns up the gain on a stereo or public-address system. In the simple laser oscillator shown in Figure 2, one mirror is totally reflective while the other transmits a small portion of the radiation outside the system (output beam). The mirrors are carefully aligned so the radiation that originates from the medium is reflected back into the medium many times with very small losses from the mirrors. If the net gain in amplification exceeds the total losses, then a highly directional, coherent, and extremely bright output beam is created.

History

Charles H. Townes at Columbia University laid the groundwork for an optical amplification device when he created the first maser in early 1954. Townes coined the term maser as an acronym for microwave amplification by stimulated emission of radiation. His ammonia beam maser operated in the microwave range of the electromagnetic spectrum shown in Figure 1. Two Soviet scientists, Nikolai G. Basov and Aleksandr M. Prokhorov, made similar discoveries just a few months later. All three men shared the Nobel

Prize in Physics in 1964 for their contributions to maser and laser science.

Immediately after these discoveries were made public, other scientists set out to extend the capabilities of the maser. Nicolaas Bloembergen of Harvard University developed a continuous three-level pumping scheme to obtain a continuous population inversion on one microwave resonance transition. Townes and Arthur L. Schawlow coauthored a very influential paper in 1958 on the possibility of optical masers or lasers. Recently, some credit has been given to Gordon Gould, a graduate student at Columbia in the late 1950's, for his notebook entries on developing the first laser.

History recognizes Theodore H. Maiman at the Hughes Research Laboratories for creating the first experimentally successful laser in July, 1960. Maiman's pulsed ruby laser transmitted at 694 nm in the visible deep red range of the spectrum and was pumped by a flashlamp. Announcing this great scientific milestone proved almost as difficult as making the laser. Maiman first attempted to publish his findings in Physical Review Letters but his paper was rejected by the editors. He instead announced his discovery at a New York news conference on July 7, 1960. His findings were finally published in Nature magazine, August 6, 1960. See a copy of this article in Appendix 1.

The first continuous-wave laser was developed by Ali Javan at the Bell Telephone Laboratories later that same

year and publicly announced in February, 1961. Javan's first helium-neon gas laser transmitted at 1152 nm in the near infrared range of the spectrum. This laser system was extended one year later to transmit at the more familiar wavelength of 633 nm in the red. The He-Ne laser has a very simple design and is extremely reliable. This inexpensive laser is used today in many schools and workplaces in a great variety of ways.

CHAPTER I:
GENERAL LASER THEORY

1. LASER CHARACTERISTICS

Lasers are categorized by the materials they are made from and their operating characteristics. Lasers have been made from atoms, molecules, ions, and organic dyes in different gases, liquids, gels, plastics, and crystalline solids. Some lasers have continuous-wave (c-w) output beams while the others have pulsed beams. Several hundred thousand wavelengths are available today with discrete or tunable outputs. Arthur Schawlow proved [1] "that nearly anything will lase if you hit it hard enough" under the right conditions. He demonstrated this when he prepared a serving of Knox gelatine (similar to Jello), pumped it with a pulsed N_2 laser causing it to lase, then ate it. Lasers are made from so many different materials and employ so many ingenious operating techniques that it is beyond the scope of this paper to even list them. There are, however, four fundamental characteristics that all these devices share. All lasers are highly directional, monochromatic, coherent, and irradiant.

Directional

The output beam from a laser radiates in one direction illuminating only the target. For example, you cannot see the beam path of a c-w laser operating in the visible range unless (1) the beam is pointed directly at your eye--a very unhealthy procedure, or (2) the beam partially reflects off particulates floating in the air. This characteristic is quite useful in applications where aiming the beam with extreme precision is desirable (eg. surgery, range-finding etc.)

Monochromatic

Laser light has a single frequency or wavelength and is thus described as monochromatic (literally meaning "one color"). The output frequency of a laser is proportional to the energy difference between allowed atomic or molecular transition levels. Ideal laser light is the result of one transition scheme, therefore only one frequency is emitted which is limited only by the linewidth of the transition.

In contrast, a thermally-pumped light source, such as an ordinary incandescent light bulb, radiates light composed of many frequencies as its tungsten filament spontaneously decays through many transition schemes. A light bulb's "white" light is actually a mixture of all the frequencies

in the visible range of the electromagnetic spectrum. The light emitted by even the most spectrally pure thermal source cannot compare to the monochromatic properties of a laser. These properties have made the laser a valuable tool in atomic and molecular spectroscopy in the modern laboratory.

Coherent

Coherence refers to a relationship between a signal at one point in space and time, and the same signal at another point in space and time. Lasers exhibit superb temporal and spatial coherence.

First, ideal lasers are temporally coherent because their beam amplitude and phase constant do not change at the same point in space between two different times. Real lasers, operating at steady-state conditions, have extremely stable beam amplitudes but do suffer some phase modulation and drift very slowly. Also, the output signals of real lasers may change from unavoidable mechanical and electronic limitations. However, the relationship between the amplitude and the phase of the output signal at one time is strongly correlated with the amplitude and phase at a much later time. This strong correlation allows the phase of the output signal to be reasonably predicted at any given point in space.

Lasers are spatially coherent because their beam amplitude and phase constant do not change between two

different points in space at any one time. Young's experiment, illustrated in Figure 4(a), demonstrates the spatial coherence of a point source of incoherent light and compares this with a laser, Figure 4(b). Note how the wavefront at points A and B are the same in both cases yet the laser does not require the pinhole source.

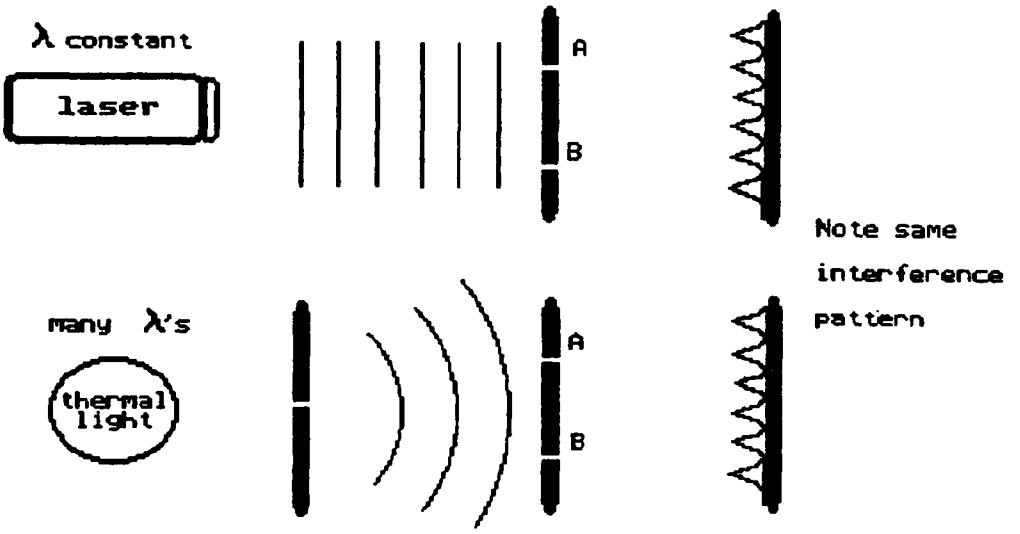

Figure 4. A comparison of the spatial coherence between an incoherent light source (a) and a laser (b). (Reproduced, in part, from [3])

Temporal and spatial coherence has given the laser awesome potential in industrial applications. For example, temporal coherence is the cornerstone of such precise timing devices as ring-laser gyroscope navigation systems. Spatial coherence accounts for a laser's highly irradiant beam. This characteristic allows the total beam power to be

concentrated into a small area which transforms the laser into a clean, precise "cutting" tool in materials fabrication.

Irradiant

Laser light is much "brighter" or has greater irradiance than ordinary light. Irradiance, I, is the amount of energy per unit time per unit area (or power per unit area). Note, irradiance has recently replaced the older, less precise term, intensity, in modern optics.

To compare the irradiance of coherent laser light with incoherent light almost seems unfair. First, since a laser is highly directional and spatially coherent, laser light can be directed at a target very far away with very little beam divergence or energy attenuation. The beam energy of an incoherent light source, however, radiates in all directions and decreases proportionally to the inverse square of the distance.

Second, since a laser is monochromatic, a low-wattage laser can transmit its total beam energy at one particular wavelength. In contrast, a high-wattage incoherent source would be needed to attain the same "brightness" at that wavelength since its total beam energy is distributed among many wavelengths.

Finally, pulsed lasers have especially high irradiance since they can transmit energy in extremely small time

periods. For example, a pulsed CO_2 laser transmitting a 5 J pulse with a 0.5-μsec duration delivers 10 MW of power.

2. EMISSION AND ABSORPTION OF RADIATION

A helium discharge lamp normally casts a pinkish-white light. However, if you view the lamp through a transmission diffraction grating, you will see distinct bands of yellow, violet, green, blue, and red. The discharge lamp transmits many different frequencies, each diffracted at a different angle, each represented by their unique color in the visible spectrum. These frequencies are defined by the following relationship, originally proposed by Planck, and later used by Niels Bohr in 1913 as one of the postulates for his model of the atom:

Planck's Law $$f = \frac{E_2 - E_1}{\hbar} \qquad (1\text{-}1)$$

where f = frequency
E = energy level
$\hbar = h/2\pi$
h = Planck's constant

Laser physics is based on the concept that every element in nature has its own set of quantum energy levels, and any movement from one level to the next involves some exchange of energy. If energy is absorbed by an atom (or molecule or ion), then the atom moves up to a higher quantum energy level. If the atom releases energy, the atom moves down to a lower energy level. Bohr claimed that the frequency of the energy absorption or emission is the difference between the initial and final levels, divided by Planck's constant.

The movement of an atom from one energy level to another is called an energy transition or quantum jump. In the case of the discharge lamp, the helium atoms are pumped to higher energy levels by an electric current. The helium atoms do not stay at these unstable, artificially high levels for long and radiate their excess energy to return to the lower energy levels. These atomic transitions produce the beautiful spectral lines mentioned earlier.

Spontaneous Transitions

The previous discussion was a typical example of a spontaneous emission of electromagnetic radiation. Spontaneous emission occurs when atoms release their internal energy, without external inducement, and drop to lower energy levels. Note that spontaneous emission is only a downward transition. This process is also called spontaneous decay, fluorescence, energy decay, and energy relaxation.

There are actually two forms of downward spontaneous transitions, radiative or non-radiative. Radiative emission releases electromagnetic energy in the form of randomly directed photons. Non-radiative emission releases mechanical energy through vibrations which heat the surrounding medium. These vibrations are a form of acoustic radiation in which the fundamental particle is referred to as a

phonon. Both transitions release incoherent energy at the transition frequency defined by Planck's Law.

One model commonly used to illustrate the radiative emission process is shown in Figure 5. In this figure, an atom at a higher energy state drops to a lower energy emitting a photon of electromagnetic energy. There are some problems with this simplistic approach that will be discussed in the next section.

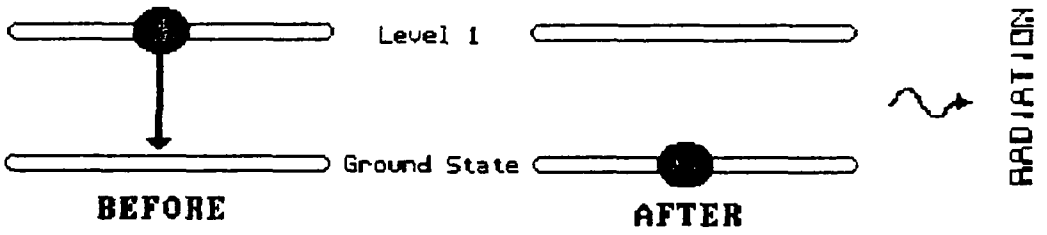

Figure 5. Simple photon-atom model of spontaneous emission.

Stimulated Transitions

Stimulated transitions occur when an atom encounters energy that equals the difference between its present energy state and another state. Note that a stimulated transition can either move an atom up to a higher energy state (absorption) or down to a lower one (emission).

Stimulated transition, triggered by electromagnetic energy at the proper frequency, is the key principle to the laser. The photon-atom model in Figure 6 demonstrates stimulated absorption and emission. In the first case, an atom at the ground state absorbs the energy of an incident photon and jumps to a higher energy level. In the next case, an atom, already at a higher energy level, encounters an incident photon, and drops down to a lower level emitting an additional photon of electromagnetic energy. The most remarkable aspect of stimulated emission is that the resulting radiation is coherently amplified in exactly the same frequency and direction as the stimulating radiation.

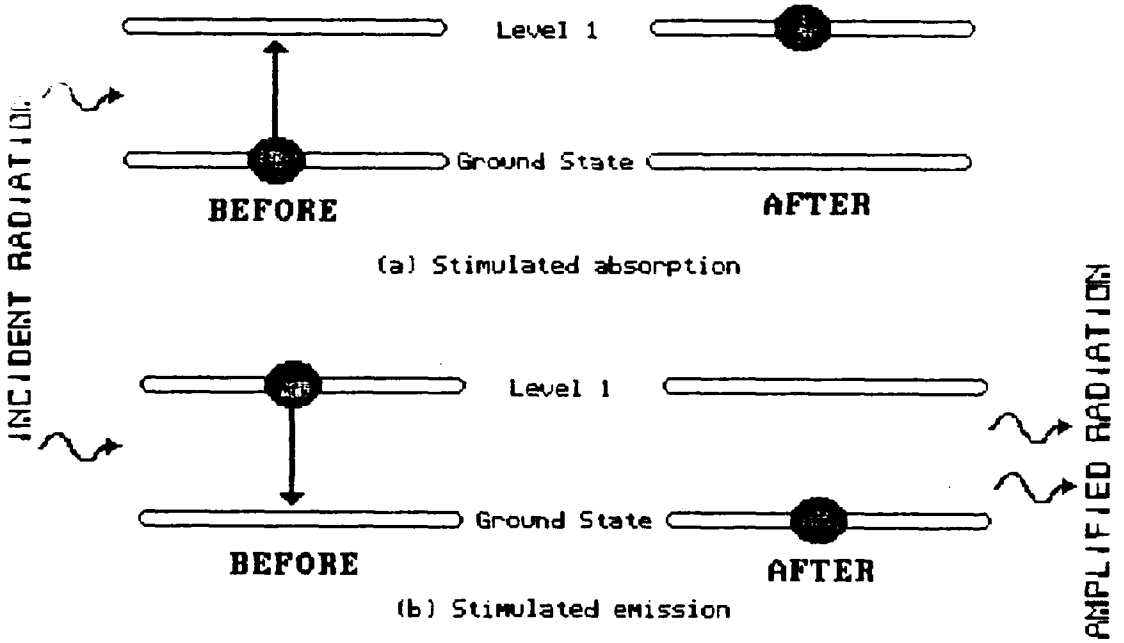

Figure 6. Simple photon-atom model of stimulated absorption and emission.

Of course, both transition processes are much more complex. Two important quantum mechanical considerations are overlooked by the photon-atom model: the wave nature of the electromagnetic radiation and the statistical nature of the laser medium.

For example, the wave nature of spontaneous emission is better understood if you consider each atom behaving like an oscillating electric dipole antenna. Each antenna (atom) releases its excess energy by independently transmitting electromagnetic radiation with a different frequency and phase angle. The result is an incoherent, multi-frequency signal.

In stimulated transitions (absorption or emission), the atoms behave like passive resonant antennas that are set oscillating by an external signal. The wave motion of each atom is not random but driven by the same incident signal; therefore, the atoms are oscillating coherently at the same frequency as the stimulating radiation.

Also, the simple photon-atom model implies that individual atoms move from one energy level to another in discrete "jumps". Quantum theory asserts that most atoms are not exactly in one energy level at any given time. The instantaneous quantum state of any one individual atom is actually a combination of quantum states that changes with time.

Transition Rates

As mentioned earlier, spontaneous transitions occur when an atom releases excess energy through radiative and non-radiative emission. The spontaneous transition (or decay) rate from energy Level 2 to 1 is directly proportional to the population of Level 2 and is given by the following equation:

$$\text{Spontaneous Transition Rate} \qquad \left.\frac{dN_2}{dt}\right]_{spon} = -\left.\frac{dN_1}{dt}\right]_{spon} = -\gamma_{21} \cdot N_2 \qquad (1\text{-}2)$$

where N_2 = population of atoms at energy level 2
N_1 = population of atoms at energy level 1
γ_{21} = total spontaneous transition rate, or decay rate, from level 2 to level 1 (radiative plus non-radiative emission)

Now, suppose we apply an external signal that equals the energy difference between Levels 1 and 2. When the signal is applied to atoms in the lower energy level, they make a stimulated transition or "jump" upward to a higher level. This stimulated absorption occurs at a rate proportional to the strength of the external signal times the number of atoms in the starting level. The signal strength is represented by the number of photons per unit volume, or energy density.

$$\text{Stimulated Absorption Rate} \qquad \left.\frac{dN_2}{dt}\right]_{stim\ up} = K \cdot n \cdot N_1 \qquad (1\text{-}3)$$

where N_1 and N_2 = initial population of atoms at energy

levels 1 and 2
K = proportionality constant
n = photon (energy) density

The same external signal applied to a population of atoms at the higher energy level will cause the atoms to jump downward in a stimulated emission of radiation.

$$\text{Stimulated Emission Rate} \quad \left[\frac{dN_2}{dt}\right]_{\text{stim down}} = -K \cdot n \cdot N_2 \qquad (1\text{-}4)$$

Note that the same proportionality constant, K, and photon density, n, are used in both equations above. Therefore (1) the probability for either stimulated absorption or emission to occur is exactly the same, and (2) the net flow of atoms will always be from the most populated energy level to the least populated at a given time. The net stimulated transition is actually the sum of the stimulated emission and stimulated absorption.

Spontaneous and stimulated transitions occur simultaneously and independently. Therefore, their results may be added together:

$$\begin{array}{lcccccc} \text{Total Transition Rate} & = & \text{Stimulated Transition Rate Upwards} & + & \text{Spontaneous Transition Rate Downwards} & + & \text{Stimulated Transition Rate Downwards} \end{array}$$

$$\left.\frac{dN_2}{dt}\right]_{tot} = \left.\frac{dN_2}{dt}\right]_{stim\ up} + \left.\frac{dN_2}{dt}\right]_{spon} + \left.\frac{dN_2}{dt}\right]_{stim\ down}$$

$$\left.\frac{dN_2}{dt}\right]_{tot} = (K \cdot n \cdot N_1) - (\gamma_{21} \cdot N_2) - (K \cdot n \cdot N_2)$$

$$= [K \cdot n\ (N_1 - N_2)] - \gamma_{21} \cdot N_2 = -\left.\frac{dN_1}{dt}\right]_{tot} \qquad (1\text{-}5)$$

Equation (1-5) is the crux of laser theory. It states that in the absence of external radiation, only spontaneous emission occurs. Also, if an external signal is applied to a collection of atoms, then a stimulated transition occurs but could be in either direction: up (stimulated absorption) or down (stimulated emission). The direction of the stimulated transition depends only on the number of atoms in the different energy levels.

The first term in brackets represents the total rate at which atoms make stimulated transitions between energy levels. If the lower-energy population is larger than the higher-energy population, $N_1 > N_2$, then external radiation is absorbed and there is a net stimulated transition upwards. However, if $N_2 > N_1$, then external radiation causes a stimulated transition downward. The additional energy released by the atoms coherently amplifies the input radiation and the result is stimulated emission. In this case, the second term representing spontaneous emission contributes to the "noise" of the net emission.

3. ATOMIC POPULATIONS

An atomic population is the number of atoms at a given quantum energy state at a particular time. Atomic populations are most often represented by an energy-level population diagram. A typical diagram for a collection of atoms is shown below in Figure 7.

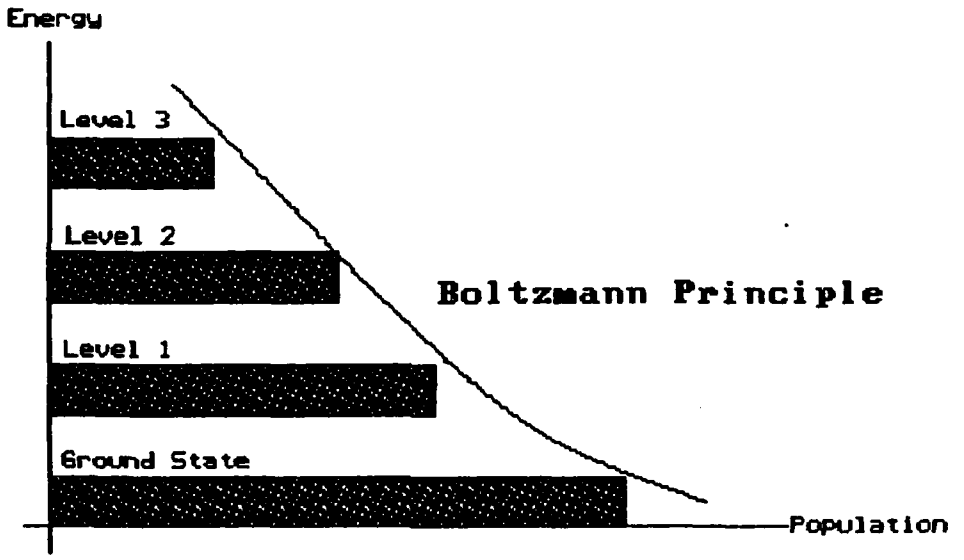

Figure 7. Typical energy-level population diagram.

Consider a collection of atoms at equilibrium and constant temperature. Since all transitions in stable matter are towards lowest energy, the majority of atoms will populate the lowest levels at equilibrium. Random molecular collisions may cause some atoms to occupy higher energy states, but the ground state will always have the largest

population. The population decrease from the ground state to the highest energy levels is called the Boltzmann Principle.

Boltzmann Populations

Ludwig Boltzmann (1844-1906) discovered that for a collection of atoms in thermal equilibrium at constant temperature, the ratio of populations between any two energy levels depended only on the temperature of the system and the energy difference between levels.

Boltzmann's Principle

$$\frac{N_2}{N_1} = \exp\left[\frac{-(E_2-E_1)}{kT}\right] \qquad (1\text{-}6)$$

where N_1, N_2 = atom populations at levels 1 and 2
E_1, E_2 = energy at levels 1 and 2
k = Boltzmann's constant
T = temperature

This exponential function is shown in Figure 7. Note that increasing the temperature of the system will increase the populations of atoms in the higher energy states, but the populations of the lower states will always be greater. According to the Boltzmann Principle, it is impossible for more atoms to "naturally" occupy a higher energy state than the next lower state. Overcoming the Boltzmann Principle was the greatest theoretical problem to solve before developing the laser.

Population Inversions

For stimulated emission to occur, a population inversion must exist between two energy levels. A population inversion is a non-equilibrium condition when more atoms exist in a higher quantum energy level than a lower energy level. When a population inversion is attained, "potential energy" is essentially stored between the two levels, ready to be released in a controlled stimulated emission.

A population inversion can be obtained by "pumping" atoms from a lower energy state to a higher energy state. Population inversions are difficult to maintain because the pumped atoms immediately begin to spontaneously decay back to their original energy level. Therefore, there are two important factors to consider when attempting to create an inverted population:

(1) the rate of spontaneous decay between levels
(2) the strength, rate, and efficiency of your pumping technique.

The key to attaining a population inversion is to have at least one "allowed" and one "forbidden" energy transition. An allowed transition occurs when atoms with excess energy spontaneously decay to the next lowest energy level very quickly (microseconds). Energy levels with allowed transitions have short lifetimes and are extremely unstable.

In Figure 8, the second excited energy level has an allowed transition.

The time for spontaneous emission to occur from the first excited level to the ground state, however, is relatively long (several hundred seconds), and is called a forbidden transition. Energetic atoms accumulate at this level, creating a population inversion and a chance for stimulated emission to occur between the first excited level and the ground state. Since the atoms have a comparatively long lifetime at this energy level, this is called a metastable state. In effect, the energetic atoms are trapped in the metastable state like a pool of water until stimulated emission occurs. After stimulated emission, the atoms "drain" to the lower levels very quickly, only to be pumped up again.

The four-level scheme in Figure 9 works the same way. Even though the atoms are initially pumped higher, the four-level scheme has some advantages. First, the population inversion occurs with respect to the second and first excited levels--not the ground state--which for most systems is much easier to accomplish. Second, if the transition from the first excited energy level to the ground state is allowed (fast), the pumping mechanism has an inexhaustible "reservoir" of ground state atoms to pump to higher levels.

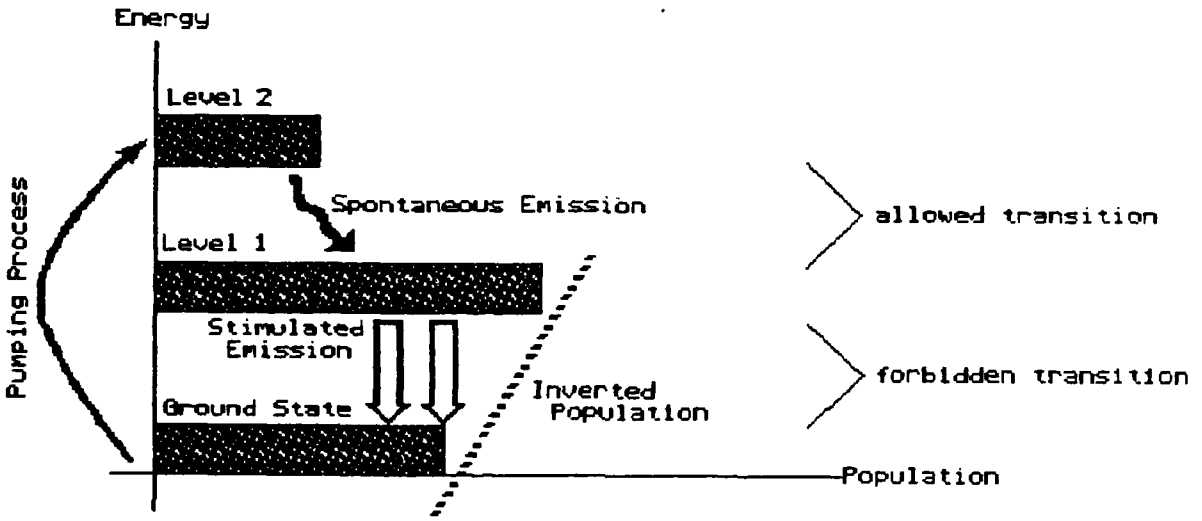

Figure 8. Inverted population diagram (three-level).

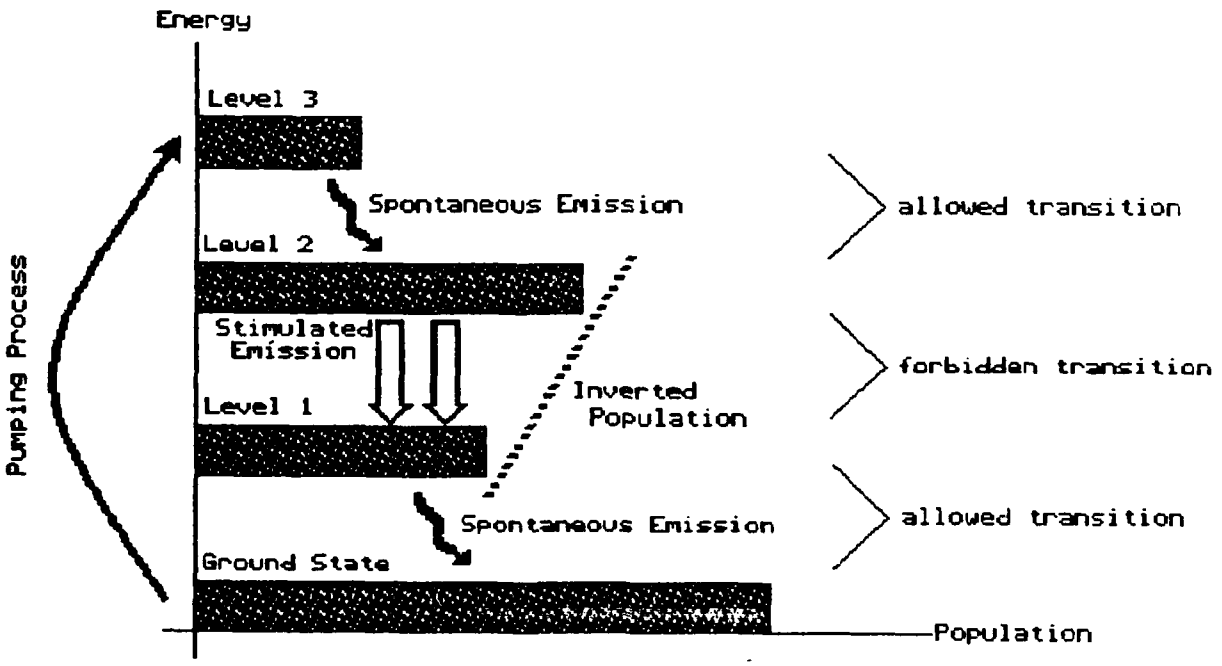

Figure 9. Inverted population diagram (four-level).

4. LASER PUMPING TECHNIQUES

To attain a population inversion, a pumping process is needed to excite atoms into their higher quantum-mechanical energy levels. Several pumping methods exist but all involve selectively adding energy to the laser medium from an external source. Electrical gas discharge and optical pumping are the two most prevalent laser pumping methods used today.

Electrical Gas Discharge

Electrical gas discharge pumping usually works by increasing the kinetic energy of pumping atoms which collide with the active lasing material. Electrical discharge pumping may be continuous or pulsed depending on the system design and lasing gas pressure. In either case, an electrical discharge is applied across the laser medium to increase the kinetic energy of the pumping atoms. The pumping atoms then collide with the lasing atoms which are excited to higher energy levels.

Keep in mind that the pumping "atoms" may actually be atoms, molecules, or ions, and are different from the active lasing material. For example, in the He-Ne laser, the excited helium (pumping) atoms collide with the neon (lasing) atoms. In any case, electrical gas discharge pumping

usually involves some type of energy transfer through collisions between particles.

Optical

Optical pumping is the method in which a strong, external light source is used to irradiate a laser medium. If the light source has the appropriate frequency and energy defined by Planck's Law, then the lasing atoms absorb the external radiation and rise to a higher energy level. Note, the photons emitted from the light source must possess the transition energy between the upper and lower pumping levels in order to be absorbed. If this is the case, then each atom can absorb one photon of light energy and jump to the higher quantum-energy level. Lasers may be optically pumped by sunlight, flashlamps, even other lasers.

Choosing the correct light source depends heavily on the thickness of the high-energy absorption band. While some lasing materials have wide absorption bands, others are much narrower. The wide-band materials are easily pumped by using intense lamps that emit photons in a wide range of frequencies.

Narrow-absorption band materials may be accommodated by using another laser. Since an ideal laser has one output frequency, this is a very efficient optical pumping method. Theoretically, every proton from the pumping laser is

capable of raising an atom of the primary laser to a higher energy level.

Other Pumping Methods

Below is a list of other pumping methods taken directly from Anthony E. Siegman's text, LASERS, 1986 [1]:

a. (Electrical) **Gas discharges** (previously mentioned), both dc, rf, and pulsed, including glow discharges, hollow cathode, arc discharges, and many kinds of pulsed axial and transverse discharges, and involving both direct electron excitation and two-stage collision pumping.

b. **Optical pumping** (previously mentioned), using flashlamps, arc lamps (pulsed or dc), tungsten lamps, semiconductor LEDs, explosions and exploding wires, other lasers, and even gas films and direct sunlight.

c. **Chemical reactions**, including chemical mixing, flash photolysis, and direct laser action in flames. It is instructive to realize that the combustion of one kg of fuel can produce enough excited molecules to yield several hundred kilojoules of laser output. A chemical laser burning one kg per second, especially if combined with a supersonic expansion nozzle, can thus provide

several hundred kW of c-w laser output from what becomes essentially a small "jet-engine laser"

d. **Direct electrical pumping,** including high voltage electron beams directed into high-pressure gas cells, and direct current injection into semiconductor injection lasers.

e. **Nuclear pumping** of gases by nuclear-fission fragments, when a gas laser tube is placed in close proximity to a nuclear reactor.

f. **Supersonic expansion of gases,** usually preheated by chemical reaction or electrical discharge, through supersonic expansion nozzles to create the so-called gasdynamic lasers.

g. **Plasma pumping in hot dense plasmas,** created by plasma pinches, focused high-power laser pulses, or electrical pulses. There are also widely believed rumors that X-ray laser action has in fact been demonstrated in a rod of some laser material pumped by the ultimate high-energy pump source, the explosion of a nuclear bomb.

5. LASING

Lasing is the process in which stimulated emission is reflected back through the laser medium to create a self-sustained optical oscillation inside the laser cavity. You may ask, "How does lasing start?" and "How is it sustained?"

Before lasing can occur, a pumping process must establish a population inversion between two energy levels of the laser medium. Since the excited atoms face a forbidden transition, the population spontaneously decays slowly from the metastable level to other lower levels. (Recall that a "forbidden" transition does not imply the downward transition is impossible, just that it occurs relatively slowly. Conversely an "allowed" transition is very quick.) Note, this spontaneous emission is transmitted in all directions at various frequencies.

Lasing begins when a photon of radiation is ejected as the atom spontaneously decays from the metastable energy level with a transition frequency, f, defined by Planck's Law. When the photon encounters other excited atoms, it causes them to undergo stimulated emission, resulting in coherent amplification. The first photon created by spontaneous decay is the external optical signal mentioned in Section 2. In effect, the first photon acts as the "seed" to an incredibly swift chain reaction resulting in stimulated emission. See Figure 10 on the following page.

To encourage stimulated emission at one frequency, a laser medium that strongly favors one particular transition is chosen. To sustain lasing, special mirrors must be added to the laser cavity.

Resonant Laser Cavity

To create a laser oscillator, optical feedback elements must be added to the laser cavity. Normally, this is accomplished by placing two highly reflective mirrors at opposite ends of the cavity. If stimulated emission radiates along the axis of the cavity, then this radiation is reflected back through the laser medium to the opposite mirror. These mirrors are coated to reflect only the desired lasing frequency, and carefully aligned to reflect the incident radiation back along the laser cavity axis.

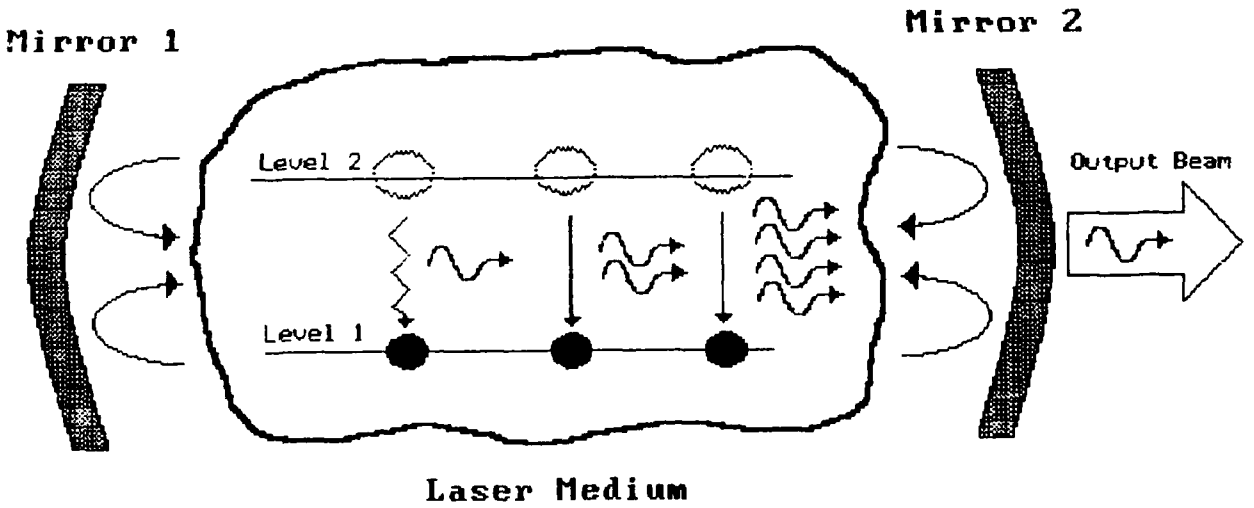

Figure 10. Amplification and lasing in a laser cavity.

As the radiation passes through the laser medium, the amplitude of the optical signal increases. When the radiation reflects off one mirror, it passes back through the medium, and the signal is reamplified. The disturbance propagating through the laser medium develops into a standing wave defined by the length of the laser cavity. If there is an integral number of half wavelengths between the mirrors, the laser cavity resonates.

Resonance Condition

$$m = \frac{L}{(\lambda/2)} \tag{1-7}$$

where m = mode number (an integral number of half wavelengths)
L = length of the cavity
λ = wavelength

Recall

$$\lambda = v/f$$

where v = wave velocity
f = wave frequency

Substituting this into (1-7) and rearranging

Longitudinal Cavity Mode

$$f_m = \frac{mv}{2L} \tag{1-8}$$

where f_m = mode frequency

The optical signal incurs a small loss each time the radiation reflects off either mirror. Also, one mirror is partially transmittive to allow a fraction of the radiation to pass outside the cavity. If the round-trip losses are greater than the amplified gains, the signal dies out. However, if round-trip gains are greater than the losses,

the signal grows exponentially until the inverted population is drained or the gain is saturated. The gain minus the losses is called the threshold condition.

The Quality Factor

The quality factor, Q, of any device, is the relationship between the device's ability to store and dissipate energy:

$$\text{Quality Factor} = \frac{\text{Energy Stored}}{\text{Energy Dissipated}}$$

The term originated in electronics, where Q is a measure of the energy-storage property (inductance) relative to the energy dissipation property (resistance) of a circuit. In the context of lasers, Q is a measure of the energy stored at the metastable energy level before being released through stimulated emission.

Consider what would happen if a mirror was removed from the laser cavity. The lasing process would stop immediately since there is no signal oscillation without optical feedback. Single-pass stimulated emission would still occur within the medium but the radiation quickly passes outside the cavity. Only an insignificant amount of energy is drained from the metastable energy level. If the system continues to pump atoms to the metastable energy level while

the system is not lasing, the population inversion is increased considerably and the energy is stored.

Now replace the mirror. Lasing is suddenly induced and a powerful pulse of energy is released as the atoms drop down to the lower state almost in unison. Removing the mirror stores energy--replacing the mirror after the extra energy is stored is called Q-spoiling (spoiling its ability to store energy), or more commonly, Q-switching (switching from an energy-storage device to an energy-release device).

A mechanical analogy of this process is illustrated in Figures 11 and 12 on the next page. In Figure 11, water is continuously pumped from a ground-level reservoir to an elevated tank (an increase of potential energy). The tank has a small hole in its base and a steady stream of water drains back into the reservoir (loss of potential energy). If the pump can first establish a "population inversion" of water between the tank and reservoir, and then just match the rate at which the water drains, we have a continuous, steady-state waterfall. In spirit, this resembles the lasing action of a continuous-wave laser.

In Figure 12, the hole at the base of the tank is plugged (the cavity mirror is removed) and water accumulates in the tank. The pump continues to operate and the tank begins to fill. Now replace the base of the tank with a spring-loaded trap door (a Q-switch) designed to open after a certain water level is reached. After enough water has

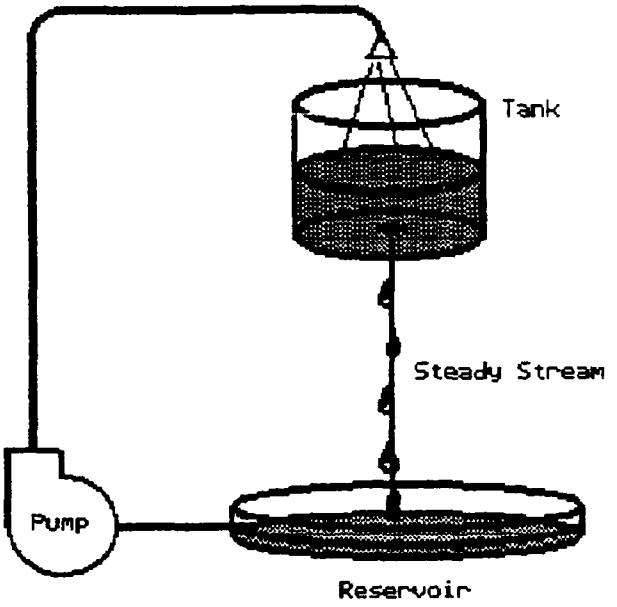

Figure 11. Mechanical analogy of a continuous-wave laser with no Q-switch.

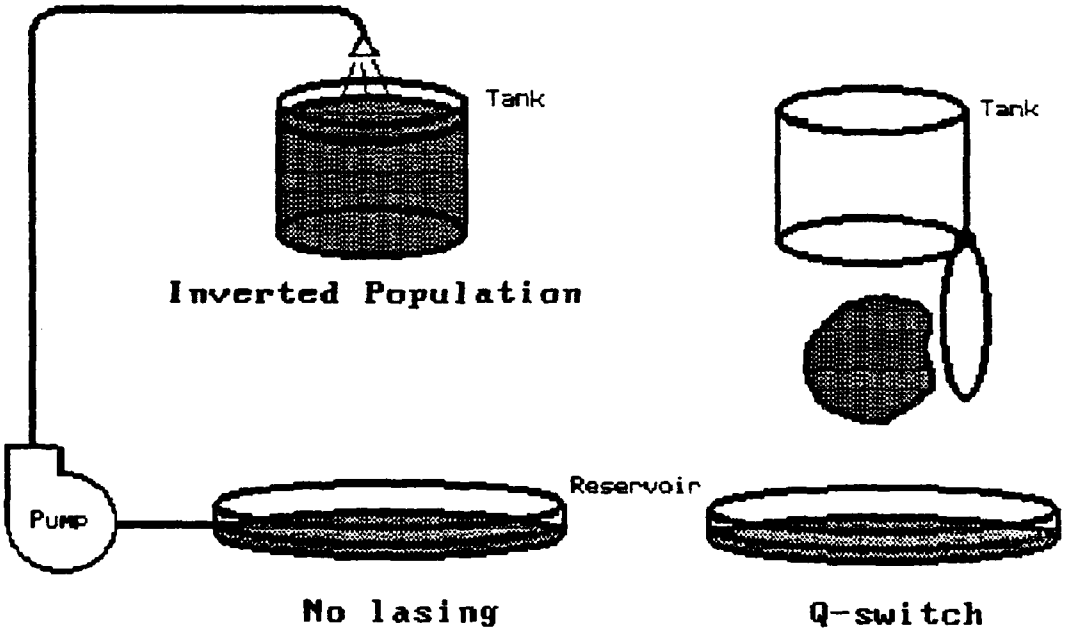

Figure 12. Mechanical analogy of a pulsed laser with a Q-switch.

been stored, a giant pulse of water is released. This is similar to the lasing action of a pulsed laser.

The obvious advantage of Q-switching is that it allows stored energy to be released in a very short time. This time interval is called the pulse duration and normally lasts only a few nanoseconds (see Figure 13). In some applications, such as nuclear fusion, a short, intense pulse of energy from a laser may be more useful than the equivalent amount of energy delivered over a much longer time.

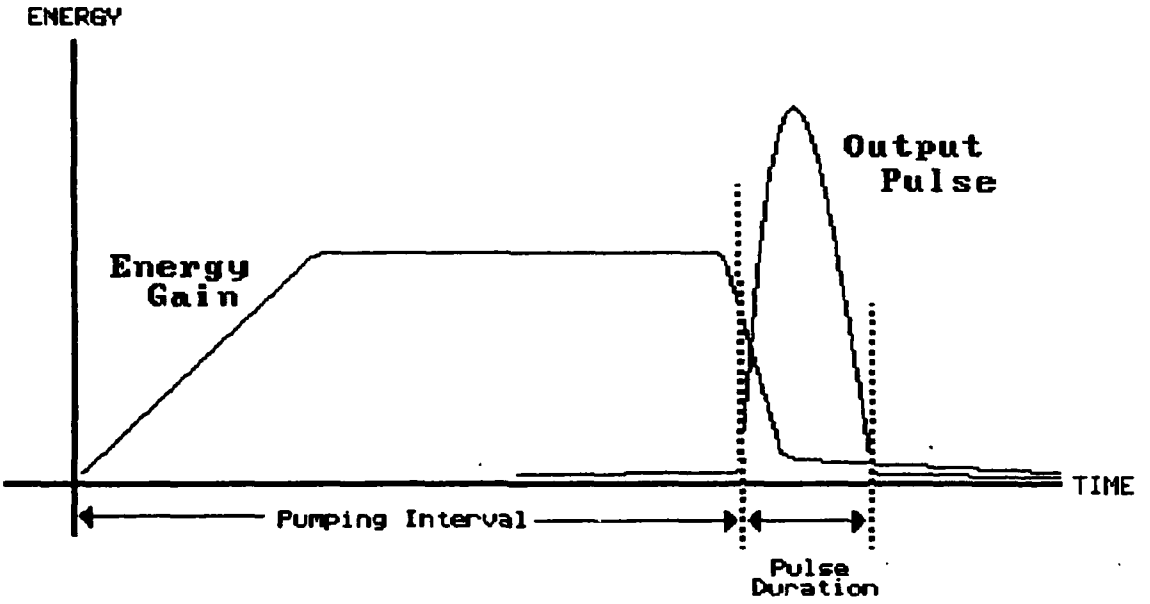

Figure 13. High-energy output pulse with short duration.

Q-switch Devices

Q-switches effectively block or remove one of the reflective mirrors of the cavity. There are two types of Q-switching devices, active and passive. Active devices use some control scheme that obstructs or deflects the laser radiation until a sufficient population inversion is established. Passive devices normally absorb the radiation until saturated. Some of the more common Q-switch devices used in practical lasers today are the following [1]:

a. **Rotating mirror Q-switch** (active) - a mirror or prism is physically rotated to block, bend, or reflect the stimulated emission. Lasing resumes when the device is properly orientated with the opposite mirror.

b. **Electrooptic Q-switch** (active) - an electrooptic crystal which becomes birefringent under the influence of an applied voltage. Any radiation passing through the crystal has its polarization rotated 90° and is absorbed by a polarizer. After the voltage is removed, the crystal becomes essentially transparent and lasing resumes.

c. **Acoustooptic Q-switch** (active) - an acoustooptic

modulator in which the index grating produced by an rf acoustic (sound) wave Bragg-diffracts (scatters) light out of the laser cavity.

d. **Saturable-Absorber Q-switch** (passive) - uses a radiation absorbing medium such as an organic dye solution. Lasing occurs after the absorbing material is saturated.

e. **Thin-film Q-switching** (passive) - an unusual offshoot of the saturable absorbers, this process uses a thin absorbing or metallic film on a glass or mylar substrate. The weak initial lasing energy is focused to a small spot on the film which quickly vaporizes. Full lasing occurs when the film at that location completely burns away.

CHAPTER II:
THE CARBON DIOXIDE LASER

1. MOLECULAR ENERGY LEVELS

Up until now, only the energy transitions of a monatomic lasing medium have been discussed. The quantum energy level of an atom was determined by the energy released or absorbed as the atom's electrons moved from one orbit to the next. The lasing medium of a carbon dioxide (CO_2) laser, however, is a diatomic molecular gas. So in addition to the energy from electron movement, we must also consider the vibrational and rotational movements of the carbon and oxygen atoms relative to each other.

CO_2 is a linear molecule with one carbon atom flanked by two oxygen atoms. Since CO_2 has over 200 possible lasing transitions between 8 and 18 μm [7], let's examine only the strongest transitions in detail. These energy transitions are primarily caused by the vibrational modes of the molecule which are significantly greater than the energy contributions from the rotational and electronic modes. The CO_2 molecule can vibrate in two distinct ways, stretching and bending.

CO_2 Stretching and Bending

The vibration modes of the CO_2 molecule are illustrated in Figure 14 on the following page. Spectroscopists have developed the following simple notation to concisely describe the excited energy levels of each mode:

Ground State	(000)		
Asymmetric Stretch	(001)...	to (00n)	quantum levels
Bending	(010)...	to (0n0)	quantum levels
Symmetric Stretch	(100)...	to (n00)	quantum levels

(a) Ground State (000)

(b) Symmetric Stretching (100)

(c) Asymmetric Stretching (001)

(d) Bending (010)

Figure 14. Vibrational modes of the CO_2 molecule.

In the ground state, the carbon atom is centered between the two oxygen atoms. In the symmetric-stretch mode the two oxygen atoms vibrate in opposite directions along the longitudinal axis of the molecule. During asymmetric-stretch vibration, the two oxygen atoms move in the same direction along the longitudinal axis of the molecule, while the carbon atom moves in the opposite direction. Finally, in the bending vibration mode, the two oxygen atoms move in the same direction perpendicular to the longitudinal axis of the molecule, while the carbon atom moves in the opposite coplanar direction.

CO_2 Transition Levels

Carbon dioxide is a simple, non-reactive, diatomic molecule with several isotopes. The various combinations of vibrational, rotational, and electronic modes yield hundreds of possible energy transitions which have been well documented. However, only two transitions, near the ground state, offer the possibility for significant lasing.

The energy-level population diagram for the CO_2 molecule is shown in Figure 15. This figure is similar to the energy diagrams shown earlier with the exceptions that CO_2 has a five-level pumping scheme and a population inversion at the fourth excited level.

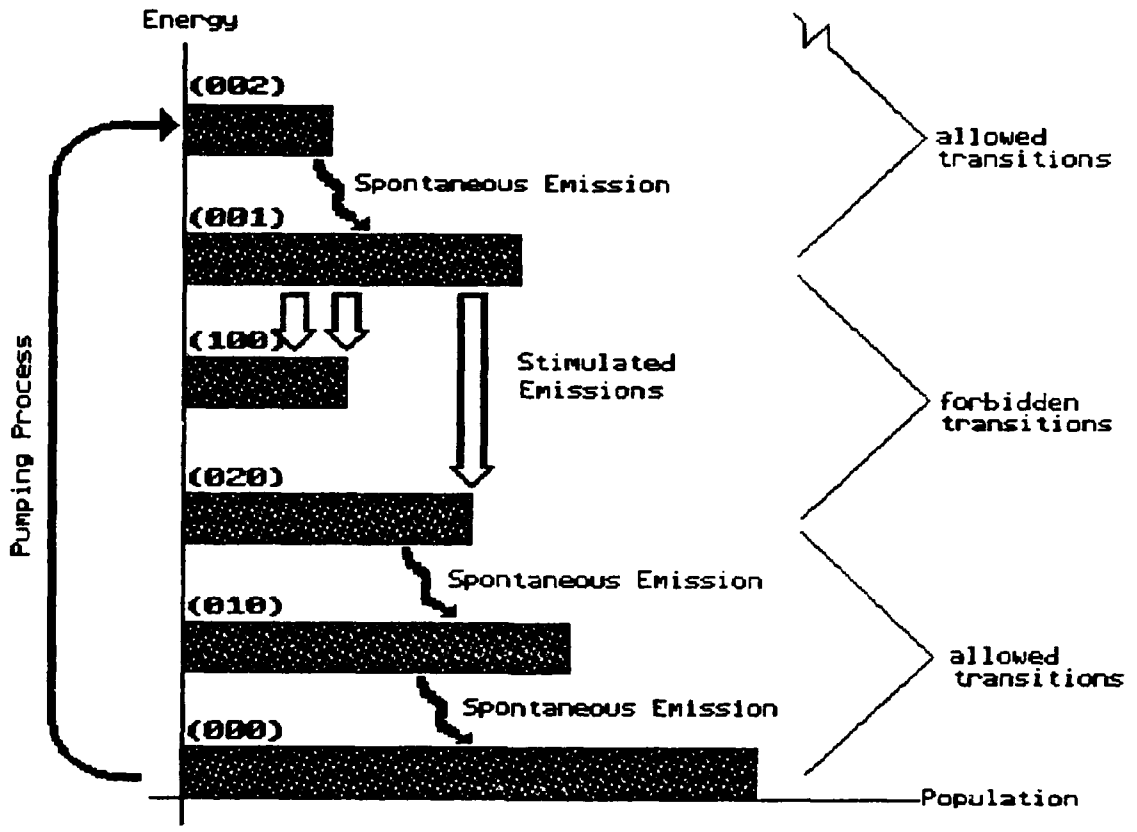

Figure 15. CO_2 energy-level population diagram.

The lasing transitions occur from the first symmetric stretch mode (001) to either the first asymmetric stretch (100) or second bending (020) modes. Radiation emitted from these transitions are in the infrared range with wavelengths of 10.6 and 9.6 μm respectively. Note that decay from the (100) and (020) modes to all other lower energy levels are allowed (fast, 0.3-20 μs) transitions. Transitions from all vibrational modes above (001) are also allowed (these are very fast, 2 ns).

CO_2 gas has several noteworthy advantages over other lasing materials. First, the CO_2 molecules are easily pumped above the forbidden transition (001). They decay very quickly to (001) to establish an inverted population. Second, the population is inverted with respect to the second and third excited energy states, not the ground state. Population inversions between higher energy levels are easier to attain, plus this scheme leaves a larger reserve of ground-state atoms to continue pumping. Finally, the CO_2 molecule transitions to (010) are to an energy level very close to the ground state; therefore, any energy losses from the spontaneous decay to the ground state are minimized.

2. THE PULSED CO_2 TEA LASER

The laser used in the experiments described in this report is a pulsed CO_2 transversely excited atmospheric (TEA) laser manufactured by Lumonics Incorporated, of Ontario, Canada. The Lasermark Model 901 was originally purchased by the Control Data Corporation of Omaha to score identification markings on magnetic storage disks. Control Data donated this laser to the Creighton University Physics Department in 1983 through a Capital Equipment Grant. This powerful CO_2 laser is easy to operate, reliable, and yields consistent output--an invaluable tool for graduate-level basic research.

CO_2 lasers operate in the infrared and have been made with continuous-wave (c-w) and pulsed output signals. Continuous-wave CO_2 lasers operate at cavity pressures of 20-50 mm Hg, are pumped by a steady glow discharge, and yield low kilowatt outputs. A pulsed CO_2 laser can operate from one to ten atmospheres and deliver several megawatts of output power. However, to achieve these tremendous power outputs, pulsed CO_2 lasers require a slightly different pumping method.

Pumping/Lasing

Pulsed CO_2 lasers are pumped by a short-duration, high-voltage electrical discharge across the laser cavity. This

discharge is created by building a high potential difference between two capacitor plates. Since capacitance is inversely proportional to the distance between the plates, the capacitor plates run the length of the laser cavity so that the discharge occurs across the diameter of the cavity, not its length. In other words, the discharge is applied transversely across the laser cavity. If the the laser cavity pressure equals one atmosphere, as in the case of the Lasermark 901, we have a transversely excited atmospheric, or TEA, laser.

Soon after Patel announced his development of the first pure CO_2 gas laser in 1964 [3], Legay and Sommaire discovered that a more efficient pumping method was possible by simply adding molecular nitrogen gas to the CO_2 [3]. They determined that it would be much easier to excite N^2 gas by an electrical discharge than pure CO_2. The excited N_2 molecules could then collide with the CO_2 molecules causing them to rise to higher vibrational energy states. Since the energy of the lowest N_2 vibrational mode was nearly equal to the energy of the (001) mode of CO_2, the transfer of energy through mechanical collisions could be quite efficient. Patel quickly developed a new laser with a CO_2-N_2 lasing gas mixture which proved to be much more efficient.

Later in 1964, Patel discovered another way to increase the CO_2 laser power output. He learned that adding helium to the lasing gas mixture increased the rate of transition after lasing to the ground states. The helium, in effect,

"dampened" the vibrational motion of the CO_2 molecules, and caused them to reach their grounds states more quickly.

Presently, the lasing gas of nearly all CO_2 lasers is actually a mixture of CO_2, N_2, and He. In general, the CO_2 and N_2 are mixed in equal parts, each approximately 7-10% of the total gas mixture, with He making up the balance. Note, each laser design uses a slightly different mixing ratio which is empirically determined for the maximum efficiency of that particular system. *Lumonics recommends a* CO_2:N_2:He mixture ratio approximately equal to 1:1:8 be used with the Lasermark 901. The present mixture ratio of CO_2, N_2, and He for the Lasermark is 8.17%, 7.70%, and 84.13% respectively.

Before pumping the lasing gas with an electrical discharge, the Lasermark ionizes the gas mixture to uniformly accept the discharge energy. Fourteen spark plugs, seven on each side of the cavity, are fired simultaneously to bath the lasing gas with ultraviolet light. (Actually, many more frequencies of light are emitted which account for the bright purple flash, but only the UV is important for this purpose.) This intense burst of UV ionizes the lasing gas, or in other words, strips electrons away from their molecules, to form a conducting plasma. The conducting plasma uniformly distributes the discharge energy throughout the cavity for an efficient discharge pumping sequence.

In summary, the CO_2 is the lasing material of the lasing gas mixture. The lasing gas is irradiated with UV light which ionizes the mixture, preparing it for the

electrical discharge. The high-voltage discharge excites the N_2 molecules which collide with the CO_2 molecules causing them to reach higher vibrational energy levels. The CO_2 molecules relax almost immediately to lower energy states, releasing their excess energy through stimulated emission which is reinforced by optical feedback elements at both ends of the laser cavity. After lasing, the He and CO_2 molecules collide which dampens the vibrational energy of the CO_2 molecules and increases their rate of transition to the ground state. This completes one cycle of the energy-transition process shown in Figure 16 below.

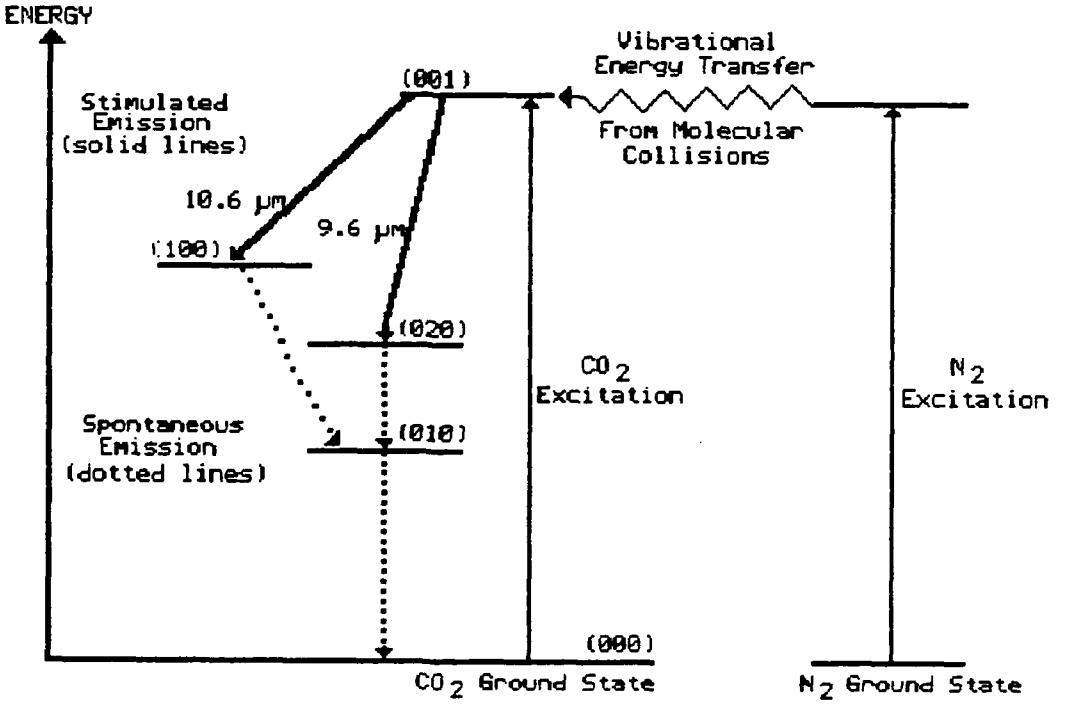

Figure 16. Energy transitions of a CO_2 molecule.

Q-switching and Efficiency

Recall that the quality factor of any device is the relationship between the device's ability to store and dissipate energy. The quality factor and a variety of Q-switch devices were described in the first chapter of this report for a number of different laser systems. In each case, a Q-switch was needed to postpone lasing until enough energy was "stored". This was normally accomplished by inducing a massive optical loss, like rotating or blocking a mirror, until a large population inversion was achieved. The simple beauty of the pulsed CO_2 laser is that no physical Q-switch is needed.

The Lasermark 901 has no Q-switch for two simple reasons:

(1) The pumping process is extremely fast and efficient
(2) Spontaneous emission from the upper level is extremely slow

Note that CO_2 molecules are pumped by molecular collisions rather than absorbing external radiation. The molecular-collision pumping scheme has two advantages. First, the molecular collisions occur very quickly, on the order of 10^8 to 10^9 collisions per second per mole [7]. Second, all of the collisions help boost the CO_2 molecules to higher energy states. If the CO_2 molecules were pumped by external radiation (through stimulated absorption), that same radiation would also help drain the upper energy levels (through

stimulated emission). Thus, the collision-pumping process is more efficient than radiation absorption. Finally, the spontaneous emissions from the upper energy levels are very slow, approximately 0.3 emissions per second per mole [7]. Therefore, the inversion develops faster than spontaneous emission can induce lasing. In effect, the pulsed CO_2 laser has a natural Q-switch.

The system efficiency of CO_2 lasers improved by several orders of magnitude in the early development years [3]. The first continuous-wave laser developed by Patel in 1964 was only 0.0001% efficient. The addition of nitrogen gas, later that same year, increased efficiency to 0.1%. In 1965, Patel applied a dc electrical discharge directly across the lasing gas mixture and boosted efficiency to 3%. A few months later, Patel cooled the lasing gas to -60°C which improved efficiency to 5%. The next big advance occurred later in 1965 when Patel discovered that adding helium gas increased efficiency above 6%. The ratio of the three-gas mixture and other conditions were then adjusted to marginally improve the operating efficiency of particular laser systems. The Lasermark 901 operates with an efficiency of approximately 15% [7]. Based on the energy levels of the CO_2 molecule, the maximum theoretical efficiency of a CO_2 laser operating at a wavelength of 10.6 microns is approximately 40% [3].

CHAPTER III: DAMAGE EFFECTS ON THIN ACRYLIC TARGETS

1. EXPERIMENTAL WORK

The overall objective of this experiment was to assess the damage inflicted on thin acrylic slides by pulsed infrared radiation fired from a CO_2 laser. Acrylic is a clear, lightweight, synthetic plastic made from acrylic acid, $H_2C{:}CHCOOH$. This target material was chosen for its ability to absorb beam energy in the infrared range and exhibit various degrees of damage from slight heat deformation to deep scoring.

Target damage effects were studied as the static air pressure surrounding the target area and the beam energy density were systematically varied. Target damage was objectively quantified by measuring the change in mass (mass loss) of each acrylic slide after being fired upon by the laser. Targets were placed in a test chamber which was evacuated from one to approximately 0.01 atmospheric pressure. The output beam was focused through an optical lens so that beam energy density could be varied by placing the target at different distances from the focal point of the lens.

Equipment

The following equipment was used during this experiment and is shown in Figure 17 below:

a. Lasermark 901 pulsed CO_2 laser
b. Test chamber
c. Two zinc-selenide (ZnSe) windows
d. Germanium (Ge) lens
e. Target holder
f. Mylar sheet attenuators
g. Energy meter
h. Helium-neon (HeNe) laser
i. Oscilloscope/Camera with high-speed Polaroid film
j. Mechanical pump
k. Mercury manometer
l. Particulate and dehumidifying filters
m. Bottle of medical-grade air
n. Bottle of CO_2:N_2:He mix
o. Scale
p. Microscope
q. 1/16-inch acrylic slides (targets)

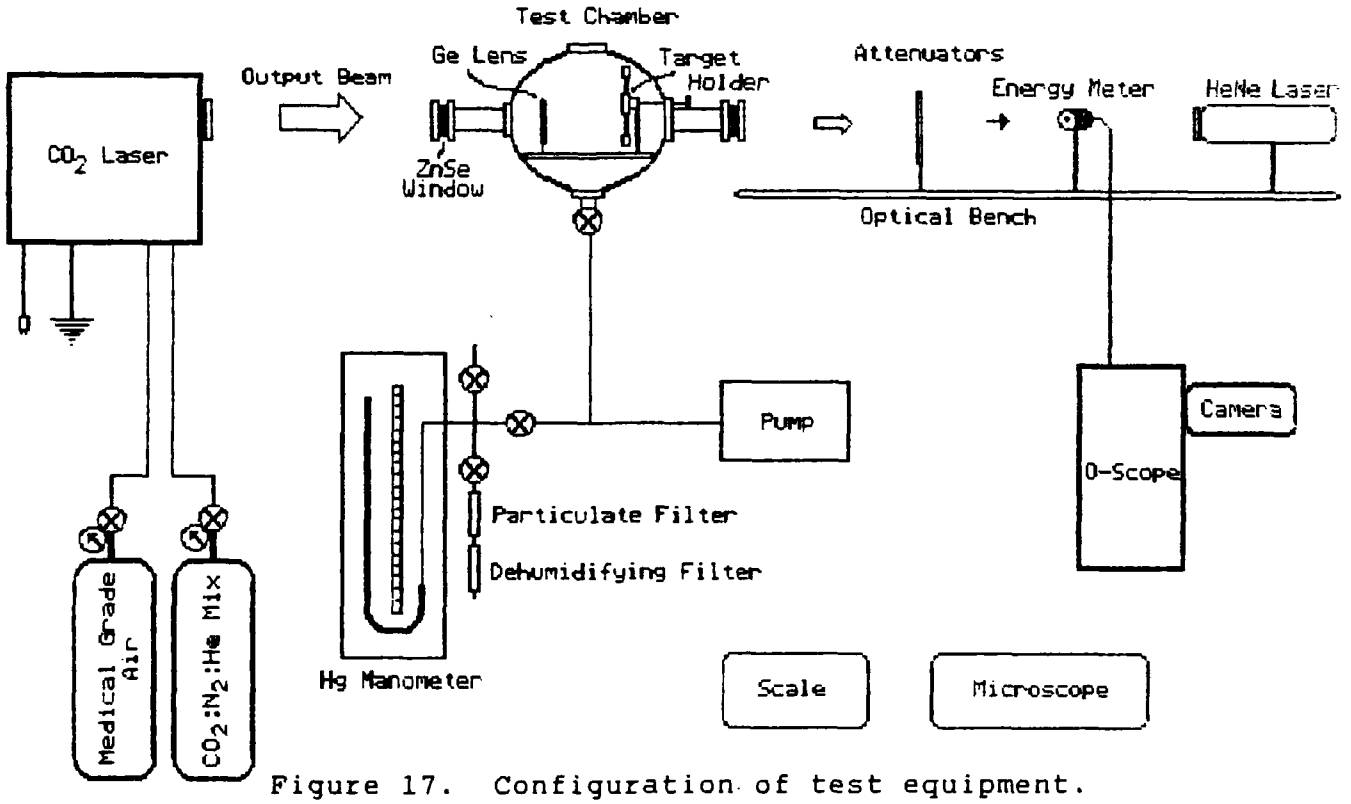

Figure 17. Configuration of test equipment.

a. Lasermark 901 pulsed CO_2 laser: The operating principles of the CO_2 laser are discussed thoroughly in Chapters I and II. A summary of the most significant performance specifications of the Lasermark 901 is given in Table 1 below. (See the Operator's Instruction Manual, reference [5], for a complete list of all specifications.)

Item	Specification
wavelength	10.6 microns
peak output energy	5 Joules
pulse duration	0.1-2 microseconds
average power	10 megawatts
firing rate	90 shots/minute

Table 1. Specifications of the Lasermark 901 CO_2 laser.

b. Test chamber: Cylindrical steel chamber, lying on its side (longitudinal axis), open at one end, 30 cm diameter, 45 cm long. Four ports located at the center of the side walls, normal to the longitudinal axis of the chamber. From the front view, the four portals are located 90 degrees apart at the 3, 6, 9, and 12 o'clock positions.

Standard steel nipple fittings are bolted to the 9 and 3 o'clock ports which serve as input and output (respectively) ports for the laser beam. Zinc-selenide optical windows are attached to the ends of the nipples. A valve is attached to the 6 o'clock port which leads to the pump and manometer. The 12 o'clock port

is fitted with a glass window and serves as a top-side viewing port.

The front face of the chamber is sealed with a transparent, 1½-inch thick, circular acrylic plate with a rubber gasket. Before reducing the air pressure inside the chamber, this plate is clamped to the front flange of the chamber with three 4-inch C-clamps. The plate is primarily used as an easy-access port to the target holder and germanium lens inside the chamber, yet can also be used for viewing during the experiment.

c. Zinc-selenide (ZnSe) windows: Two 2-inch diameter ZnSe plane windows were fitted to the input/output nipples. See Figure 18 for window specifications (reproduced from reference [6]). Note that each ZnSe window has a transmission coefficient of approximately 75 percent at 10.6 microns.

d. Germanium (Ge) lens: One 2-inch diameter Ge positive meniscus lens with a 10 cm focal length. This lens was used to focus the beam energy. See Figure 19 for complete lens specifications (reproduced from reference [6]). Note that the Ge lens has a transmission coefficient of approximately 45 percent at 10.6 microns.

Zinc Selenide ZnSe

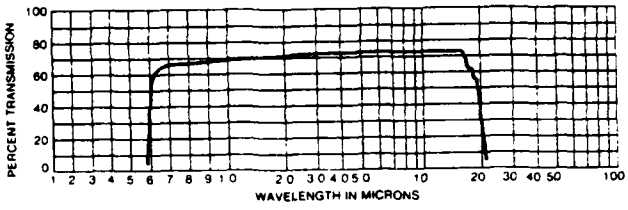

Zinc Selenide is used for infrared windows, lenses and prisms where transmission in the range 0.58 microns to 22 microns is desired. The refractive index is near 2.4. Zinc Selenide has a very low absorption co-efficient and is used extensively for high power infrared laser optics. It is non-hygroscopic.

Zinc Selenide is a relatively soft material and scratches rather easily. The low absorption of the material avoids the thermal runaway problem of Germanium. Zinc selenide requires an antireflection coating due to its high refractive index if high transmission is required.

Zinc Selenide Refractive Index vs. Wavelength

λμm	n	λμm	n	λμm	n
2.75	2.44	12.5	2.39	17.8	2.34
5.00	2.43	13.5	2.38	18.5	2.33
7.50	2.42	15.0	2.37	19.3	2.32
9.50	2.41	16.0	2.36	20.0	2.31
11.0	2.40	16.9	2.35		

Zinc Selenide Windows

Specifications	Standard	State-of-the-Art
Material:	ZnSe chemical vapor deposited	
Diameter Tolerance:	+0.000", −0.005" (+0.00mm, −0.13mm)	+0.0000", −0.0001" (+0.000mm, −0.0025mm)
Thickness Tolerance:	±0.010" (±0.25mm)	±0.0001" (±0.0025mm)
Clear Aperture:	90% Central Diameter	100% Central Diameter
Parallelism:	As Indicated	1 arc sec
Flatness:	As Indicated	1/400 λ @ 10.6 μm
Surface Quality: (scratch-dig)	20-10	5-2
Coating:	AR coating @ 10.6 μm. R < 0.5% per surface. Durability per MIL-M-13508C.	A variety of AR, filter and beam-splitter/partial reflector coatings are available. See Coatings Section.

Figure 18. Optical specifications of ZnSe plane windows.

Germanium Ge

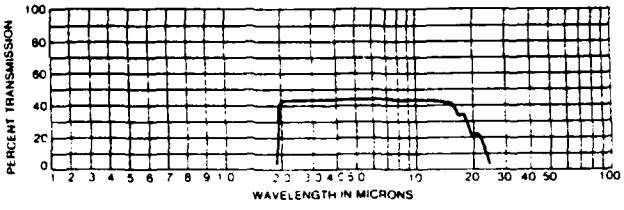

Germanium is used widely for lenses and windows in infrared laser systems. Its high index of refraction (greater than 4) makes it of particular interest. Its useful transmission range is from 2 to 12 microns. Germanium is opaque in the visible.

Germanium has the property of thermal runaway; that is, the hotter it gets the more the absorption increases. It is the most widely used material for infrared lasers.

Germanium Refractive Index vs. Wavelength

λμm	n	λμm	n	λμm	n
2.06	4.10	3.00	4.05	8.66	4.00
2.15	4.09	3.42	4.03	9.72	4.00
2.44	4.07	4.26	4.02	11.04	4.00
2.58	4.06	6.24	4.01	13.02	4.00

Germanium Positive Meniscus Lens

Specifications	Standard	State-of-the-Art
Material:	Ge Standard optical quality	
Design Wavelength:	10.6 μm	
Effective Focal Length (EFL):	±1% @ Design Wavelength	±0.1% or less
Clear Aperture:	90% Central Diameter	100% Central Diameter
Edge Thickness Variation (ETV):	0.001"	Up to 1" diam. 0.0001" Over 1" diam. 0.00001"
Diameter Tolerance:	+0.000", −0.005" (+0.00mm, −0.13mm)	+0.0000", −0.0001" (+0.000mm, −0.0025mm)
Thickness Tolerance	±0.010" (±0.25mm)	±0.0001" (±0.0025mm)
Standard Bevel:	0.020" ±0.010"	No bevel
Surface Irregularity:	1/40 λ @ 10.6 μm	1/400 λ @ 10.6 μm
Surface Quality: (scratch-dig)	20-10	5-2
Coating:	AR coating @ 10.6 μm. R <.5% per surface. Durability per MIL-M-13508C	AR coatings with R <.1% per surface. Broad-band AR coatings of high durability.

Figure 19. Optical specifications of Ge positive meniscus lens.

e. Target holder: Two thin circular steel plates, each 1/8 inch thick and 6 inches in diameter. The target holder has six, equally spaced, 2-inch diameter apertures (see below, Figure 20). Target slides are placed over the apertures and clamped between the two plates with three tightening bolts and securely held by O-rings. During operation, the target holder rotates (like the chamber of a six-shot revolver) placing a new slide in the laser's line of fire. The target holder is manually rotated by a knob outside the test chamber at the 3 o'clock port which is connected with a flexible shaft to a gear box inside the chamber.

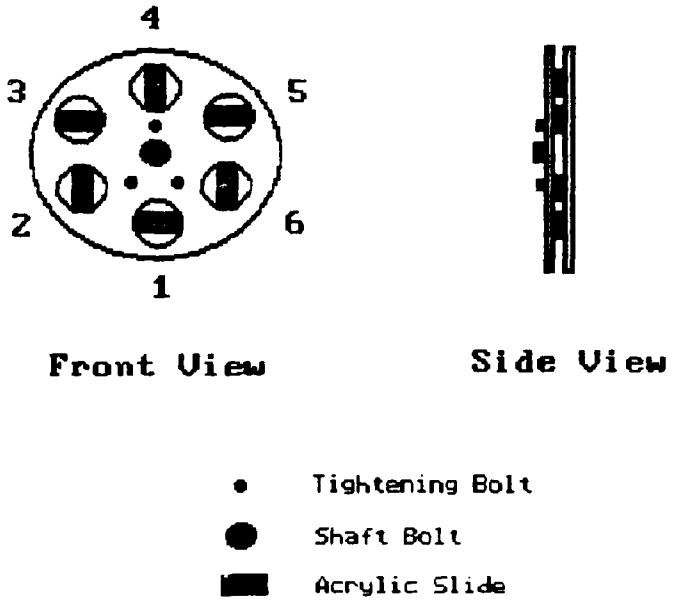

Figure 20. Target holder assembly.

f. Mylar sheet attenuators: Two thin mylar plastic sheets (overhead projector transparencies), each 0.20 mm thick and approximately 12 cm square. Placed in front of the energy meter to attenuate the beam energy and protect the meter from an input signal overload. Each sheet has a transmission coefficient of approximately 20 percent.

g. Energy meter: Thin-foil heat-flux meter which senses the amount of heat energy absorbed at the meter face and translates this into a proportional electrical output signal.

Parameter	Specification
responsivity	1 Joule/177 Volts
damage threshold	1 megawatt/cm^2
*window area	0.2 cm^2
**maximum energy	0.02 Joules

Table 2. Specifications of the energy meter.
* directly measured
** based on calculations given in the Procedure of Section 2.

h. Helium-neon laser: Typical low-energy, continuous-wave HeNe laser used to align all optical elements along beam path.

i. Oscilloscope/Camera: Standard laboratory two-channel oscilloscope with Polaroid camera mount. Camera loaded with Type 67, high-speed professional film, to record transient signal response from energy meter. Optimum

oscilloscope switch settings: 5 ms single-sweep, 0.05 Volts/cm.

j. Mechanical pump: Electric-motor driven piston pump lubricated with high-vacuum oil.

k. Mercury (Hg) manometer: Simple, U-shaped, Hg manometer hand-made from 10 mm (outer-diameter) Corning (glass) rubber hose and three Fisher (glass) stopcocks. Stopcocks and fittings lubricated with Apiezon grease. Manometer filled with slightly less than one pound of Hg. Absolute chamber pressure is read directly by measuring the heights of the two columns of Hg and computing the difference.

l. Particulate and dehumidifying filters: Two glass tube filters connected in tandem at one air inlet of the system (see Figure 17). First filter is filled with "indicating" desiccant which changes colors from blue to white as the desiccant crystals absorb moisture. Second filter is filled with "angel hair" (extremely thin glass fibers) that screen out particulates down to approximately 1 micron in length. Note: the particulate filter is behind the desiccant filter to catch any desiccant particulate.

m. Medical-grade air: High-pressure bottle of medical-

grade air which flows directly into the Lasermark 901 at a rate of 6 standard cubic feet per minute with a static pressure of 18 psig. This extremely pure air flows between three high-voltage electrode plates in the spark gap trigger switch to inhibit electrical arcing and laser misfiring.

n. CO_2:N_2:He gas: High-pressure bottle of the following gas mixture: 8.17% carbon dioxide/ 7.70% nitrogen/ 84.13% helium. The CO_2 gas serves as the laser medium. The N_2 supplies molecules that are easily excited to higher energy states and serves to mechanically pump CO_2 molecules through intermolecular collisions. The He gas dampens the vibrational energy of the CO_2 molecules (again through intermolecular collisions) and increases their rate of transition to the ground state.

o. Scale: Precise, electronic scale used to weigh the targets before and after they have been fired upon.

p. Microscope: Measuring microscope used to visibly examine the extent of damage to the target sample by measuring the damage area.

q. Acrylic slides: Thin, transparent acrylic slides, approximately 1x2 inches in length were used as targets. The slides were cut from a single sheet of

1/16-inch acrylic, each slide weighing 2 grams nominally. Damage was determined by measuring the amount of mass removed from the target after being fired upon; therefore, each slide was carefully weighed before and after each trial. To prevent inaccurate measurements, the slides were handled only with gloves and metal tweezers.

Construction

Designs for the first test chamber, test chamber stand, optical bench, lens holders, and target holder were submitted to the Physics Department Machine Shop on 5 Oct 87. The design for the Hg manometer was submitted to the Chemistry Department on 20 Nov 87. The unfilled glass manometer was delivered on 15 Dec 87 and mounted on a board. One pound of Hg, one desiccant filter, and one particulate filter were purchased from the Chemistry Department on 19 Jan 88.

The manometer was filled with Hg on 21 Jan 88. Since this was designed as an absolute-scale manometer, the air inside the manometer needed to be removed before pouring the Hg into the glass tubing. This was accomplished by sealing the 12 o'clock inlet with a lubricated stopcock, connecting the 3 o'clock inlet to the mercury bottle, and connecting the 6 o'clock inlet to the mechanical pump, see Figure 21.

The stopcock at the 3 o'clock position was removed and sealed with two rubber stoppers. A thin glass tube was

connected to the mercury bottle straw and inserted through a rubber stopper past the glass intersection of the manometer. A small C-clamp was placed on the plastic straw of the Hg bottle and the manometer system was evacuated.

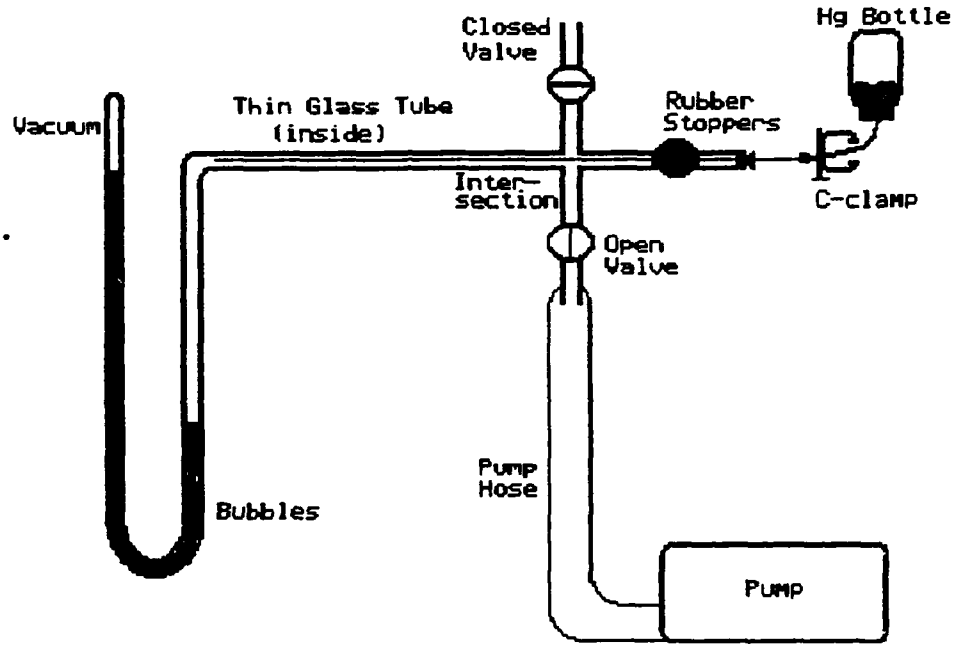

Figure 21. Equipment used to fill the manometer with Hg.

After approximately 15 minutes, the C-clamp was slowly released and the Hg entered the glass manometer. Since the Hg bottle itself contained a small air pocket above the Hg fluid at atmospheric pressure, the Hg quickly poured into the manometer along with a few small air bubbles. Fortunately, the Hg was new and clean, and these small bubbles were easily removed from the system by slowly tilting and

shaking the manometer. These actions caused the bubbles to slowly rise to the top of the right column and exit the system. The pump was switched off and disconnected.

Note that enough Hg must be poured into the manometer to establish at least a 760 mm difference in height between the left and right columns--the equivalent of one atmosphere of pressure. The curve at the bottom of the manometer and the extra height at the top of the left column must be taken into account. This extra height of tubing is necessary to determine if there is any overpressure of the system above one atmosphere. The small empty volume atop the left column of Hg must be completely evacuated for an accurate absolute pressure measurement.

Work had been progressing well with test chamber and other support equipment despite the holiday season. The test equipment was delivered and set up on 22 Jan 88. The initial test chamber was not the one shown in Figure 17, but a long rectangular box made from ½-inch acrylic. The large-area front and back access plates were bolted on and reinforced with ½-inch acrylic ribs. Rubber gaskets sealed components that could be removed and all corners were glued together for an airtight seal. In the original design, the optical bench was placed inside the chamber and a plano-convex ZnSe lens was added to recollimate the beam before reaching the outlet nipple.

Five days later, on 27 Jan 88, disaster struck during the first leak-check of the new test chamber. The pump was

connected to the test chamber and the chamber pressure reduced. As the pressure was SLOWLY being reduced, we noticed the chamber would creak and flex along the front and rear access plates. After correcting numerous small leaks around the access plate and nipple bolts, the chamber reached an internal pressure of approximately 150 mm Hg (note the ambient atmospheric pressure in the lab on that day was 742 mm Hg). At 9:32 p.m. the test chamber suddenly imploded totally destroying the chamber and manometer.

Miraculously, the laser, ZnSe windows, and parts of the target holder and optical bench were not damaged by the flying debris. Although the manometer was broken into many pieces near the valve intersection, atmospheric pressure quickly pushed the Hg up the left column and there was no Hg spill. Fortunately the Ge and ZnSe lens and energy meter were removed and safely stored during the leak check. It was determined that the equivalent of nearly 6,650 lbf was directed at the centroid of the front access plate at the moment the test chamber imploded. Stress fractures near the bolts developed and quickly propagated causing a catastrophic structural failure.

A second test chamber, target holder, and optical bench assembly was quickly designed the following week from undamaged components and parts of existing equipment in the Department that could be modified. A new manometer was ordered and delivered three weeks later. The new cylindrical chamber, made from ½-inch thick steel and a 1½-inch

acrylic front access plate, was completed on 28 Feb 88. The manometer was filled and the new chamber put together the next day.

On 29 Feb 88, the new system was successfully leak-checked down to 7 mm Hg--presumably the limit of the mechanical pump for an evacuated volume that large. This leak-check was almost non-climactic compared to the experience one month earlier. The chamber quietly pumped down and appeared to be quite solid. As the minor leaks were corrected, the front access plate would tightly compress against the rubber gasket from the increased difference in pressure. Our first indication that the chamber had been evacuated occurred when the C-clamps holding the front plate slipped off and fell to the ground. The second chamber provided easy access to the targets inside, was air-tight and structurally sound.

The remaining lab equipment was assembled to begin the experiment. The Ge lens and target holder were placed in the test chamber, and a HeNe laser was used to carefully align all the optical elements along the CO_2 laser beam path. All that was needed now was to begin taking data.

2. BEAM ENERGY AS A FUNCTION OF PRESSURE

The objective of this part of the experiment was to measure the change in beam energy as a function of chamber pressure. It is well known that infrared radiation is slightly attenuated as it passes through air. My goal was to determine if the change in beam energy was significant as the chamber pressure was reduced from one to 0.01 atmospheres.

Procedure

The Ge lens was removed from the test chamber and the energy meter was installed on the optical bench. The energy meter was connected to the oscilloscope. The laboratory oscilloscope was set to trigger a single sweep with one input signal from the meter. To prevent the oscilloscope from accidentally triggering from the laser's electromagnetic pulse, the meter-oscilloscope connection was shielded with Reynolds aluminum foil connected to ground.

Realizing the damage threshold for the meter was 1 MW/cm^2, a worst-case scenario was determined to protect the meter with an appropriate number of mylar attenuating sheets. In a worst-case scenario, the Lasermark could deliver all of its energy in the leading spike with a minimum pulse duration of 0.1 μs. The maximum energy the meter could absorb without damage would be the following:

$$\text{max energy} = (\text{damage threshold})\left[\begin{matrix}\text{min pulse duration}\\ \text{of Lasermark}\end{matrix}\right]$$

$$= (1\ \text{MW/cm}^2)(0.1\ \mu\text{s}) = 0.1\ \text{J/cm}^2$$

or

$$\text{max energy} = (\text{damage threshold})\left[\begin{matrix}\text{min pulse duration}\\ \text{of Lasermark}\end{matrix}\right]\left[\begin{matrix}\text{window}\\ \text{area}\end{matrix}\right]$$

$$= (1\ \text{MW/cm}^2)(0.1\ \mu\text{s})(0.2\ \text{cm}^2)$$

$$\boxed{E_{MAX} = 0.02\ \text{J}\quad \text{(entering the meter)}}$$

Throughout the experiment, the ZnSe windows would be in the beam path. In addition to the windows, an unknown number of mylar sheets might also be needed in the beam path to attenuate the beam energy and protect the meter. The transmission coefficient of the two ZnSe windows was found to be approximately 75 percent per window (see Figure 18). From earlier graduate work [8], the transmission coefficient of similar mylar sheets was found to equal 32.7 percent per sheet; therefore,

$$E_{MAX} = \left[\begin{matrix}\text{total transmission}\\ \text{coefficient}\end{matrix}\right]\left[\begin{matrix}\text{max output energy}\\ \text{of Lasermark}\end{matrix}\right]$$

$$0.02\ \text{J} = (0.75)(0.75)(0.327)^N\ \ (5\ \text{J})$$

where N = the number of mylar sheets

Then

$$0.327^N = \frac{(0.02\ J)}{(0.75)^2(5\ J)}$$

$$N = \frac{1}{\ln\ (0.327)} \quad \ln\left[\frac{(0.02\ J)}{(0.75)^2(5\ J)}\right]$$

$$N = 4.4 \text{ sheets}$$

From this calculation, five mylar sheets were required to protect the energy meter. This calculation assumes (1) the worst-case scenario, (2) the sheets of mylar used in reference [8] had the same coefficient of transmission as the mylar samples used in this experiment, and (3) no atmospheric attenuation.

The test chamber was evacuated and five mylar sheets were installed on the optical bench. The laser was fired, and the output signal from the meter observed on the oscilloscope. No output spike could be seen at the lowest scale. One sheet of mylar was removed, and the procedure repeated. A very small spike was observed at the lowest scale, but well below the energy damage threshold of 0.02 J of the meter. Two more mylar sheets were removed, one at a time, until a clear, easily measured spike was seen on the oscilloscope. With only two mylar sheets in place, the beam energy reaching the meter was still well below the damage threshold. Finally, it was determined that only one sheet of mylar was required to protect the meter in this configuration.

The beam energy was measured with the test chamber pressure at 6 mm Hg and one mylar sheet in place. A second mylar sheet was added and the energy measured. This procedure was repeated at atmospheric pressure, 737 mm Hg.

Results and Discussion

No noticeable change in energy was measured at the two pressure extremes. Note that the beam inlet to the chamber is separated from the outlet by only 65 cm, see Figure 22 below.

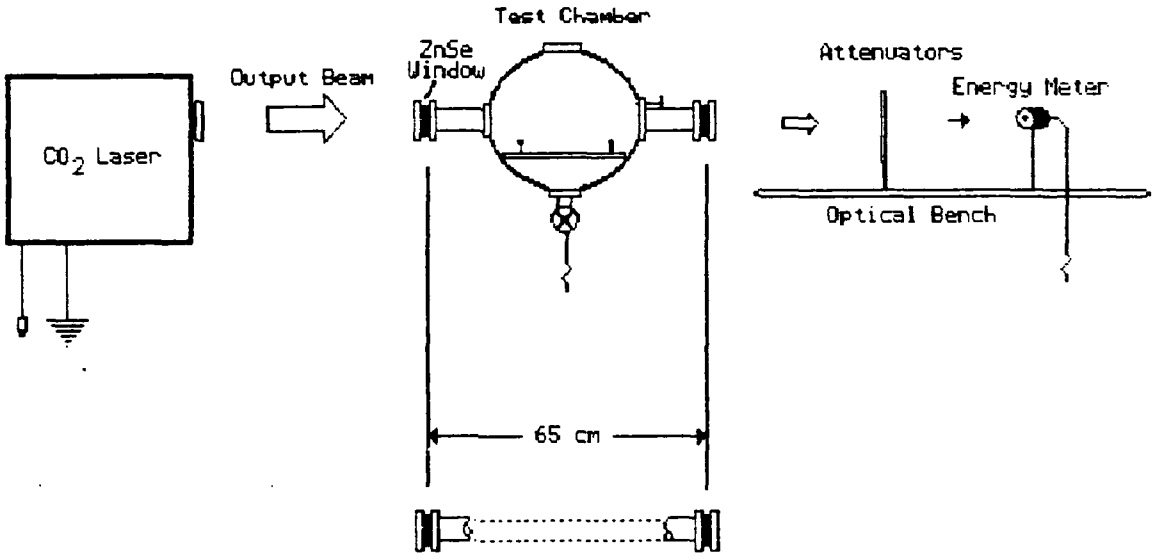

Figure 22. Illustration of the beam path.

Even though the measurements were taken at the two chamber pressure extremes, 6 and 737 mm Hg, the beam is passing through a linear column of air only 65 cm long. Even at atmospheric pressure, there simply is not enough air mass to significantly weaken the beam over this short distance. Therefore, the change in beam energy from atmospheric attenuation is not significant in this experiment.

The beam energy and transmission coefficient of the mylar sheets were found in the following manner:

$$\text{energy delivered} = \frac{\text{(energy measured)}}{\text{(total transmission coefficient)}}$$

$$\text{or} \qquad E = \frac{E_M}{T}$$

where

E_M = (o-scope measured)(o-scope setting)(meter response)
$T = (T_W)^N\ (T_T)^N$

and $(T_W)^N$ = transmission coefficient of N ZnSe windows
$(T_T)^N$ = transmission coefficient of N transparencies

In the first case

E_{M1} = (2.6 ± 0.1 cm)(0.5 V/cm)(1 J/177 V)

$E_{M1} = 7.3 \pm 0.3$ mJ at 6 and 737 mm Hg

$T_1 = (0.75)^2\ (T_T)^1$ for one transparency

In the second case,

E_{M2} = (2.6 ± 0.1 cm)(0.1 V/cm)(1 J/177 V)

$E_{M2} = 1.5 \pm 0.05$ mJ at 6 and 737 mm Hg

$T_2 = (0.75)^2\ (T_T)^2$ for two transparencies

Equating the two equations

$$E = \frac{E_{M1}}{T_1} = \frac{E_{M2}}{T_2}$$

$$\frac{T_2}{T_1} = \frac{E_{M2}}{E_{M1}}$$

$$\frac{(0.75)^2\ (T_T)^2}{(0.75)^2\ (T_T)^1} = \frac{1.47\ mJ}{7.34\ mJ}$$

$$T_T = 0.20$$

$T_T = 20\ \%$ | transmission coefficient for one transparency

Note that the value for the transmission coefficient of one transparency is close to 32.7 % measured by Ronk in his work [8]. Keep in mind, the transparencies used in Ronk's experiment were only 0.077 mm thick while those used in this experiment were 0.20 mm.

Returning to the fundamental equation for energy delivered:

$$E = \frac{E_M}{T} = \frac{E_{M1}}{T_1} = \frac{7.34\ mJ}{(0.75)^2(0.20)} = 0.065\ J$$

The energy delivered by the CO_2 laser measured in this experiment was substantially less than 0.75 ± 0.16 J given by Ronk in his work [8]. Note, however, Ronk changed the location of the meter many times, thoroughly mapping the beam area for "bright" and "dark" areas of energy. Since the goal of this experiment was to determine the relative change of energy as a function of chamber pressure, the

meter was not moved and may have been located in a "dark" area. Ronk's values are doubtedly closer to the true output energy of the laser.

3. MASS LOSS AS A FUNCTION OF FIRINGS

The objective of this part of the experiment was to measure the target mass loss as a function of the number of firings at a fixed pressure. The laser was fired in five separate firing sequences 10, 20, 30, 40, and 50 times at 737 mm Hg. In addition to this, the distance between the Ge lens and the target was varied from 5 to 15 cm to observe how an optical detonation near the target might change the mass loss. My goal was to determine the rate at which mass is removed from the target per firing and how this might be affected by inducing an optical detonation.

Procedure

A large sheet of 1/16-inch acrylic was cut into small rectangular slides, approximately 1x2 inches long. Each slide was carefully weighed with an electronic scale and recorded. Since a mass loss of only a few milligrams was expected at the low extreme of the experiment, the slides were never directly touched. Each slide was handled only while wearing gloves or using metal tweezers to eliminate the chance of depositing skin oils and moisture on the slides. If a slide was dropped, it was immediately replaced with a new sample.

One slip of heat-sensitive paper and five acrylic slides were inserted in the six apertures of the target

holder. The target holder was placed in the test chamber. Next, the Ge lens was positioned 5 cm from the first target. The test chamber was sealed at one atmosphere of pressure (738 mm Hg). One shot was fired at the heat sensitive paper to record the beam area at that target distance. The first acrylic slide (second target) was rotated into position and ten shots were fired at the approximate rate of 3 shots per 2 seconds (or 90 shots/minute). This procedure was repeated for 20, 30, 40, and 50 shots each for the four remaining slides. During each trial, the number of optical detonations per number of shots was counted and recorded.

The test chamber was opened and allowed to ventilate. The target holder was removed from the chamber and the acrylic slides removed from the holder. Each slide was visibly examined for damage, then weighed. One new slip of heat-sensitive paper and the original five acrylic slides were placed in the target holder. Note, the original slides were used again to streamline data acquisition. If new slides were used each time, initial masses would need to be weighed, etc. If the laser actually burned through the acrylic, a new slide would be used.

The Ge lens was positioned one centimeter farther away, the chamber sealed and the firing sequence repeated. This entire procedure was repeated for target distances from 5 to 15 cm in 1 cm steps (or -5 cm to +5 cm from the lens focal point, see Figure 23).

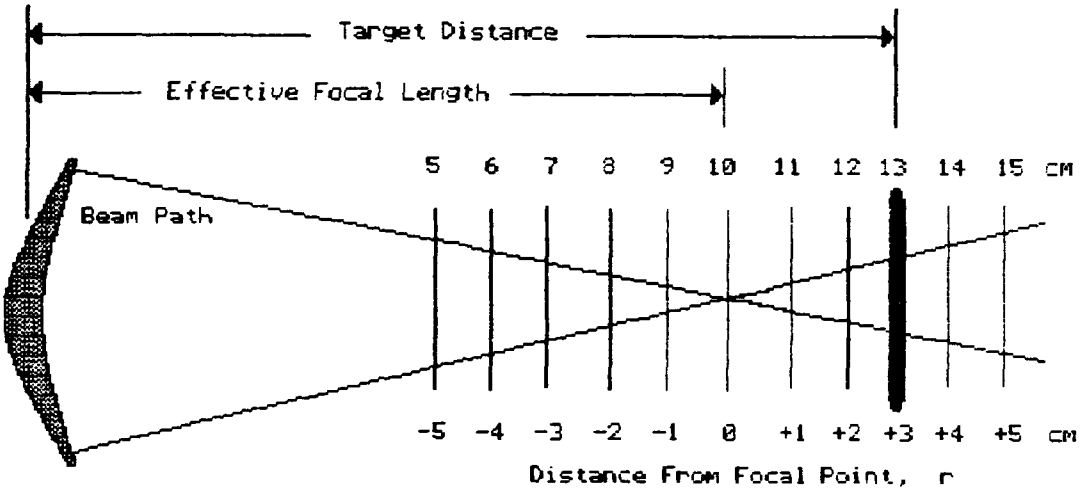

Figure 23. Target distance relative to lens focal length.

Results and Discussion

Data filling 11 tables, each with 28 measurements, were gathered. A computer program was written in GWBASIC 2.0 to load this data into random-access storage files on an MSDOS 2.0-compatible personal computer. A second, interactive program was written to plot this information in a variety of ways.

One might expect that the mass loss would generally increase with the number of firings. This research has shown that if the effects of optical detonations are ruled

out, this is true. However, as the target is moved closer to the effective focal length of the Ge lens, the possibility of an optical detonation increases and the mass loss decreases.

An optical detonation is a small "explosion" in the air near the focal point. This phenomena is caused by using a lens to focus all of the beam energy to a very small volume. A megawatt-class laser can produce sufficient optical intensity at the focal point to cause a very rapid ionization of the air, creating a high-density plasma. Electrons are almost instantaneously stripped from their atoms and a plasma develops, accompanied by a bright flash and shock wave (bang!). According to Siegman [1], the electron density in this plasma becomes so high that its index of refraction drops almost instantly to zero. The plasma then acts like a tiny, highly reflecting ball that scatters essentially all the laser energy out of the beam. Huston [7] has studied the optical detonations produced by the Lasermark in great detail. The reader is highly encouraged to read his thesis.

The next 11 pages of figures and tables illustrate the target mass loss as a function of firings. Note that the number of optical detonations per number of firings is indicated above the appropriate data point. The table below the figure has all the information shown in the figure, plus the target distance from the lens, chamber pressure, and beam area burned onto the heat-sensitive paper.

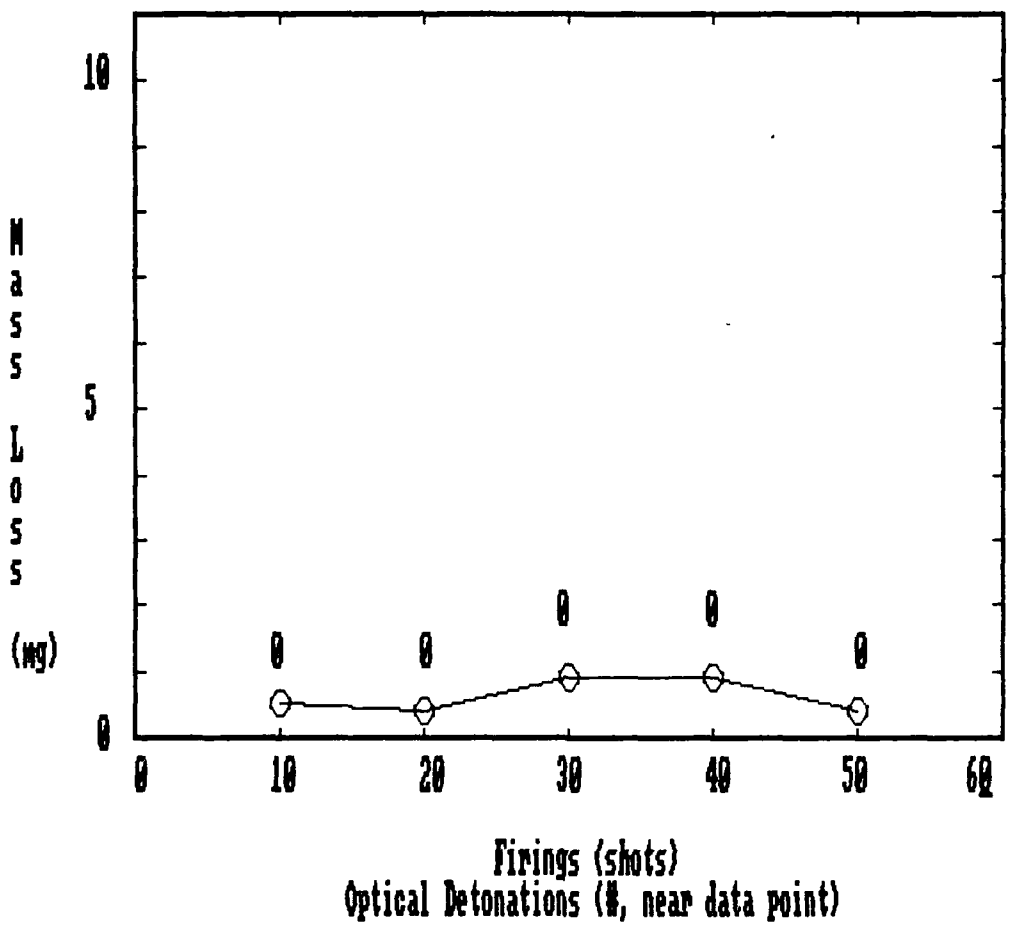

Figure 24. Mass loss versus firings at atmospheric pressure -5 cm from the focal point.

Target Distance	=	5	cm
Pressure	=	738	mm Hg
Beam Area	=	181.5	mm^2

Firings (shots)	Optical Detonations (#)	Initial Mass (grams)	Final Mass (grams)	Mass Loss (mg)
10	0	1.8008	1.8003	.4999638
20	0	1.913	1.9126	.3999472
30	0	2.2791	2.2782	.9000301
40	0	1.9436	1.9427	.9000301
50	0	2.1229	2.1225	.4000664

Table 3. Mass loss as a function of firings, -5 cm from the focal point.

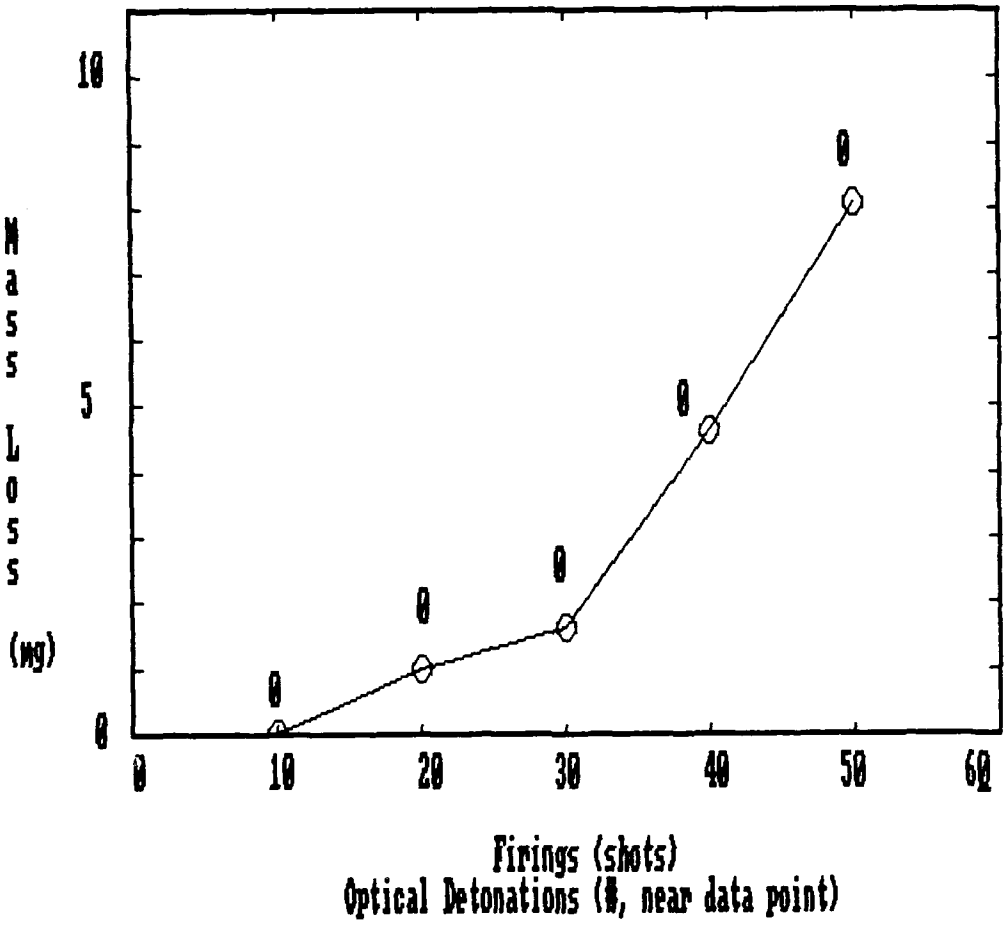

Figure 25. Mass loss versus firings at atmospheric pressure -4 cm from the focal point.

Target Distance	=	6	cm
Pressure	=	738	mm Hg
Beam Area	=	115.75	mm^2

Firings (shots)	Optical Detonations (#)	Initial Mass (grams)	Final Mass (grams)	Mass Loss (mg)
10	0	1.8003	1.8003	0
20	0	1.9126	1.9116	1.000047
30	0	2.2782	2.2766	1.600027
40	0	1.9427	1.9381	4.600048
50	0	2.1225	2.1144	8.100033

Table 4. Mass loss as a function of firings, -4 cm from the focal point.

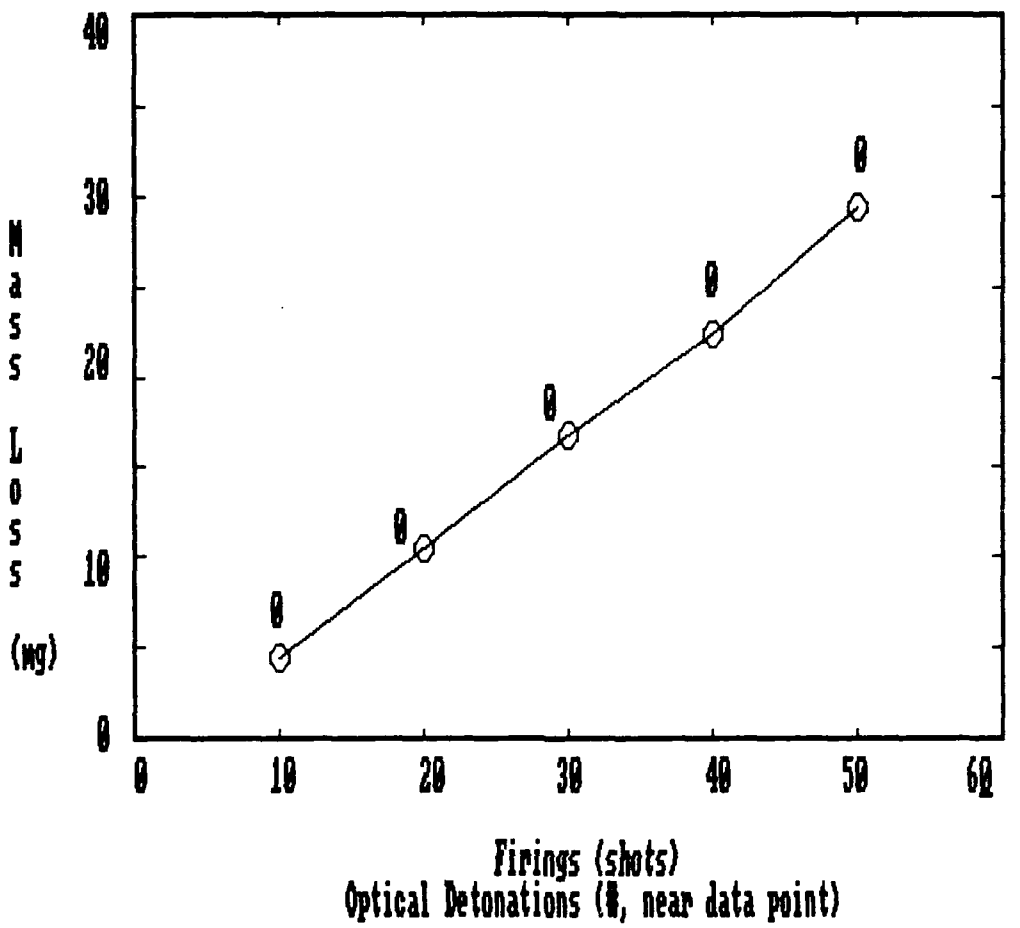

Figure 26. Mass loss versus firings at atmospheric pressure -3 cm from the focal point.

Target Distance	=	7	cm
Pressure	=	738	mm Hg
Beam Area	=	54.5	mm^2

Firings (shots)	Optical Detonations (#)	Initial Mass (grams)	Final Mass (grams)	Mass Loss (mg)
10	0	1.8003	1.7958	4.500032
20	0	1.9116	1.9012	10.39994
30	0	2.2766	2.2598	16.79993
40	0	1.9381	1.9158	22.30001
50	0	2.1144	2.085	29.39987

Table 5. Mass loss as a function of firings, -3 cm from the focal point.

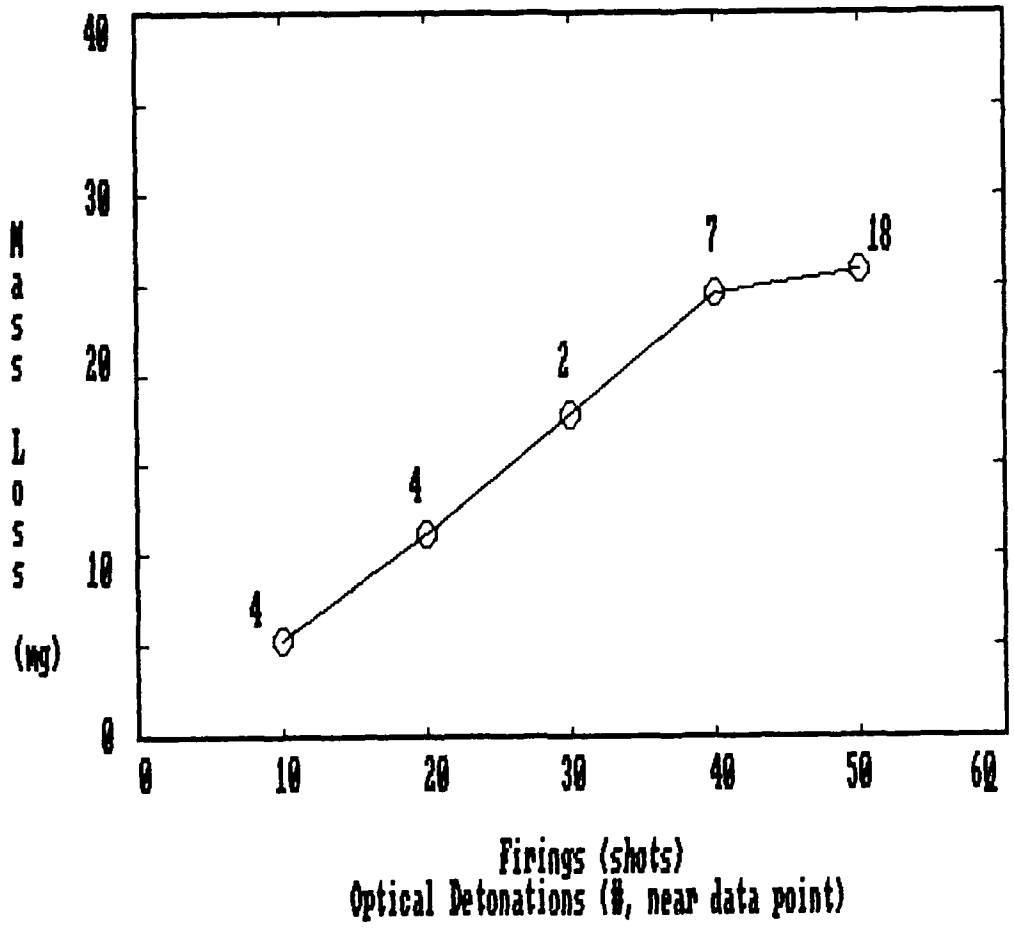

Figure 27. Mass loss versus firings at atmospheric pressure -2 cm from the focal point.

Target Distance	=	8	cm
Pressure	=	738	mm Hg
Beam Area	=	22.5	mm^2

Firings (shots)	Optical Detonations (#)	Initial Mass (grams)	Final Mass (grams)	Mass Loss (mg)
10	4	1.7958	1.7905	5.299926
20	4	1.9012	1.89	11.20007
30	2	2.2598	2.242	17.79985
40	7	1.9158	1.8913	24.50001
50	18	2.085	2.0592	25.79999

Table 6. Mass loss as a function of firings, -2 cm from the focal point.

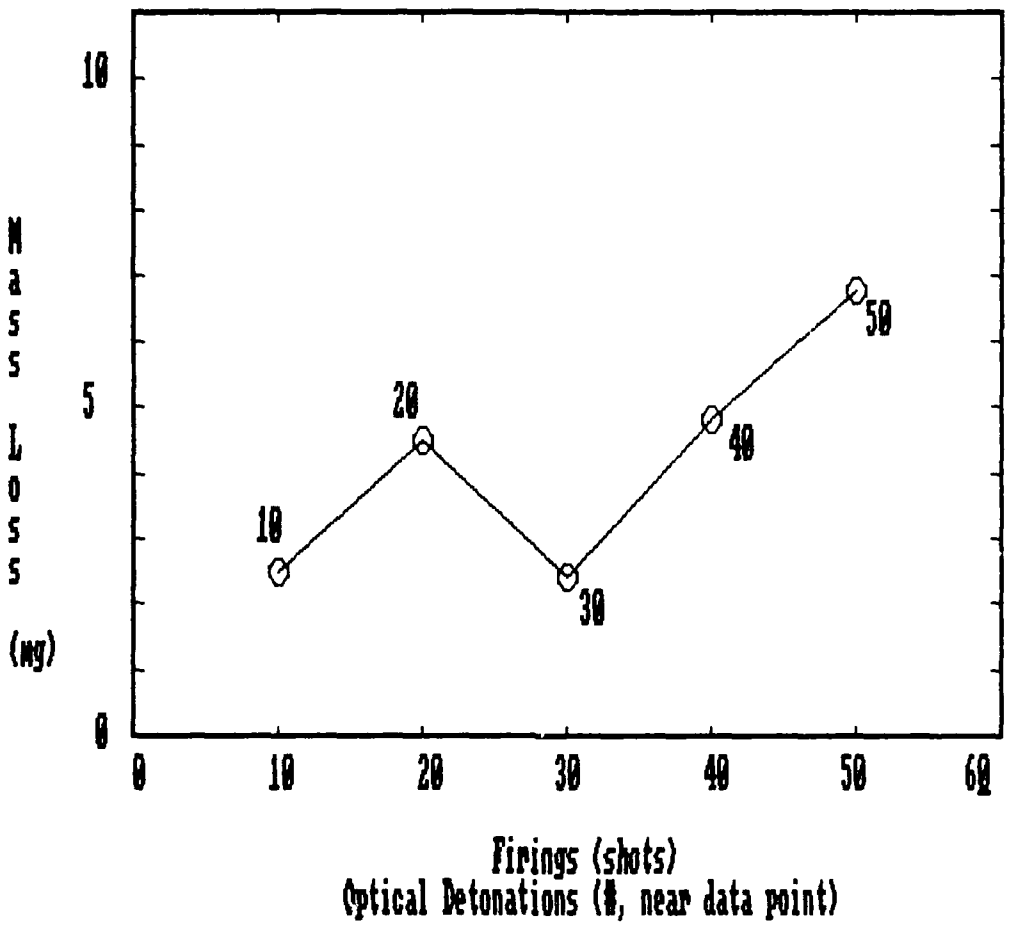

Figure 28. Mass loss versus firings at atmospheric pressure -1 cm from the focal point.

Target Distance	=	9	cm
Pressure	=	738	mm Hg
Beam Area	=	3.75	mm^2

Firings (shots)	Optical Detonations (#)	Initial Mass (grams)	Final Mass (grams)	Mass Loss (mg)
10	10	1.7905	1.788	2.500057
20	20	1.89	1.8855	4.500032
30	30	2.242	2.2396	2.40016
40	40	1.9642	1.9594	4.799962
50	50	2.0484	2.0416	6.799937

Table 7. Mass loss as a function of firings, -1 cm from the focal point.

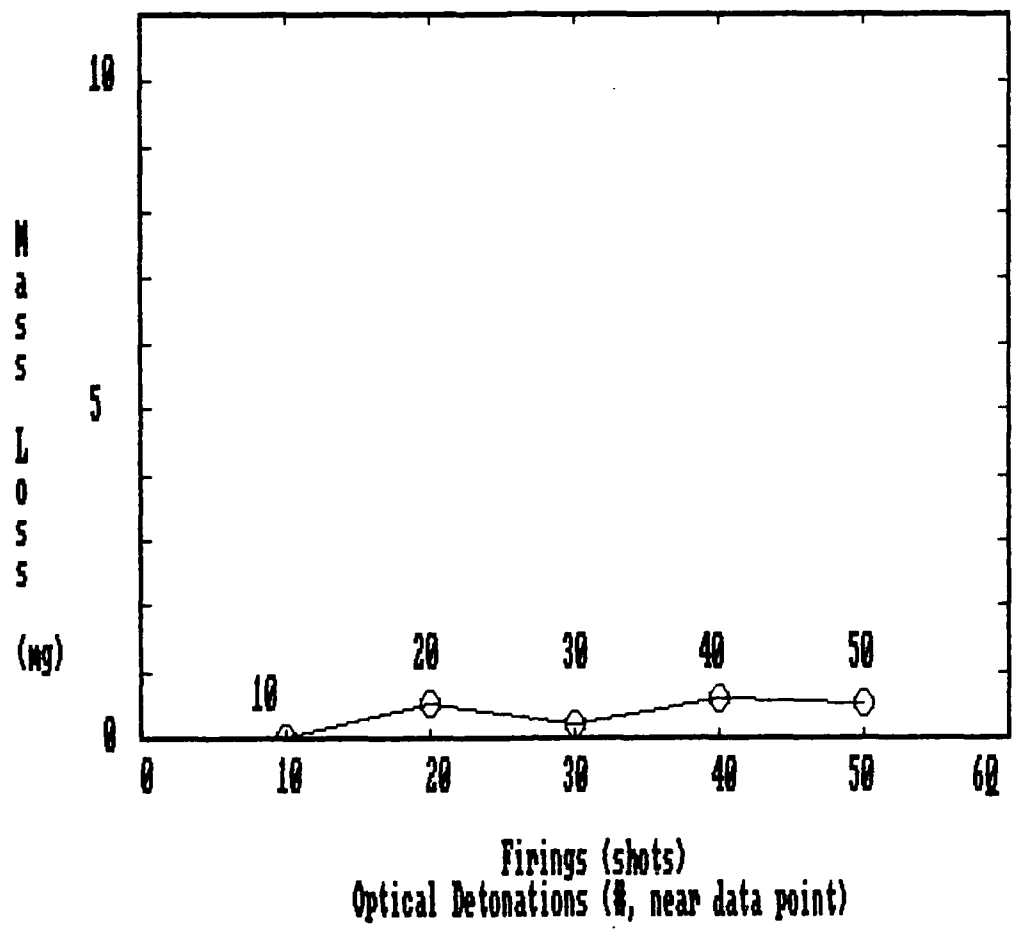

Figure 29. Mass loss versus firings at atmospheric pressure 0 cm from the focal point.

Target Distance	=	10	cm
Pressure	=	738	mm Hg
Beam Area	=	2.5	mm^2

Firings (shots)	Optical Detonations (#)	Initial Mass (grams)	Final Mass (grams)	Mass Loss (mg)
10	10	1.788	1.788	0
20	20	1.8855	1.885	.4999638
30	30	2.2396	2.2394	.2000332
40	40	1.9594	1.9588	.6000996
50	50	2.0416	2.0411	.4999638

Table 8. Mass loss as a function of firings, 0 cm from the focal point.

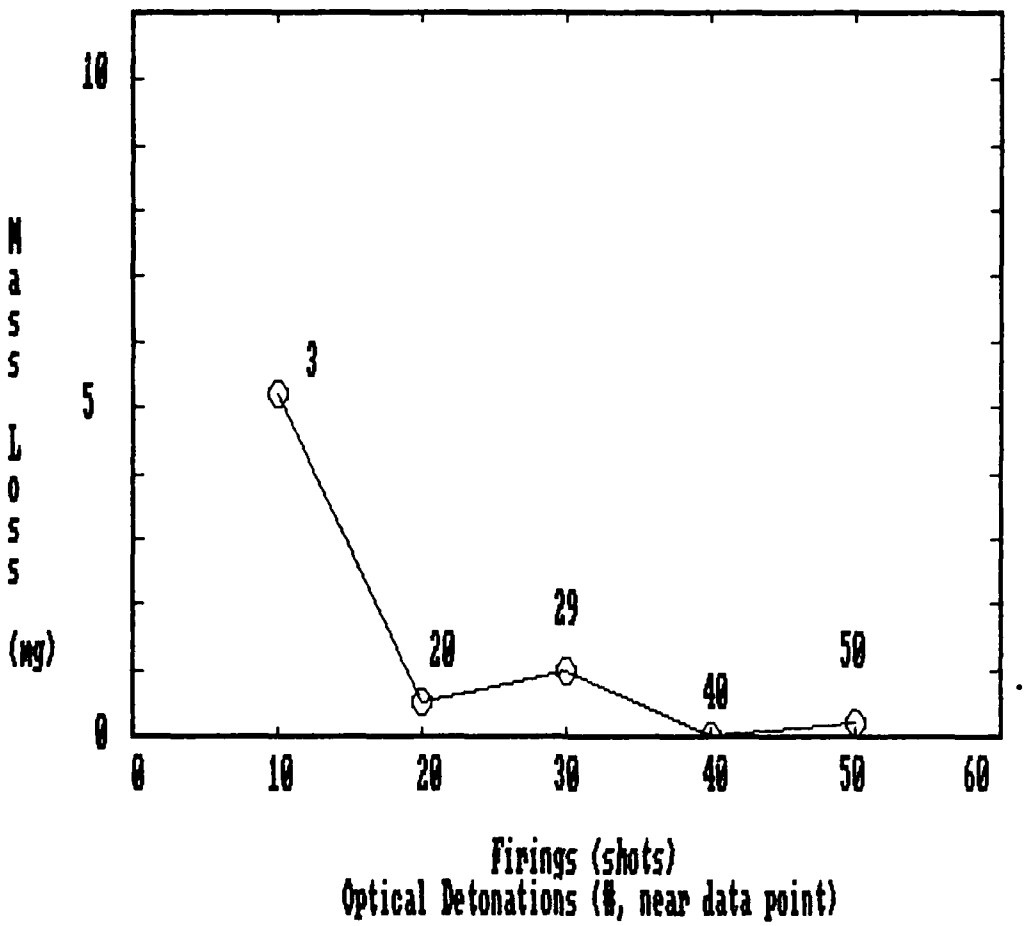

Figure 30. Mass loss versus firings at atmospheric pressure +1 cm from the focal point.

Target Distance	=	11	cm
Pressure	=	738	mm Hg
Beam Area	=	18	mm^2

Firings (shots)	Optical Detonations (#)	Initial Mass (grams)	Final Mass (grams)	Mass Loss (mg)
10	3	1.788	1.7828	5.200029
20	20	2.2575	2.257	.4999638
30	29	2.1908	2.1898	.9999275
40	40	2.0742	2.0742	0
50	50	1.8524	1.8522	.199914

Table 9. Mass loss as a function of firings, +1 cm from the focal point.

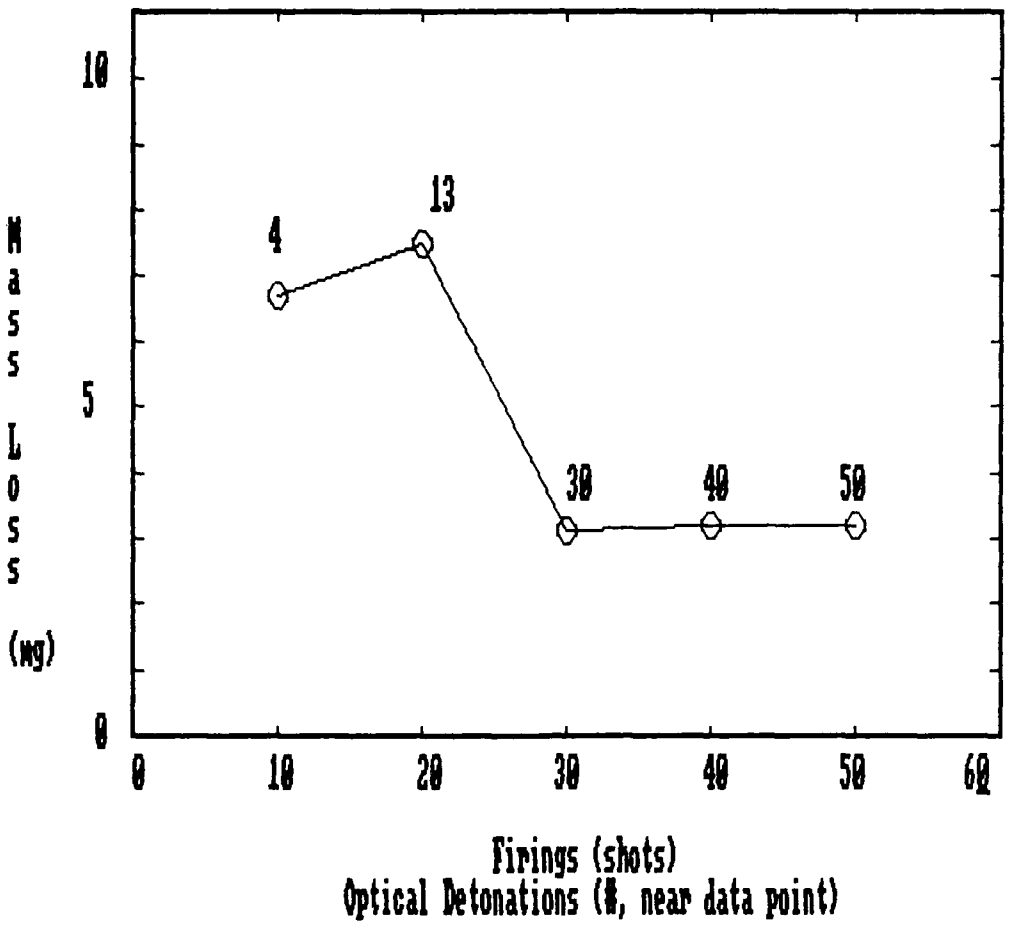

Figure 31. Mass loss versus firings at atmospheric pressure +2 cm from the focal point.

Target Distance	=	12	cm
Pressure	=	738	mm Hg
Beam Area	=	49.5	mm^2

Firings (shots)	Optical Detonations (#)	Initial Mass (grams)	Final Mass (grams)	Mass Loss (mg)
10	4	1.7828	1.7761	6.69992
20	13	2.257	2.2495	7.499933
30	30	2.1898	2.1867	3.099918
40	40	2.0742	2.071	3.199816
50	50	1.8522	1.849	3.200054

Table 10. Mass loss as a function of firings, +2 cm from the focal point.

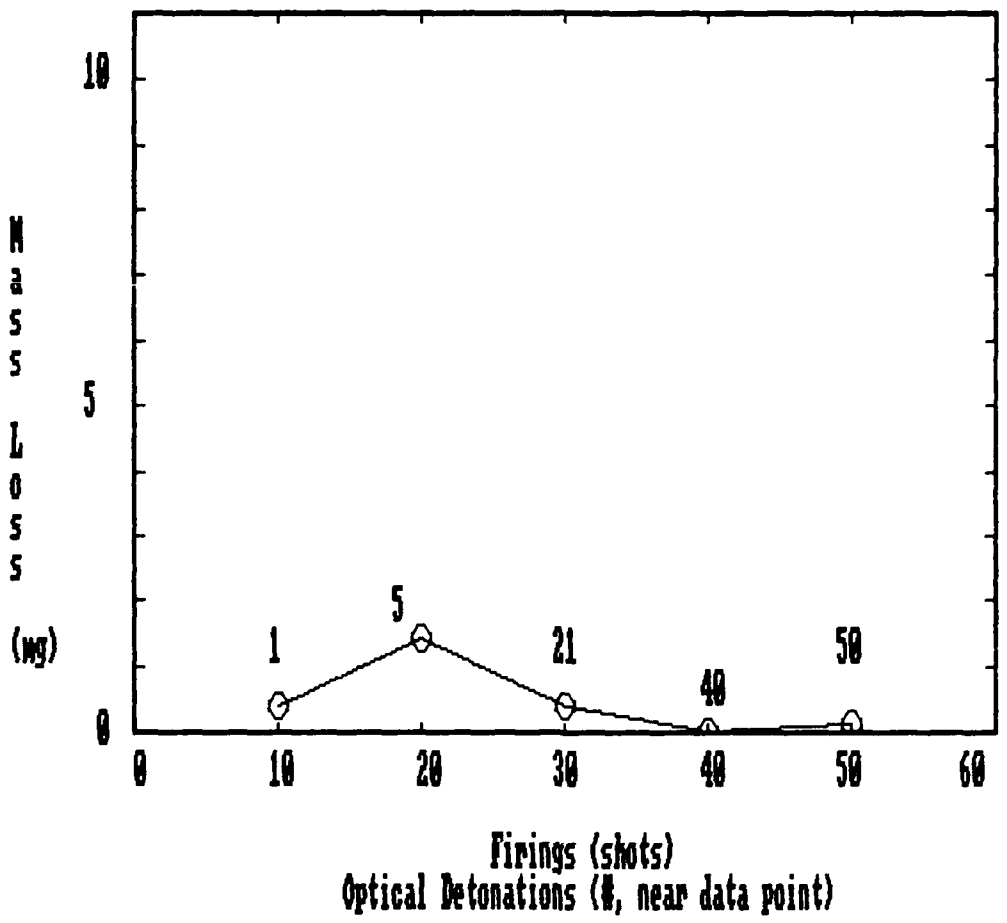

Figure 32. Mass loss versus firings at atmospheric pressure +3 cm from the focal point.

Target Distance	=	13	cm
Pressure	=	738	mm Hg
Beam Area	=	116	mm^2

Firings (shots)	Optical Detonations (#)	Initial Mass (grams)	Final Mass (grams)	Mass Loss (mg)
10	1	1.7761	1.7757	.4000664
20	5	2.2495	2.2481	1.399994
30	21	2.1867	2.1863	.4000664
40	40	2.071	2.071	0
50	50	1.849	1.8489	.1000166

Table 11. Mass loss as a function of firings, +3 cm from the focal point.

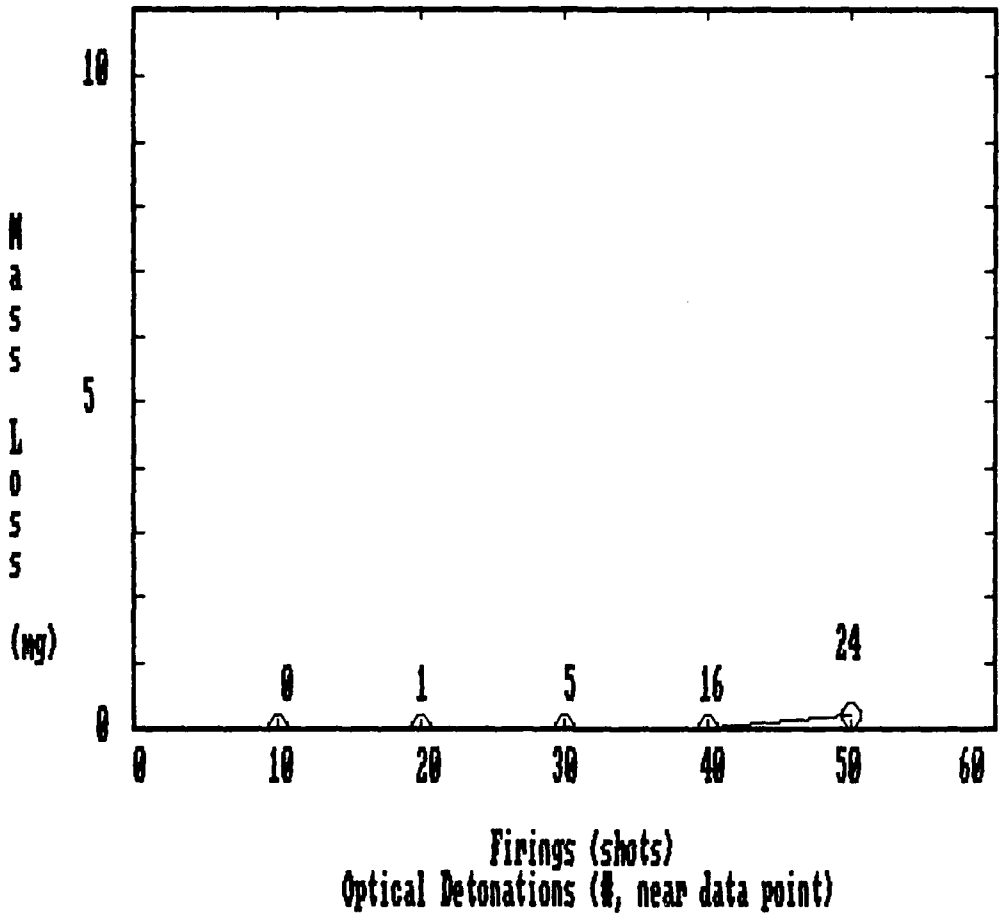

Figure 33. Mass loss versus firings at atmospheric pressure +4 cm from the focal point.

Target Distance	=	14	cm
Pressure	=	738	mm Hg
Beam Area	=	151.25	mm^2

Firings (shots)	Optical Detonations (#)	Initial Mass (grams)	Final Mass (grams)	Mass Loss (mg)
10	0	1.7757	1.7757	0
20	1	2.2481	2.2481	0
30	5	2.1863	2.1863	0
40	16	2.071	2.071	0
50	24	1.8489	1.8487	.199914

Table 12. Mass loss as a function of firings, +4 cm from the focal point.

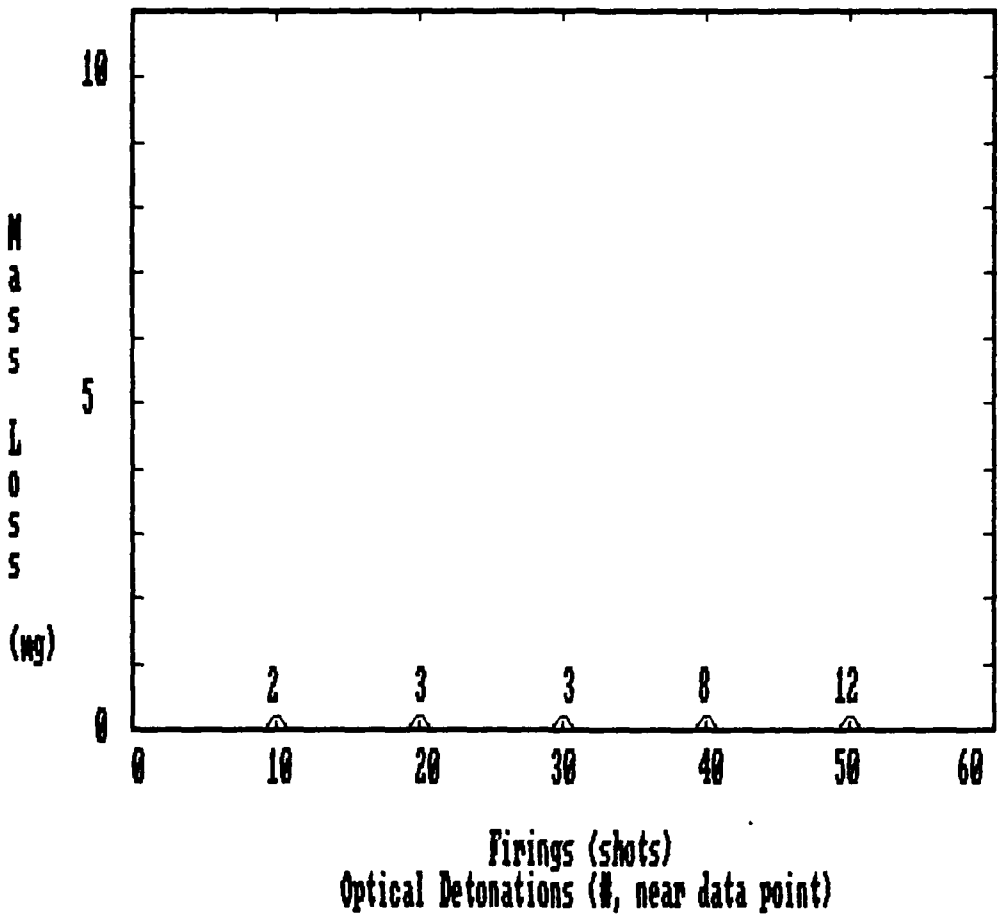

Figure 34. Mass loss versus firings at atmospheric pressure +5 cm from the focal point.

Target Distance	=	15	cm
Pressure	=	738	mm Hg
Beam Area	=	204	mm^2

Firings (shots)	Optical Detonations (#)	Initial Mass (grams)	Final Mass (grams)	Mass Loss (mg)
10	2	1.7757	1.7757	0
20	3	2.2481	2.2481	0
30	3	2.1863	2.1863	0
40	8	2.071	2.071	0
50	12	1.8487	1.8487	0

Table 13. Mass loss as a function of firings, +5 cm from the focal point.

The following observations were made while gathering and mapping the data:

a. When the targets are placed at extreme distances from the focal point (-5, +4, and +5 cm), there is no significant mass loss. At these distances, the acrylic slides experienced some heat deformation but no etching at the target area. There is probably insufficient energy density at these locations to heat the acrylic surface to a temperature high enough to cause mass loss through vaporization.

b. As the targets are moved closer to the focal point, there is significant mass loss until optical detonations occur. When the number of detonations approaches the number of firings, mass loss decreases drastically.

c. The number of optical detonations per number of firings definitely increases as the target approaches the focal point.

d. The mass loss increases linearly with the number of firings when there are no optical detonations. Note how the rate of mass loss, or the slope of the mass loss curve, is roughly independent of the target distance if optical detonations are ignored. The mass loss rate equals 0.62 ± 0.02 mg/shot.

e. When the target is moved closer to the focal point, the rate of mass loss, or slope, is nearly unchanged (if a qualitative adjustment is made to exclude the effects of optical detonations). This indicates that as beam energy density increases there is a damage trade-off at the target area. Examining the acrylic slides showed that as the damage area decreased, the damage deepness increased.

f. The acrylic slide was "burned through" after approximately 30 shots at -2 cm and 20 shots at -1 cm. No other penetrations occurred at 737 mm Hg.

g. No optical detonations were observed at the extreme ranges in front of the focal point at -5, -4, and -3 cm. However, there were sporadic detonations at symmetric positions behind the focal point at +3, +4, and +5 cm.

4. MASS LOSS AS A FUNCTION OF PRESSURE

The objective of the final part of this experiment was to measure the target mass loss as a function of chamber pressure. The laser was fired 30 times at each acrylic slide as the chamber pressure was varied from one to 0.01 atmospheres. In addition, the distance between the Ge lens and the target was varied from 5 to 15 cm to observe how an optical detonation near the target might change the mass loss. My goal was to determine the rate at which mass is removed from the target as pressure was reduced and how this might be affected by an optical detonation.

Procedure

Six acrylic slides were initially weighed, inserted into the target holder, and placed into the chamber as before. The Ge lens was positioned 5 cm from the first target. The test chamber was sealed and evacuated to 7 mm Hg.

Based on earlier runs, 30 was picked as the most effective minimum number of firings per target. The first acrylic target was rotated into position and 30 shots were fired. The second target was rotated into position and the pressure increased to 123 mm Hg by slowly bleeding filtered lab air into the system. Again, 30 shots were fired. This procedure was repeated for 241, 358, 474, and 604 mm Hg.

During each trial, the number of optical detonations per 30 shots was counted and recorded.

The test chamber was opened and ventilated. The targets were removed as before, examined, then weighed. The original six acrylic slides were placed in the target holder unless burned through. The Ge lens was positioned one centimeter farther away from the target, the chamber sealed, and the firing sequence repeated. This entire procedure was repeated for target distances from 5 to 15 cm in 1 cm steps.

Results and Discussion

Data filling 11 more tables, each with 33 measurements, were gathered. Another computer program was written to load the data into random-access storage files and plot this information.

This research has shown that mass loss generally decreases as pressure increases from 0.01 to one atmospheres. One might suspect that the beam energy is attenuated as more air fills the chamber. However, the first part of this experiment shows the beam energy does not measurably change across the short span of the test chamber at 6 and 737 mm Hg (see Section 2, this chapter). Therefore, something besides atmospheric attenuation must be considered.

Two possible causes for greater mass loss at lower pressures may be (1) the properties of the target material, and (2) the dynamics of the mass ejection from the material

surface. Most materials exhibit unexpected behavior in low pressures; the acrylic targets may undergo subtle changes, especially at the surface, which facilitates more damage. Also, reduced pressure means reduced air mass and fewer retarding collisions with the ejected target material. At higher pressures, the vaporized acrylic may not be able to clear the target area. Some of the sub-micron particulate may settle back on the slide and be included with the original mass when reweighed. Of course, optical detonations near the focal point complicate matters too. However, note that in cases where there were no optical detonations, or an equal number of detonations, mass loss can certainly be seen as a function of pressure.

The next 11 pages of figures and tables illustrate the target mass loss as a function of pressure. As before, the number of optical detonations are indicated in the figures above each data point. The tables list the information shown in the figure, plus the target distance, number of firings, and beam area.

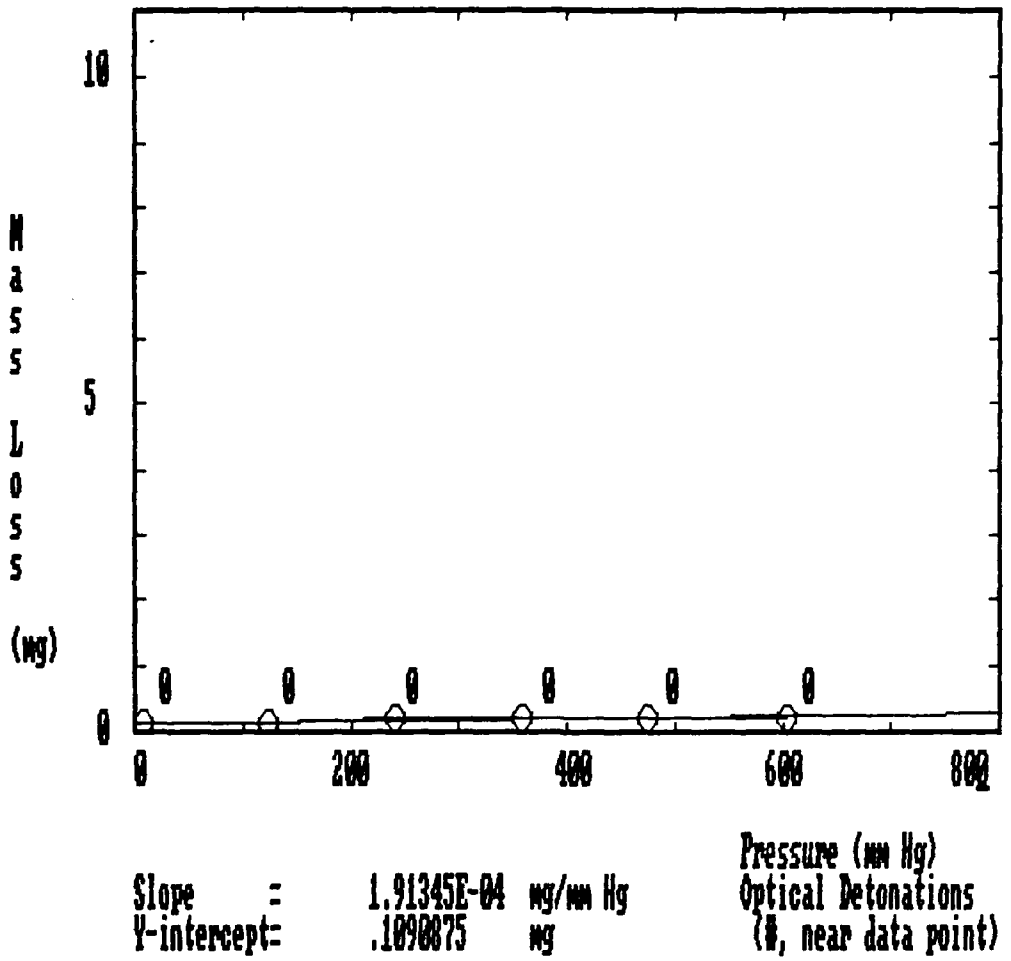

Figure 35. Mass loss versus pressure at 30 firings, -5 cm from the focal point.

Target Distance	=	5	cm
Firings	=	30	shots
Beam Area	=	181.5	mm^2

Pressure (mm Hg)	Optical Detonations (#)	Initial Mass (grams)	Final Mass (grams)	Mass Loss (mg)
7	0	2.0322	2.0321	.1001358
123	0	1.9147	1.9146	.1000166
241	0	2.0996	2.0994	.2000332
358	0	2.0058	2.0056	.2000332
474	0	1.9716	1.9714	.2000332
604	0	2.2668	2.2666	.2000332

Table 14. Mass loss as a function of pressure, -5 cm from the focal point.

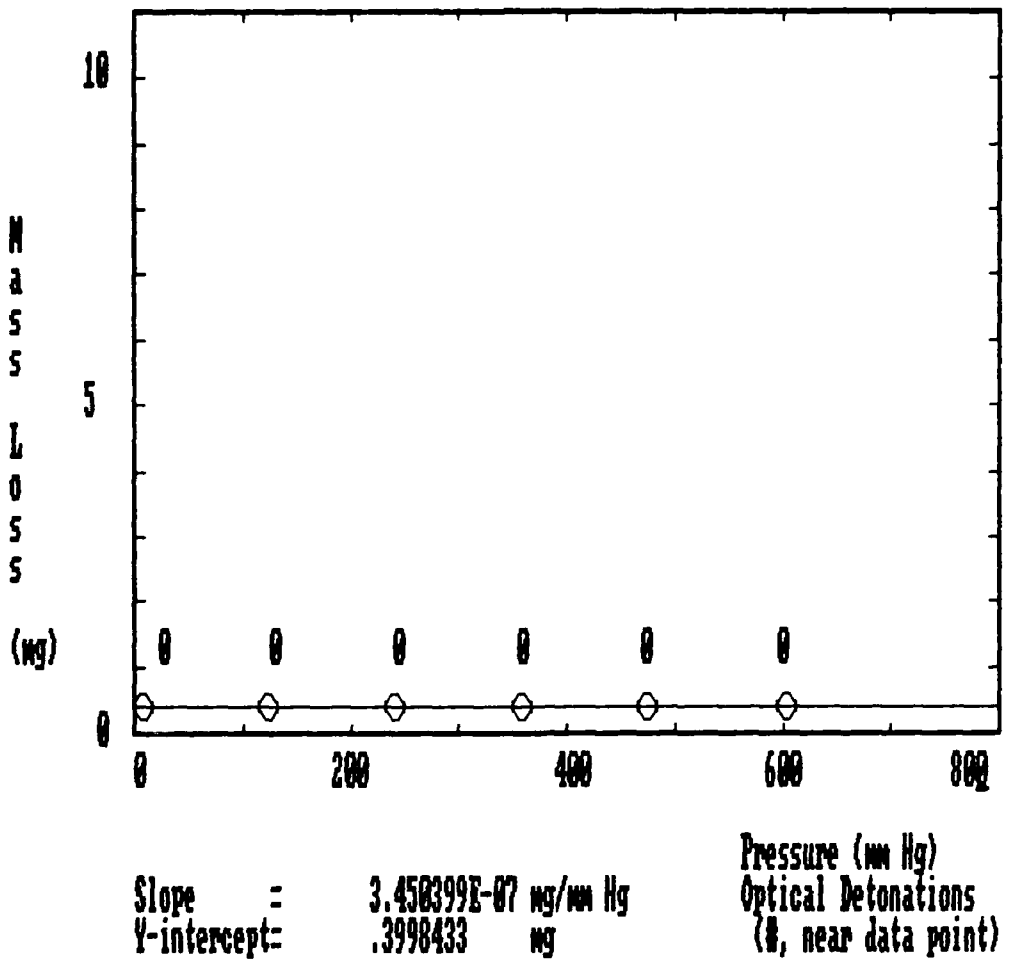

Figure 36. Mass loss versus pressure at 30 firings, -4 cm from the focal point.

Target Distance	=	6	cm
Firings	=	30	shots
Beam Area	=	115.75	mm^2

Pressure (mm Hg)	Optical Detonations (#)	Initial Mass (grams)	Final Mass (grams)	Mass Loss (mg)
7	0	2.0326	2.0322	.399828
123	0	1.9151	1.9147	.3999472
241	0	2.1	2.0996	.399828
358	0	2.0062	2.0058	.4000664
474	0	1.972	1.9716	.3999472
604	0	2.2672	2.2668	.4000664

Table 15. Mass loss as a function of pressure, -4 cm from the focal point.

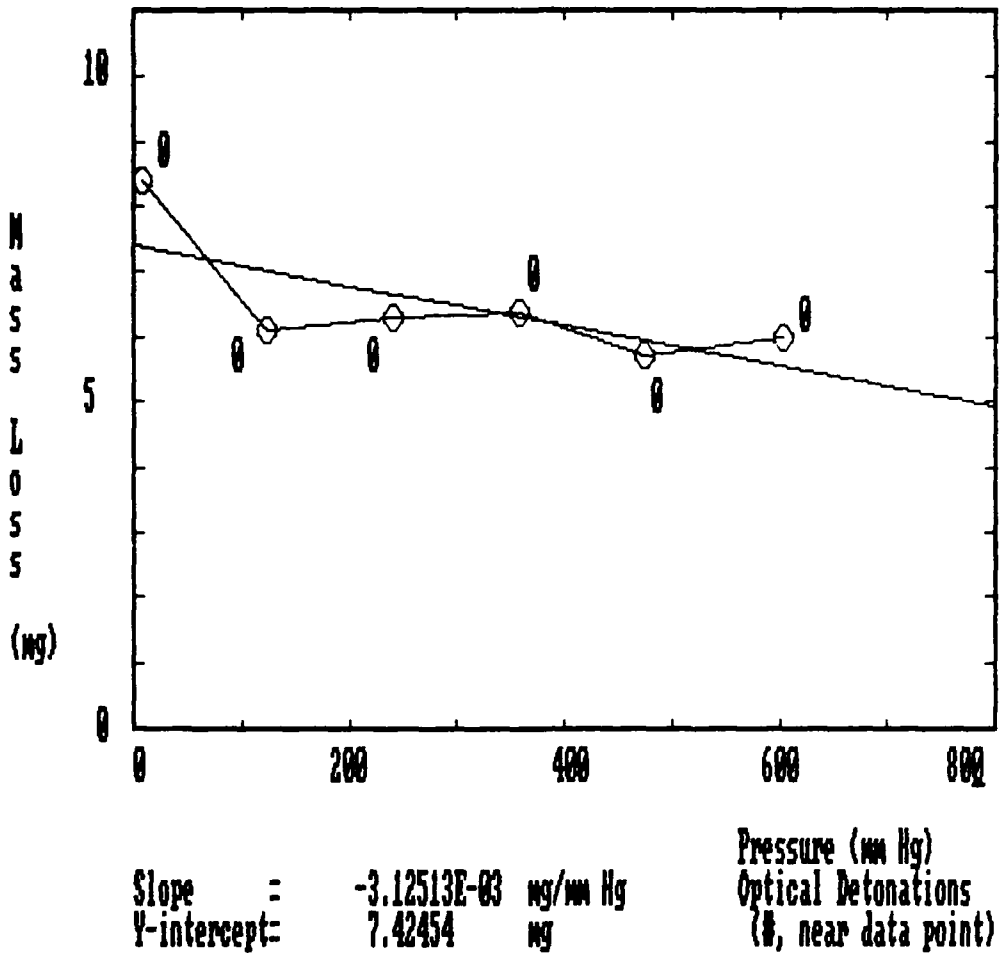

Figure 37. Mass loss versus pressure at 30 firings, -3 cm from the focal point.

Target Distance	=	7	cm
Firings	=	30	shots
Beam Area	=	54.5	mm^2

Pressure (mm Hg)	Optical Detonations (#)	Initial Mass (grams)	Final Mass (grams)	Mass Loss (mg)
7	0	2.041	2.0326	8.399963
123	0	1.9212	1.9151	6.100059
241	0	2.1063	2.1	6.300211
358	0	2.0126	2.0062	6.39987
474	0	1.9777	1.972	5.699992
604	0	2.2732	2.2672	6.000042

Table 16. Mass loss as a function of pressure, -3 cm from the focal point.

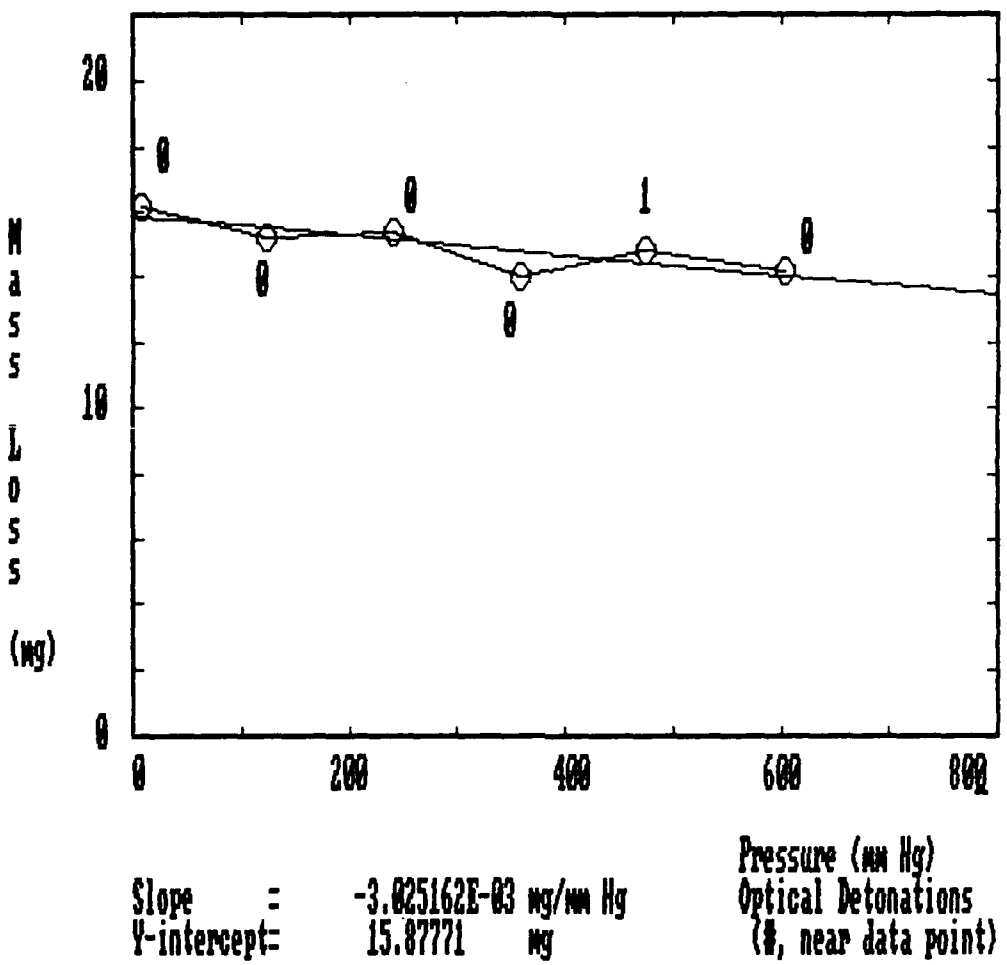

Figure 38. Mass loss versus pressure at 30 firings, -2 cm from the focal point.

Target Distance	=	8	cm
Firings	=	30	shots
Beam Area	=	22.5	mm^2

Pressure (mm Hg)	Optical Detonations (#)	Initial Mass (grams)	Final Mass (grams)	Mass Loss (mg)
7	0	1.9576	1.9414	16.19995
123	0	2.26	2.2448	15.1999
241	0	2.6954	2.68	15.39993
358	0	2.1418	2.1278	13.99994
474	1	2.0488	2.034	14.80007
604	0	2.3322	2.318	14.19997

Table 17. Mass loss as a function of pressure, -2 cm from the focal point.

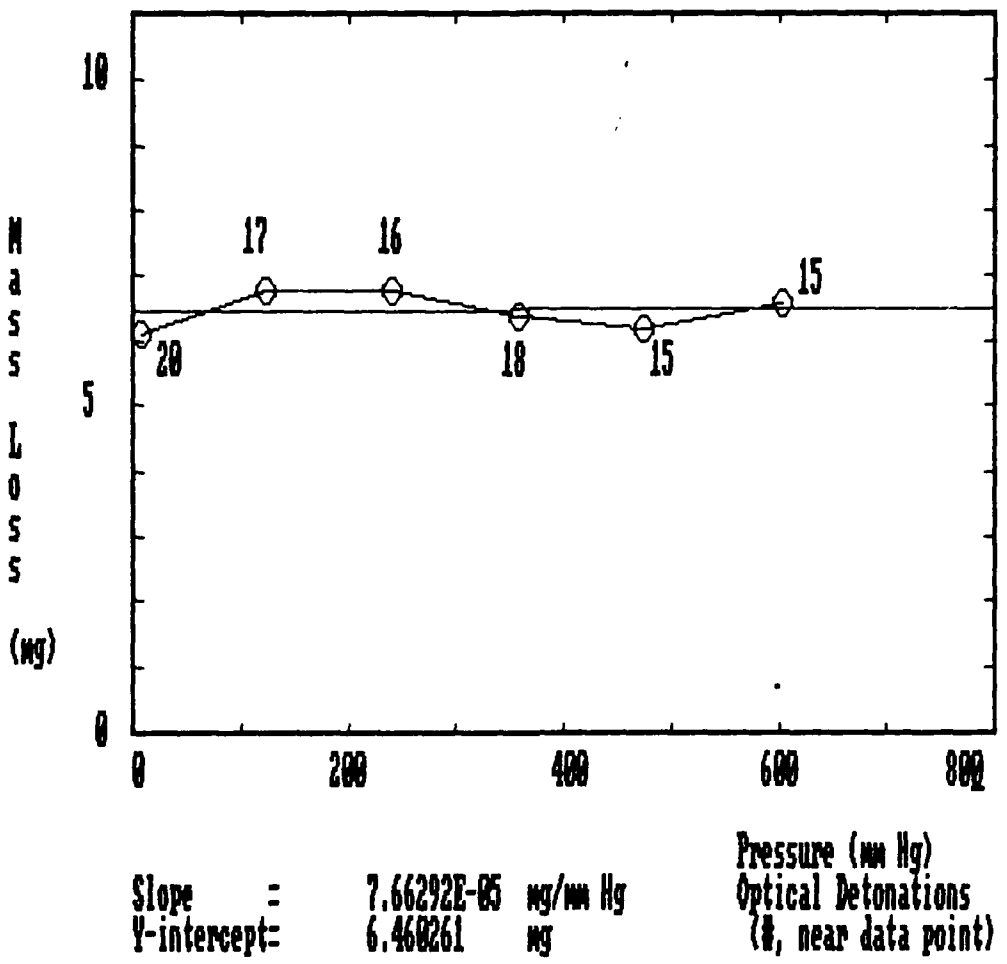

Figure 39. Mass loss versus pressure at 30 firings, -1 cm from the focal point.

Target Distance	=	9	cm
Firings	=	30	shots
Beam Area	=	3.75	mm^2

Pressure (mm Hg)	Optical Detonations (#)	Initial Mass (grams)	Final Mass (grams)	Mass Loss (mg)
7	20	1.9637	1.9576	6.100059
123	17	2.2668	2.26	6.799937
241	16	2.7022	2.6954	6.799937
358	18	2.1482	2.1418	6.400109
474	15	2.055	2.0488	6.200075
604	15	2.3388	2.3322	6.599903

Table 18. Mass loss as a function of pressure, -1 cm from the focal point.

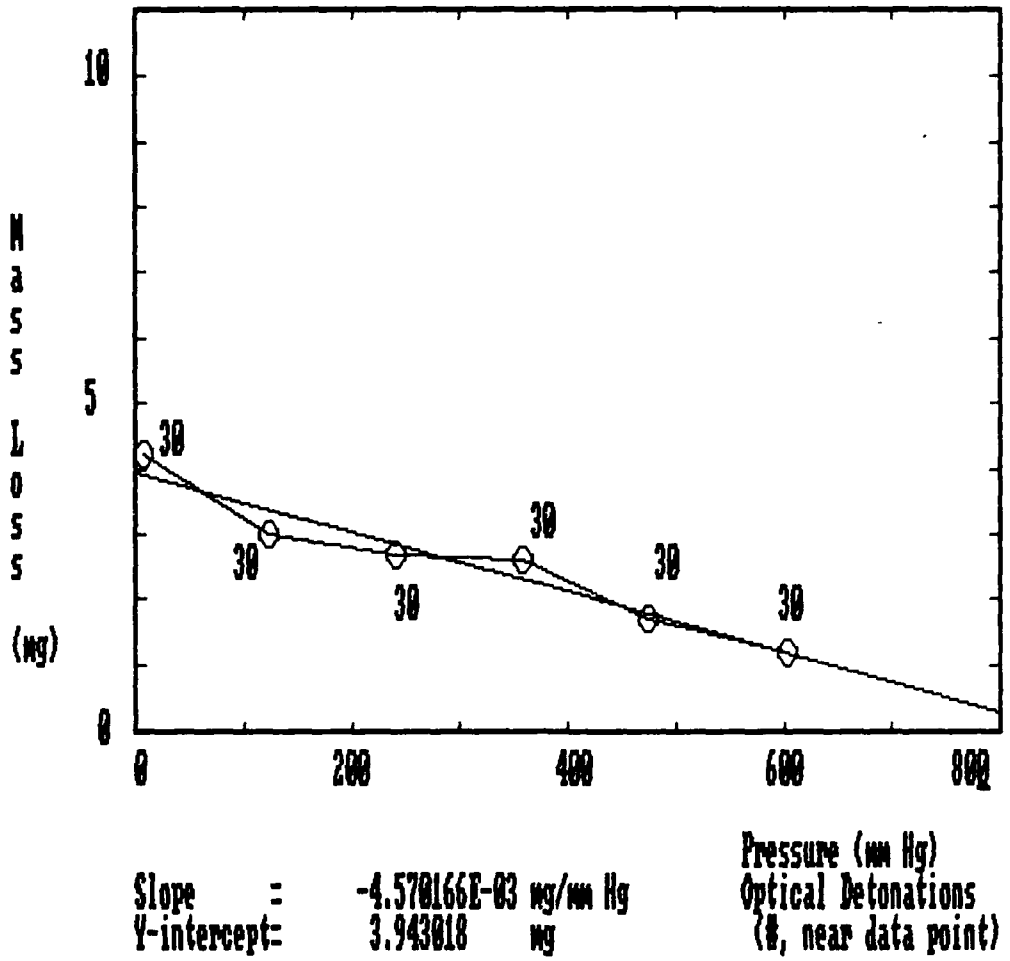

Figure 40. Mass loss versus pressure at 30 firings, 0 cm from the focal point.

Target Distance	=	10	cm
Firings	=	30	shots
Beam Area	=	2.5	mm^2

Pressure (mm Hg)	Optical Detonations (#)	Initial Mass (grams)	Final Mass (grams)	Mass Loss (mg)
7	30	2.1336	2.1294	4.199982
123	30	2.0439	2.0409	3.000021
241	30	1.9985	1.9958	2.699971
358	30	2.2539	2.2513	2.599955
474	30	2.55	2.5483	1.699925
604	30	2.0273	2.0261	1.199961

Table 19. Mass loss as a function of pressure, 0 cm from the focal point.

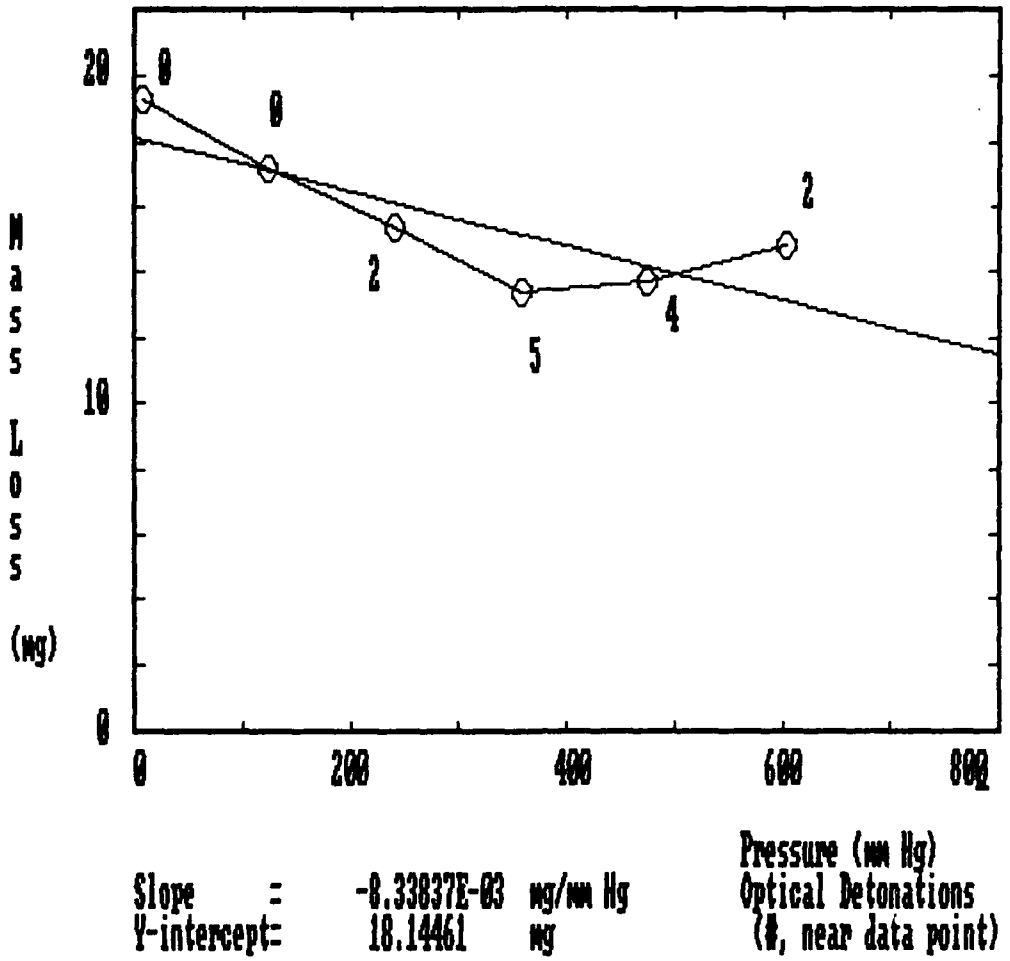

Figure 41. Mass loss versus pressure at 30 firings, +1 cm from the focal point.

Target Distance	=	11	cm
Firings	=	30	shots
Beam Area	=	18	mm^2

Pressure (mm Hg)	Optical Detonations (#)	Initial Mass (grams)	Final Mass (grams)	Mass Loss (mg)
7	0	1.8839	1.8646	19.3001
123	0	1.8468	1.8296	17.19999
241	2	2.0776	2.0622	15.39993
358	5	1.9414	1.928	13.40008
474	4	2.1743	2.1606	13.70001
604	2	1.8976	1.8828	14.80007

Table 20. Mass loss as a function of pressure, +1 cm from the focal point.

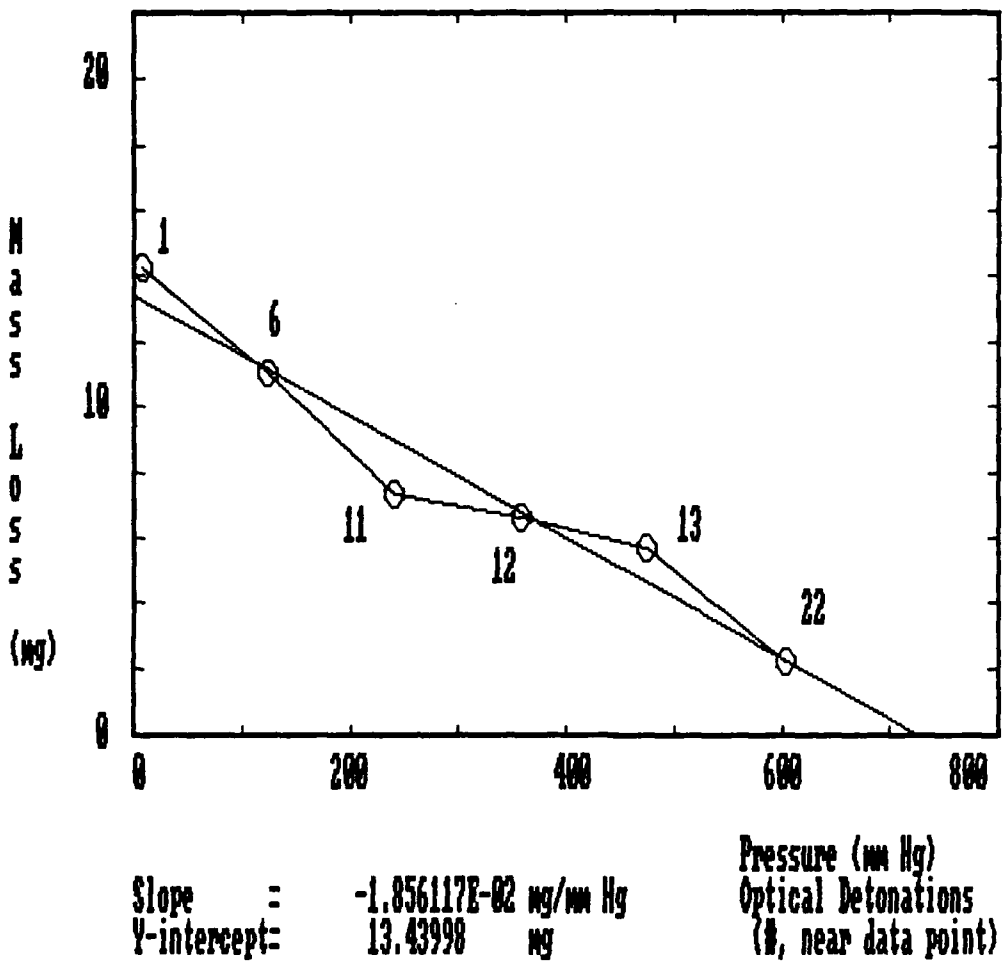

Figure 42. Mass loss versus pressure at 30 firings, +2 cm from the focal point.

Target Distance	=	12	cm
Firings	=	30	shots
Beam Area	=	49.5	mm^2

Pressure (mm Hg)	Optical Detonations (#)	Initial Mass (grams)	Final Mass (grams)	Mass Loss (mg)
7	1	1.8982	1.8839	14.29999
123	6	1.8578	1.8468	11.00004
241	11	2.0849	2.0776	7.2999
358	12	1.948	1.9414	6.599903
474	13	2.18	2.1743	5.700112
604	22	1.8998	1.8976	2.199888

Table 21. Mass loss as a function of pressure, +2 cm from the focal point.

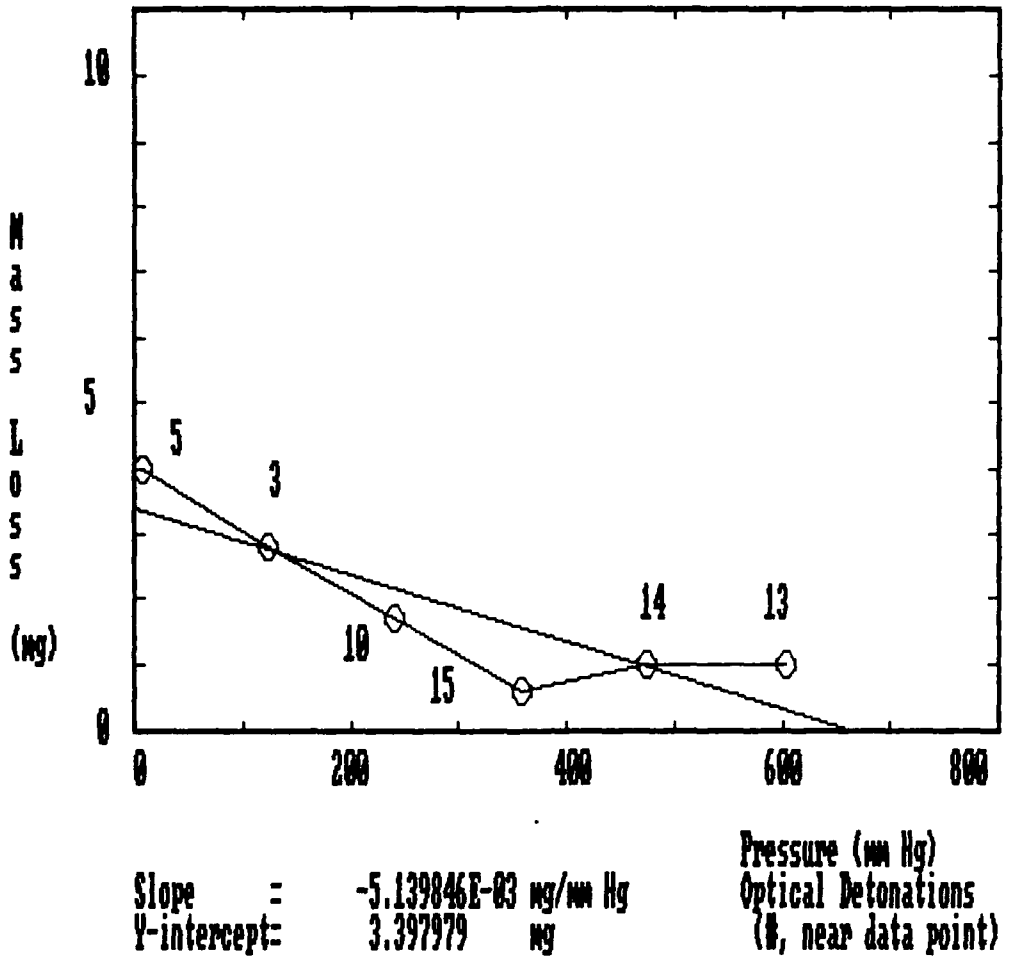

Figure 43. Mass loss versus pressure at 30 firings, +3 cm from the focal point.

Target Distance	=	13	cm
Firings	=	30	shots
Beam Area	=	116	mm^2

Pressure (mm Hg)	Optical Detonations (#)	Initial Mass (grams)	Final Mass (grams)	Mass Loss (mg)
7	5	1.9022	1.8982	3.999949
123	3	1.8606	1.8578	2.799988
241	10	2.0866	2.0849	1.700163
358	15	1.9486	1.948	.6000996
474	14	2.181	2.18	.9999275
604	13	1.9008	1.8998	1.000047

Table 22. Mass loss as a function of pressure, +3 cm from the focal point.

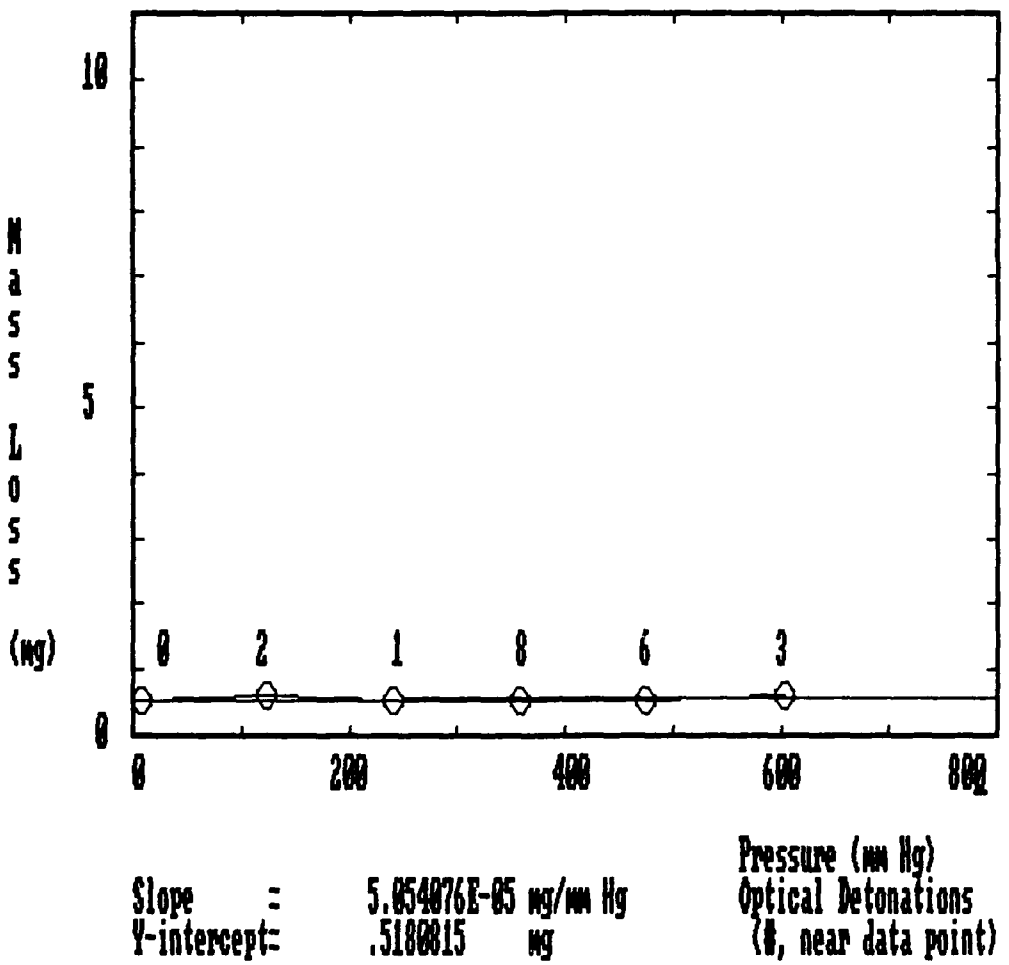

Figure 44. Mass loss versus pressure at 30 firings, +4 cm from the focal point.

Target Distance	=	14	cm
Firings	=	30	shots
Beam Area	=	151.25	mm^2

Pressure (mm Hg)	Optical Detonations (#)	Initial Mass (grams)	Final Mass (grams)	Mass Loss (mg)
7	0	1.9027	1.9022	.4999638
123	2	1.8612	1.8606	.5999804
241	1	2.0871	2.0866	.4999638
358	8	1.9491	1.9486	.4999638
474	6	2.1815	2.181	.4999638
604	3	1.9014	1.9008	.5999804

Table 23. Mass loss as a function of pressure, +4 cm from the focal point.

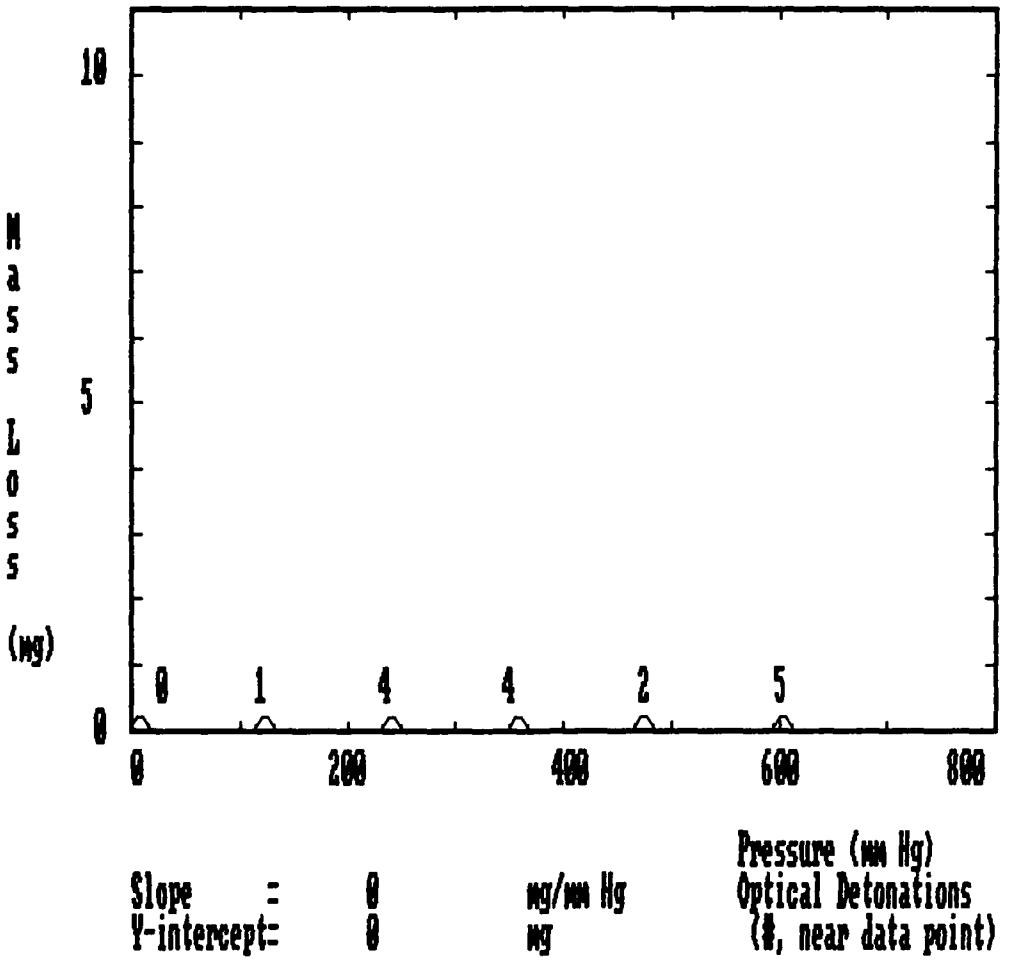

Figure 45. Mass loss versus pressure at 30 firings, +5 cm from the focal point.

Target Distance	=	15	cm
Firings	=	30	shots
Beam Area	=	204	mm^2

Pressure (mm Hg)	Optical Detonations (#)	Initial Mass (grams)	Final Mass (grams)	Mass Loss (mg)
7	0	1.9027	1.9027	0
123	1	1.8637	1.8637	0
241	4	2.0871	2.0871	0
358	4	1.9491	1.9491	0
474	2	2.1815	2.1815	0
604	5	1.9014	1.9014	0

Table 24. Mass loss as a function of pressure, +5 cm from the focal point.

The following observations were made while gathering and mapping the data:

a. When the targets are placed at extreme distances from the focal point (-5, -4, +4, and +5 cm), there is no significant mass loss. At -5 and +5 cm, the acrylic slides experienced only slight heat deformation at all pressures. At -4 and +4 cm, very slight etching was noted.

b. As the targets are moved closer to the focal point, there is significant mass loss which decreases as pressure increases.

c. The mass loss decreases linearly as pressure increases. When there are no optical detonations, or an approximately equal number of detonations, the data fit a straight line fairly well. If there is a disproportionate number of optical detonations at various pressures, the data pattern is much more scattered.

d. The number of optical detonations per number of firings definitely increases as the target approaches the focal point.

e. No optical detonations were observed at the extreme ranges in front of the focal point at -5, -4, and

-3 cm. However, there were sporadic detonations at symmetric positions behind the focal point at +3, +4, and +5 cm.

f. The optical detonations themselves appeared quite different at various pressures and target distances.

At atmospheric pressure, an optical detonation resembles a blue-white flash in the shape of a sphere, or ellipsoid. Huston mapped the optical detonations of the Lasermark [7] and discovered that the shape of the plasma cloud depended on how close the target is to the focal point of the lens. Optical detonations always occur very near the focal point; yet if the target is placed just ahead of the focal point, say from -1 to 0 cm, a truncated detonation will appear on the lens side of the target (see formation of plasma cloud, Figure 46).

At 7 mm Hg, near the focal point (-2 to +1 cm), the beam energy seemed to "sparkle" at the surface of the target during just the first or second shot. This effect may be caused by initial vaporization of the target surface, and is seen only at reduced pressures when optical detonations are scarce. The "sparkle" is probably the incandescent burning of the acrylic vapor. After the target had burned through, a yellowish-brown ribbon of sparks emanated from the target area (see Figure 47).

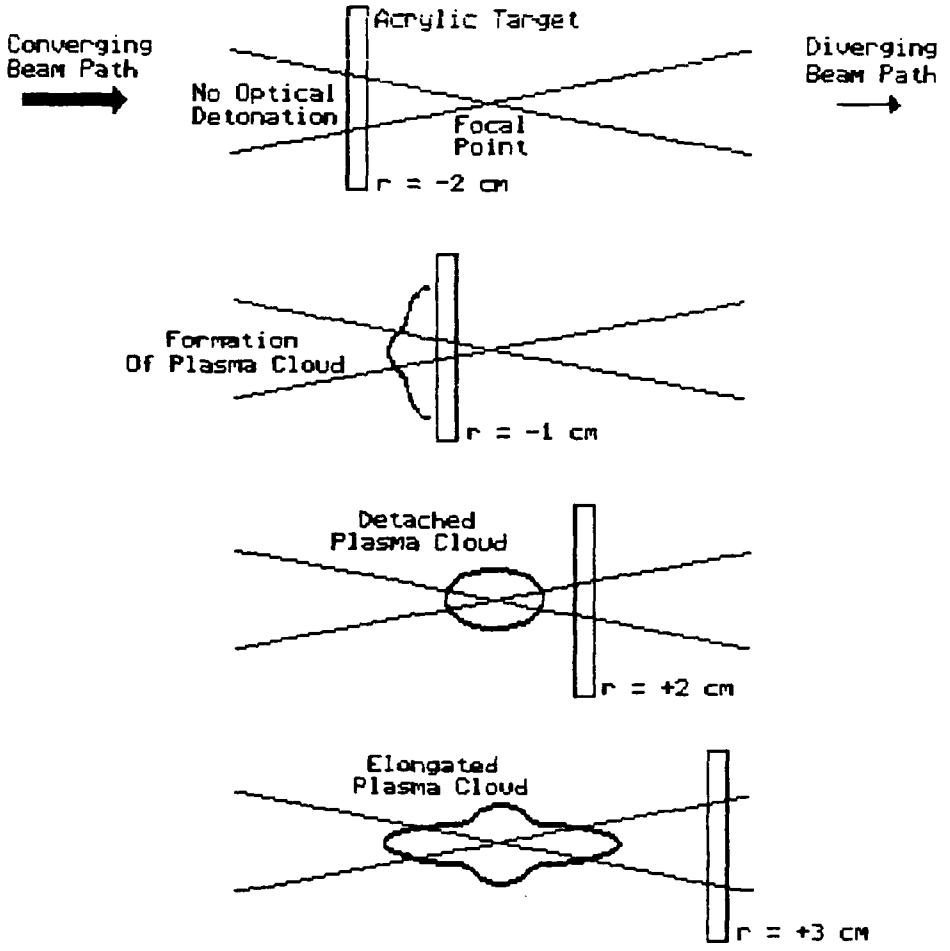

Figure 46. The changing shape of the plasma cloud at atmospheric pressure as a target is moved relative to the focal point of the Ge lens.

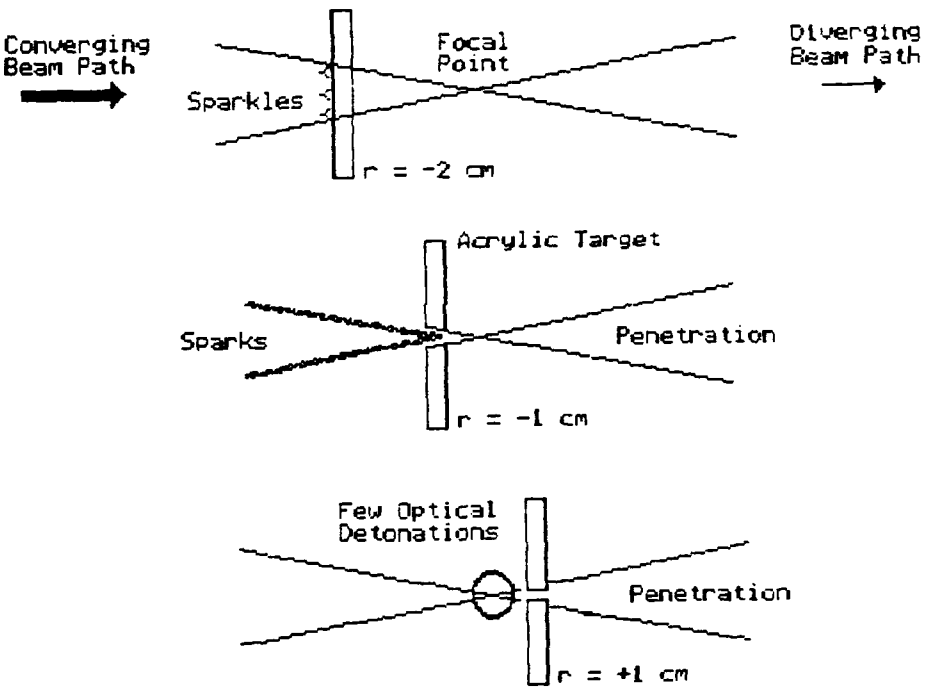

Figure 47. Appearance of the optical detonation at 7 mm Hg when the acrylic target is -2 to +1 cm from the focal point.

Note: burn-throughs occurred only from -1 to +1 cm from the focal point. Also note, every target burned through at -1 and 0 cm.

The sparkle effect was also observed beyond the focal point (0 to +5 cm) at low pressures. However, only two targets were burned through at +1 cm and no ribbon of sparks appeared. When an optical detonation did occur at low pressure, it was quite small, yet had the same color and shape as an optical detonation at atmospheric pressure at the same target distance from the focal point.

g. A thin film of acrylic powder was discovered on the target-side of the Ge lens. This was undoubtedly caused by the mass plume from the damaged target. This thin acrylic film may have slightly reduced the transmission coefficient of the lens. An energy measurement to confirm this possibility was not taken. Unfortunately, this lens will need to be replaced or resurfaced.

5. CONCLUSION

In the first part of this experiment, the beam energy was measured and found not to change as chamber pressure was reduced from one to 0.01 atmosphere. Therefore, the change in beam energy from atmospheric attenuation may be considered insignificant when the linear beam path through the pressurized test chamber is less than 65 cm.

In the second part of this experiment, the target mass loss was measured as a function of the number of firings at atmospheric pressure. Optical detonations near the target were also counted to observe how they might change the mass loss. It was found that mass loss increased linearly with the number of firings at the rate of 0.62 ± 0.02 mg/shot--ignoring the effects of optical detonations which will be discussed later.

Finally, target mass loss was measured as a function of chamber pressure for 30 firings per target. Again, optical detonations near the target were counted to observe their effects. It was determined that mass loss decreases linearly as the chamber pressure increases. However, the rate of mass loss (slope of the mass loss versus pressure) differed significantly when the distance from the focal length was changed. Figure 48 shows the different rates of mass loss as a function of pressure for various distances from the focal length. The maximum rate of mass loss occurred at +2 cm from the focal point.

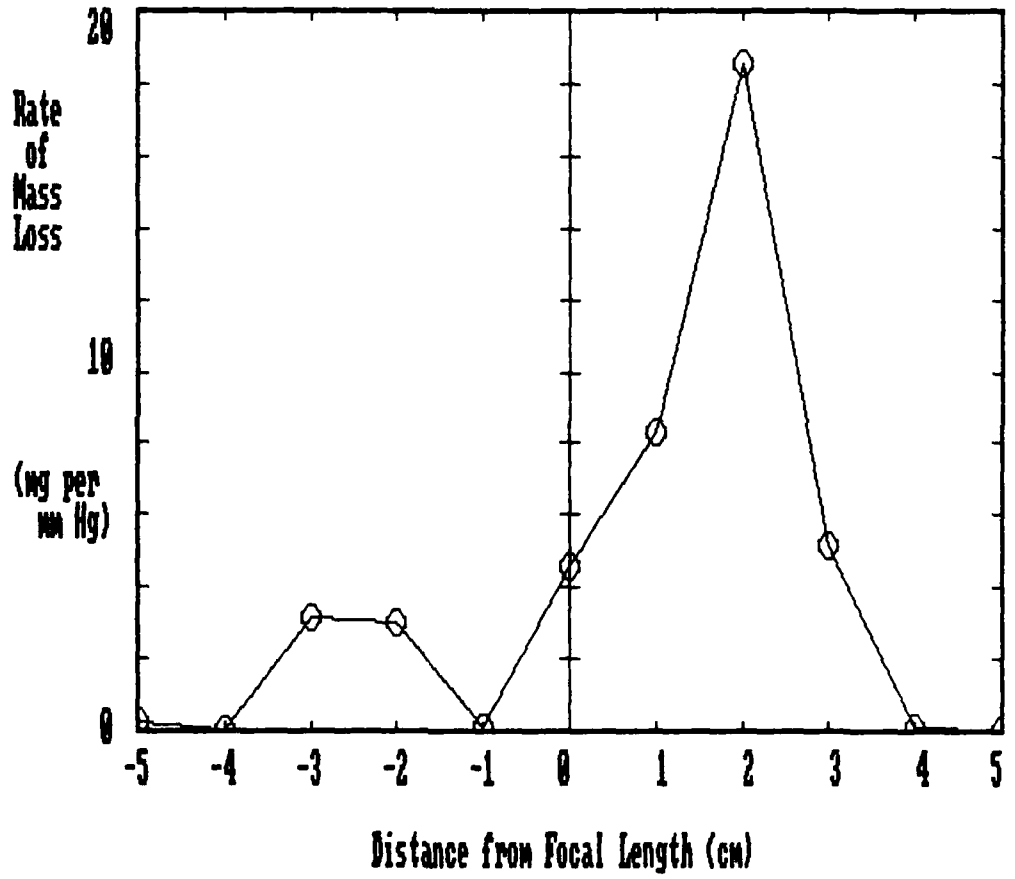

Figure 48. Different rates of mass loss as a function of pressure versus distance from the focal length.

Figure 49 summarizes all the data in the previous section and illustrates it in a new way. Mass loss is plotted as a function of distance from the focal length in constant pressure lines. Note how mass loss has two asymmetric peaks on both sides of the focal point, at 0 cm. (Figure 23 is reproduced above Figure 49 and 50 for the reader's convenience.) The two most important features of the graph are (1) the sudden drop in mass loss at the focal point for all pressures, and (2) the gradual decline in mass loss as pressure increases beyond the focal point from +1 to +5 cm. Both trends are caused by optical detonations.

The number of optical detonations during a firing sequence depended on the target distance and chamber pressure. Optical detonations increased as the target moved closer to the focal point and decreased as chamber pressure was reduced. Figure 50 clearly illustrates this phenomenon. Like before, optical detonations are plotted as a function of focal distance in constant pressure lines. Note how optical detonations increase near the focal point for all pressures. Beyond the focal point, from +1 to +5 cm, the optical detonations are sporadic, yet decrease with pressure. Even more interesting, note the apparent lack of randomness in the data from -5 to +1 cm. A solution to this puzzle might be linked to the mass ejected from the target.

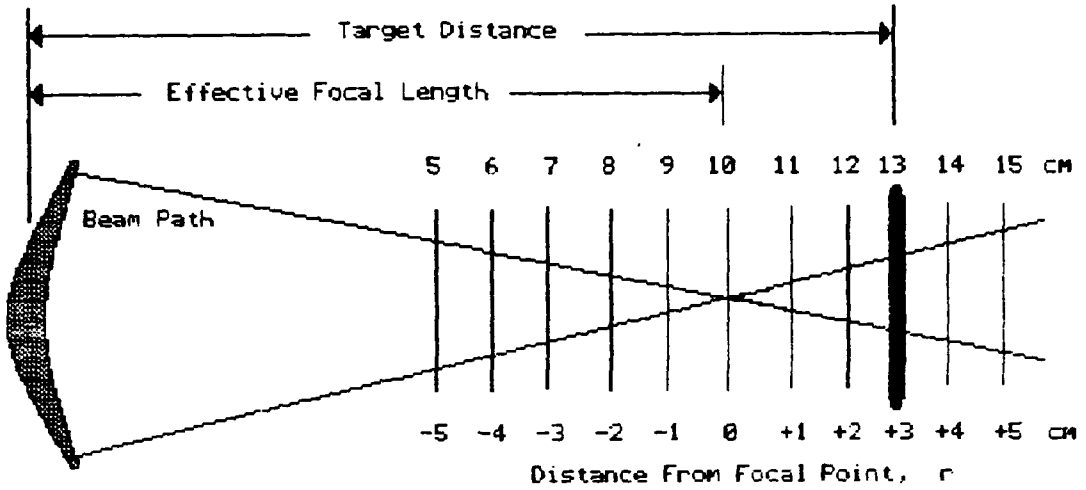

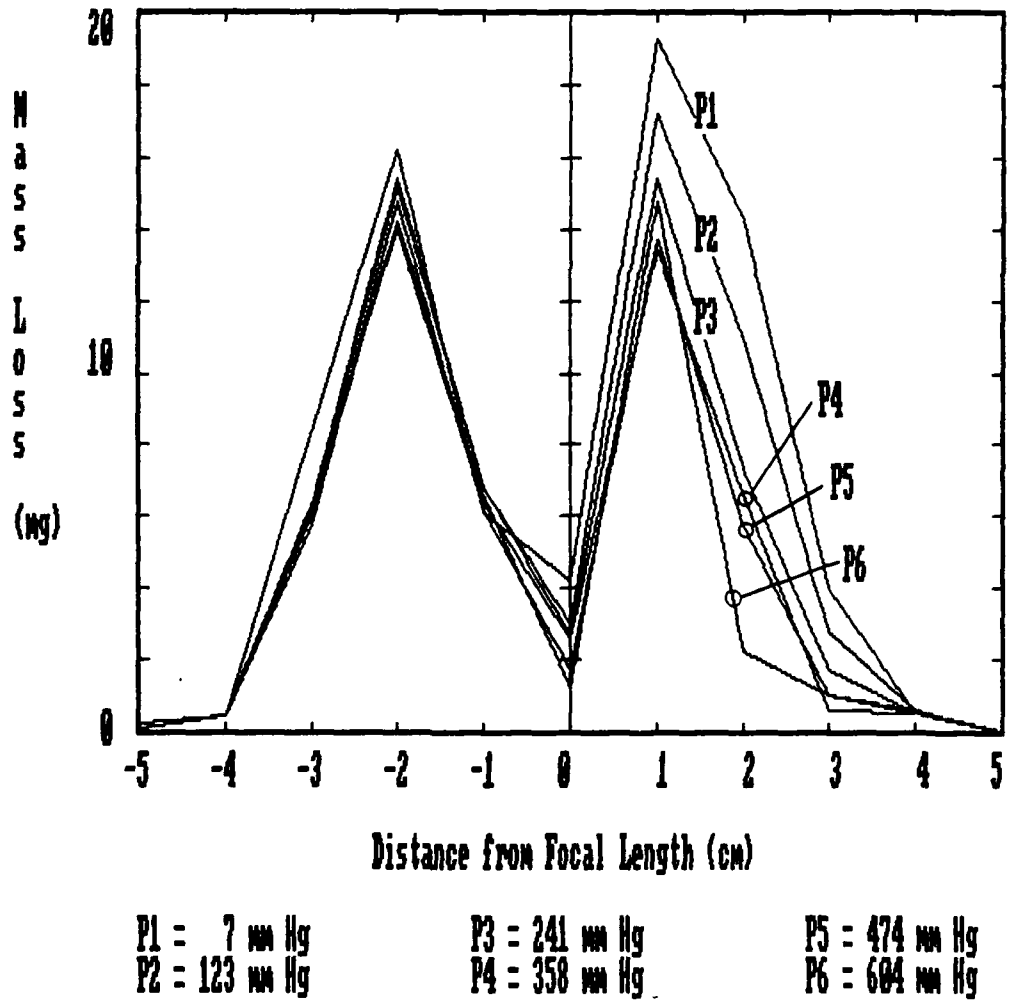

Figure 49. Summary of mass loss versus distance from focal length.

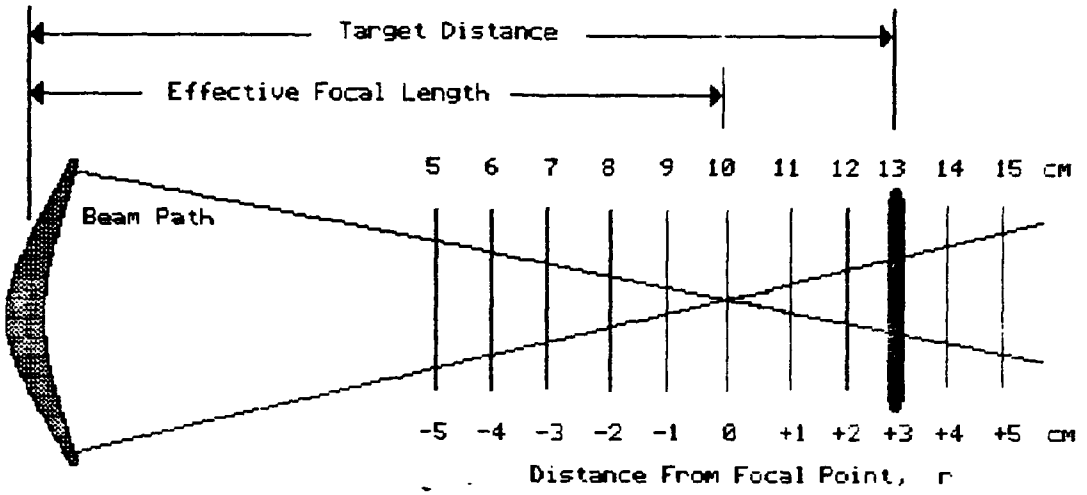

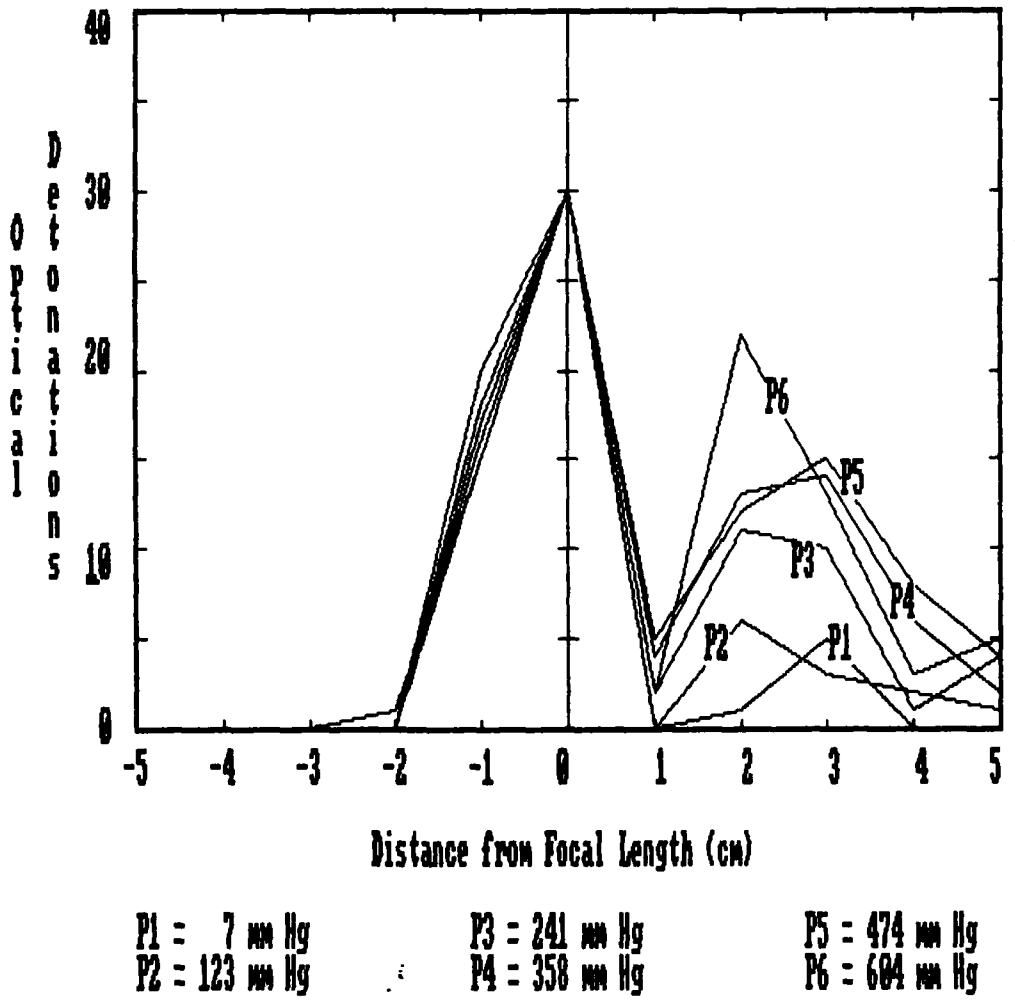

Figure 50. Summary of optical detonations versus distance from focal length.

Optical detonations may depend on the amount of particulate in the air. Huston [7] mentions that the detonation flash changed color when a different target material was used. For example, during trial runs for this experiment, the detonation flashes near a glass plate were gold-yellow (presumably from silicon atoms ejected from the glass surface) while the flashes near wood targets were silver-blue. Huston concluded the optical detonations may be triggered by particles actually removed from the target by initial irradiation. If this is true then the number of optical detonations should increase as more target material is ejected.

With this in mind, consider the case in which the target is placed ahead of the focal point, from -2 to 0 cm. The beam energy density is sufficiently high to cause an optical detonation, yet the debris from the detonation is ejected away from the focal point. The target itself is between the ejected debris and the area with the highest beam energy density. However, when the target is placed beyond the focal point, the debris is ejected directly into the focal point causing sporadic detonations shown in Figure 50. These optical detonations influence mass loss.

Comparing Figures 49 and 50 shows that optical detonations drastically decrease target mass loss. Figure 49 indicates two definite "peaks" of mass loss at -2 and +1 cm from the focal point. Compare these results to the same locations in Figure 50 where there are definite "valleys"

of optical detonations. This reciprocal relationship is consistent throughout both graphs. Optical detonations must decrease the amount of energy delivered to the target; therefore, the plasma created by the detonation must absorb and reflect beam energy.

Summary of Damage Effects

Target damage:

(1) Increases linearly (approximately) with the number of firings
(2) Increases linearly (approximately) as pressure decreases
(3) Decreases when optical detonations occur

Optical detonations:

(1) Increase with beam energy density
(2) Increase/decrease with pressure
(3) Increase with the amount of particulate in the air
(4) Absorb and reflect beam energy

Error Analysis

Unlike nuclear physics in which a statistical error analysis can be performed after obtaining thousands--or even millions--of samples, the error in this experiment must be measured by the precision of the instruments used. See Table 25 on the next page for a listing of the error introduced into this experiment.

A second run was performed to check the reproducibility of the data -1 cm from the focal length. The same pattern of mass loss was observed as a function of the number of

firings and pressure within ± 0.5 mg. Error bars and tolerances were not included in the data presented in this report so that important trends were not obscured. The mass loss values (in milligrams) shown in Tables 3-24 were printed by a GWBASIC computer program and should not be interpreted beyond two significant figures.

Variable	Measuring Device	Error
Target Distance	centimeter stick	± 1 mm
Firings	counter	± 1 count
Detonations	counter	± 1 count
Beam Area	microscope	± 0.5 to ± 2.0 mm^2
Pressure	meter stick	± 1 mm
Mass	electronic scale	± 0.1 mg

Table 25. Error associated with instruments.

6. RECOMMENDED FUTURE WORK

As with many research projects, this experiment asked more questions than it answered:

(1) What is the rate at which beam energy is attenuated by the atmosphere?
(2) What is the threshold beam energy density needed to cause an optical detonation in a standard lab atmosphere?
(3) How much of the beam energy is absorbed by the plasma created by the optical detonation? --how much is reflected?
(4) What are the damage effects to other targets? --at even lower pressures?

The answers to these questions can be sought in a variety of ways. For example, atmospheric attenuation might be measured by transmitting the beam through a very long tube evacuated by a pump. One inexpensive material for this type of test chamber would be a 10-meter section (or longer) of PVC (polyvinyl chloride) plumbing pipe which can be purchased at any homecenter or hardware store. This straightforward experiment would be an excellent research project for an undergraduate.

The remaining questions may require more exotic materials and imaginative procedures. For example, a high-speed video cassette system could be used to visually record optical detonations while acquiring data. The tape could then be played back in slow motion to make special observations.

In any case, no matter how many problems are solved, there will always be more questions waiting beyond the horizon. This is the most wonderful and challenging aspect of experimental research!

Lessons Learned

A great American historian, Henry Brook Adams (1838-1918) once said "All experience is an arch, to build upon" [9]. The following lessons, gained through experience, are offered to the next student to "build upon". They might save you personal time and departmental money--two precious resources no matter where you work or attend school.

1. NEVER design a large rectangular vacuum chamber unless it is made very strong. This is an inherently weak shape to oppose the uniform force of atmospheric pressure. Even though square or rectangular chambers normally offer more useable space, they require stronger construction materials and techniques. Failures easily occur at stress points like seams and bolt holes.

   Spherical or cylindrical chambers are much better pressure vessels since they distribute stress evenly across their entire surface. Keep the design simple, even if it is a little inconvenient. The quality of an airtight seal, cost of materials, and safety advantages

of a spherical or cylindrical design easily surpass any minor advantages in utility.

2. Lubricate all glass fittings with a non-silicon-based grease such as Apiezon. If a glass instrument breaks, and a silicon-based grease is used, the instrument cannot be reblown.

3. Shield all instrument connections to the oscilloscope. The Lasermark transmits a relatively strong electromagnetic pulse (EMP) that triggers the oscilloscope inadvertently. One method to protect the instrumentation against EMP is to wrap the instrument connections with aluminum foil. Be careful not to touch the foil to the connection itself and ground this makeshift shield to the grounding shield of the cable.

4. Keep a fresh stock of Type 667 Polaroid film. This film has a definite shelf life so do not buy large supplies of it unless you really plan to use it. Fortunately, this film is available in many professional camera stores.

5. Do not bother to evacuate the absolute-scale manometer before pouring mercury into it. Evacuating the manometer is more trouble than it's worth. Elaborate connections must be made between the empty manometer

and the mercury bottle. Pump hoses make the whole system cumbersome and dangerous to handle. If the glass tubing and mercury are clean and new, you should be able to easily "shake out" any bubbles trapped in the system.

APPENDIX 1

NATURE August 6, 1960 VOL. 187

Stimulated Optical Radiation in Ruby

Schawlow and Townes[1] have proposed a technique for the generation of very monochromatic radiation in the infra-red optical region of the spectrum using an alkali vapour as the active medium. Javan[2] and Sanders[3] have discussed proposals involving electron-excited gaseous systems. In this laboratory an optical pumping technique has been successfully applied to a fluorescent solid resulting in the attainment of negative temperatures and stimulated optical emission at a wave-length of 6943 Å.; the active material used was ruby (chromium in corundum).

A simplified energy-level diagram for triply ionized chromium in this crystal is shown in Fig. 1. When this material is irradiated with energy at a wave-length of about 5500 Å., chromium ions are excited to the $^4F_2$ state and then quickly lose some of their excitation energy through non-radiative transitions to the ^2E state[4]. This state then slowly decays by spontaneously emitting a sharp doublet the components of which at 300° K. are at 6943 Å. and 6929 Å. (Fig. 2*a*). Under very intense excitation the population of this metastable state (^2E) can become greater than that of the ground-state; this is the condition for negative temperatures and consequently amplification via stimulated emission.

To demonstrate the above effect a ruby crystal of 1-cm. dimensions coated on two parallel faces with silver was irradiated by a high-power flash lamp;

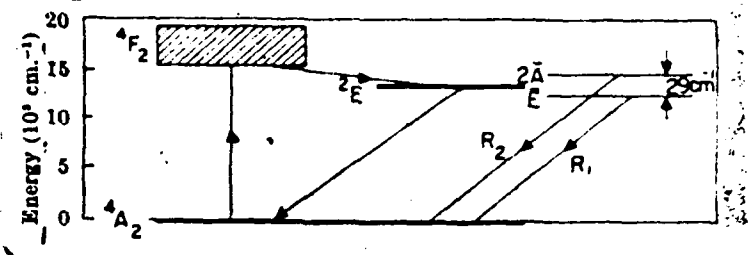

Fig. 1. Energy-level diagram of Cr^{3+} in corundum, showing pertinent processes

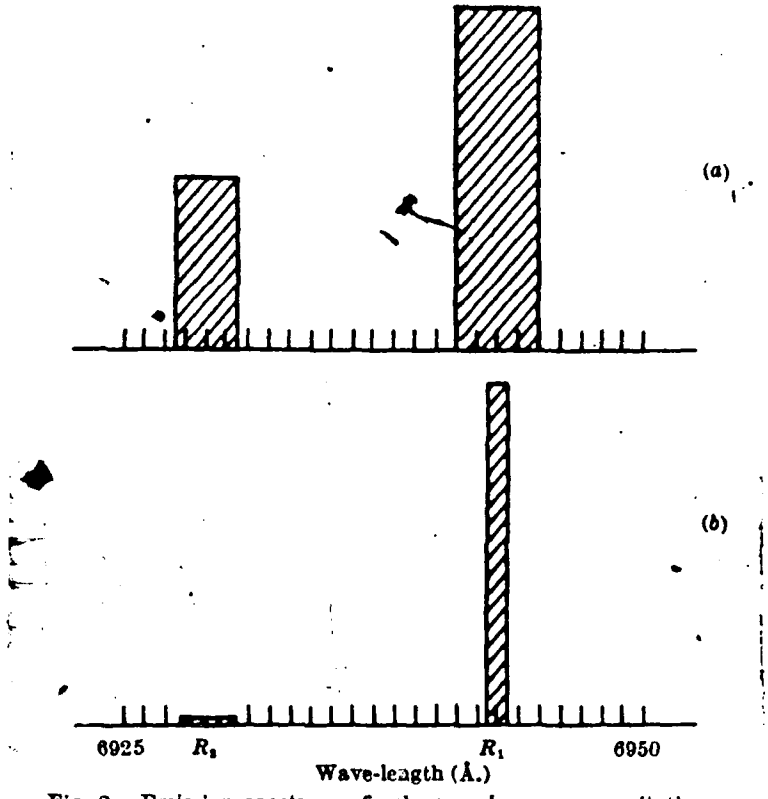

Fig. 2. Emission spectrum of ruby: *a*, low-power excitation; *b*, high-power excitation

the emission spectrum obtained under these conditions is shown in Fig. 2*b*. These results can be explained on the basis that negative temperatures were produced and regenerative amplification ensued. I expect, in principle, a considerably greater ($\sim 10^8$) reduction in line width when mode selection techniques are used[1].

I gratefully acknowledge helpful discussions with G. Birnbaum, R. W. Hellwarth, L. C. Levitt, and R. A. Satten and am indebted to I. J. D'Haenens and C. K. Asawa for technical assistance in obtaining the measurements.

T. H. Maiman

Hughes Research Laboratories,
A Division of Hughes Aircraft Co.,
Malibu, California.

[1] Schawlow, A. L., and Townes, C. H., *Phys. Rev.*, **112**, 1940 (1958).
[2] Javan, A., *Phys. Rev. Letters*, **3**, 87 (1959).
[3] Sanders, J. H., *Phys. Rev. Letters*, **3**, 86 (1959).
[4] Maiman, T. H., *Phys. Rev. Letters*, **4**, 564 (1960).

APPENDIX 2

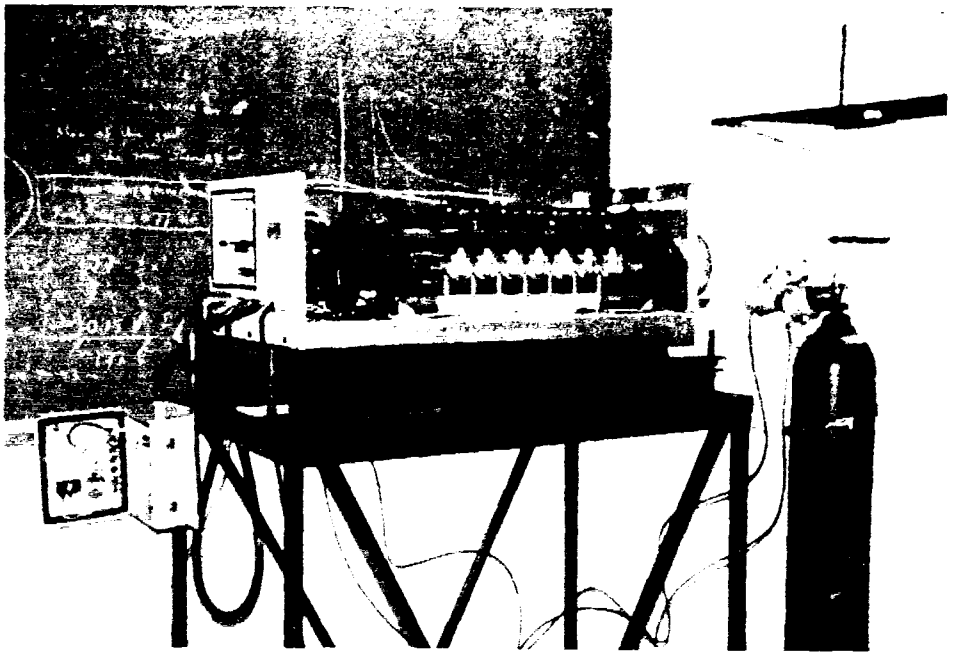

Figure A1. Lumonics CO_2 Lasermark 401.

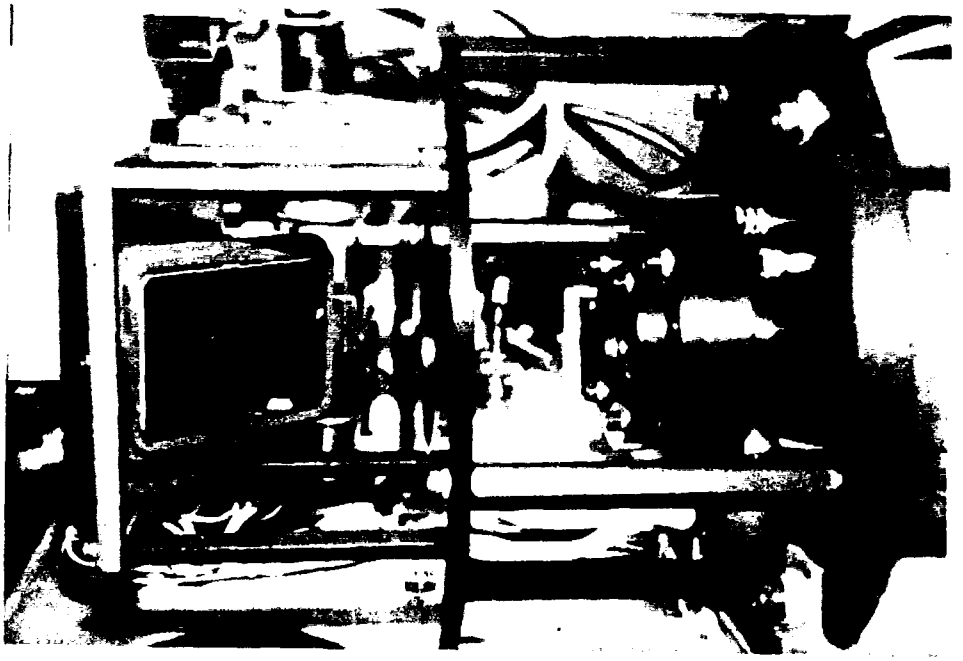

Figure A2. Close up of optical elements.

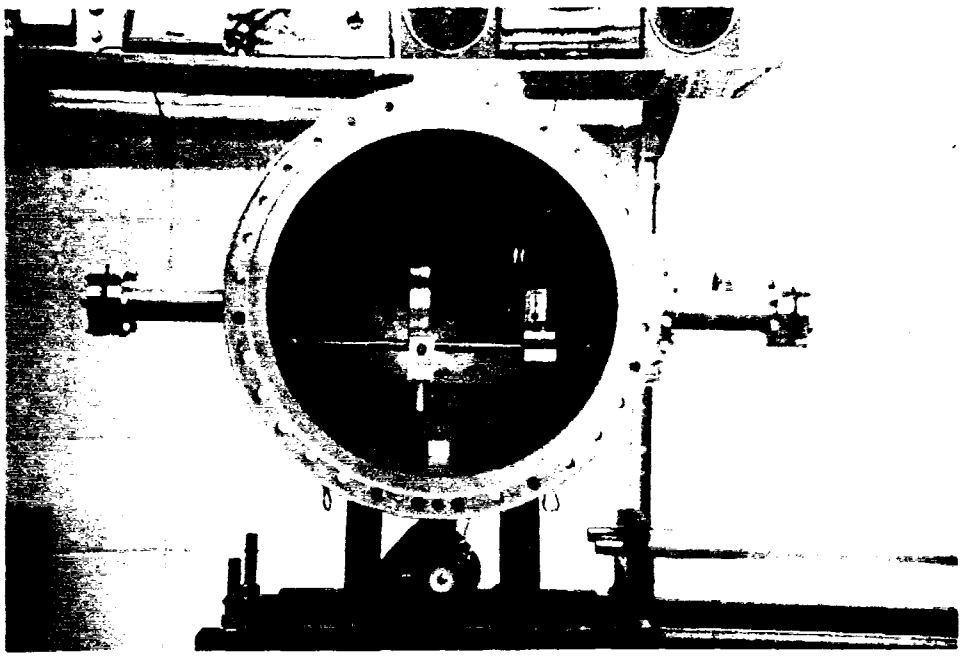

Figure A3. Test chamber.

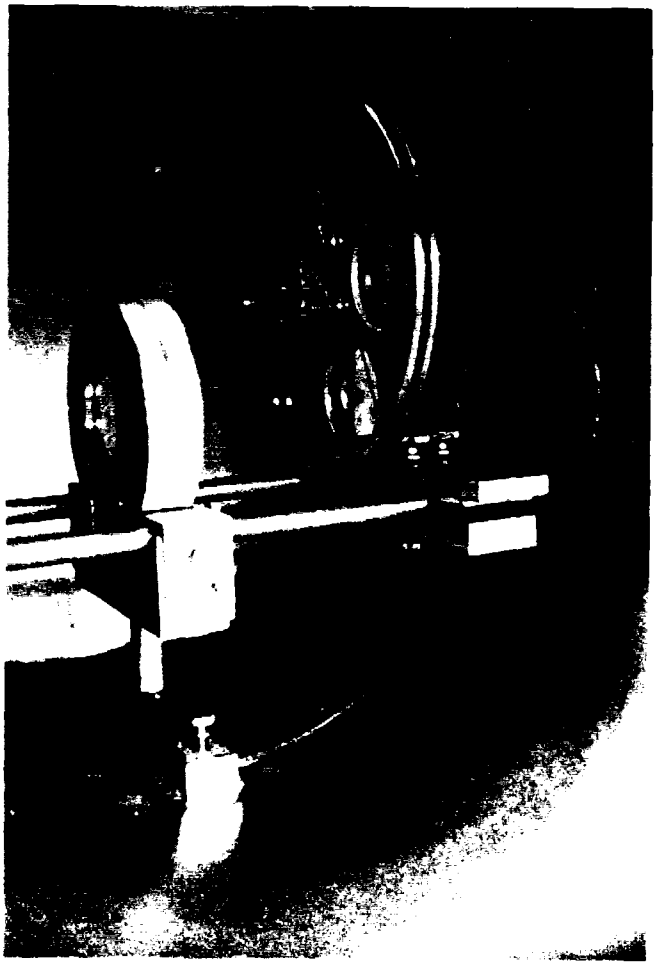

Figure A4. Lens mount and target holder.

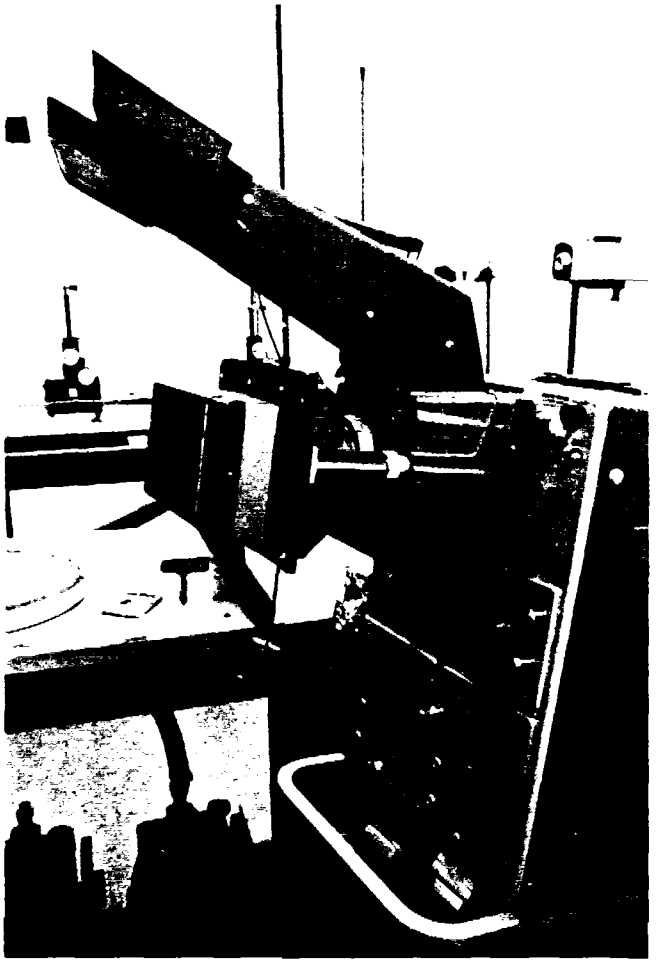

Figure A5. Dual-channel oscilloscope with camera mount.

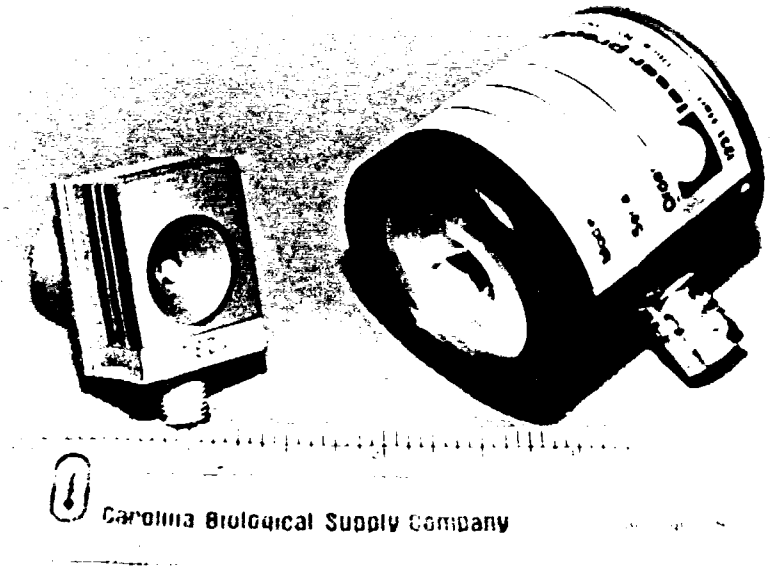

Figure A6. Power meter (not used) and energy meter.

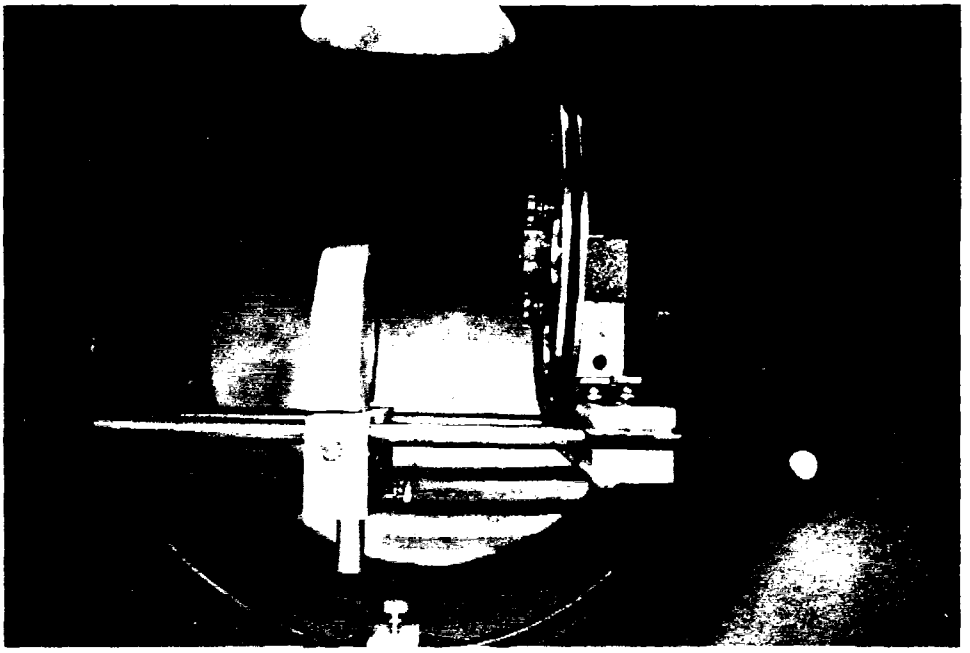

Figure A7. Front view of lens-target system.

Figure A8. Same view with optical detonation.

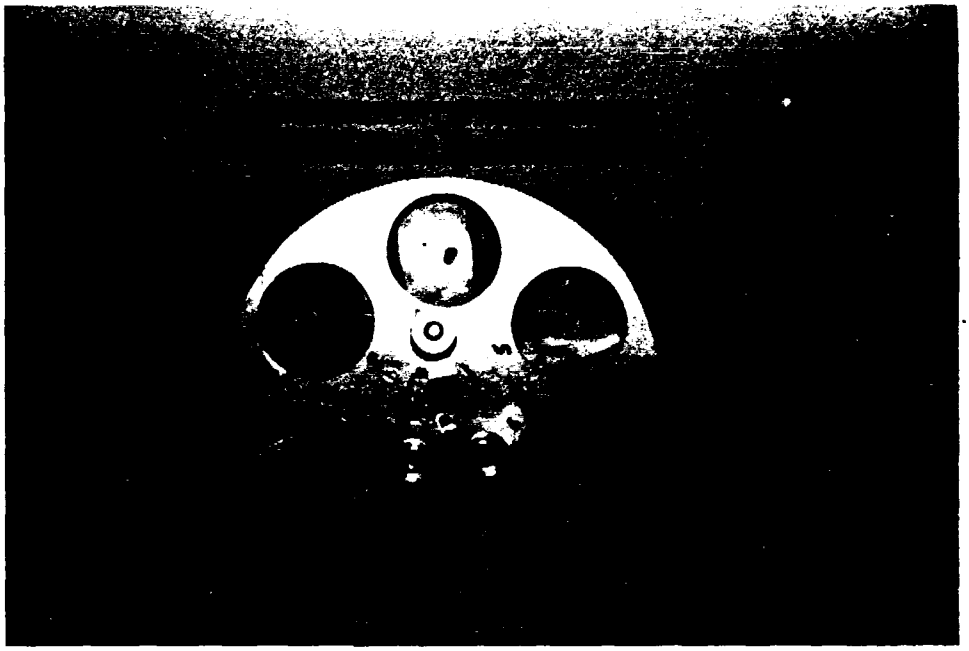

Figure A9. Target holder with six acrylic slides.

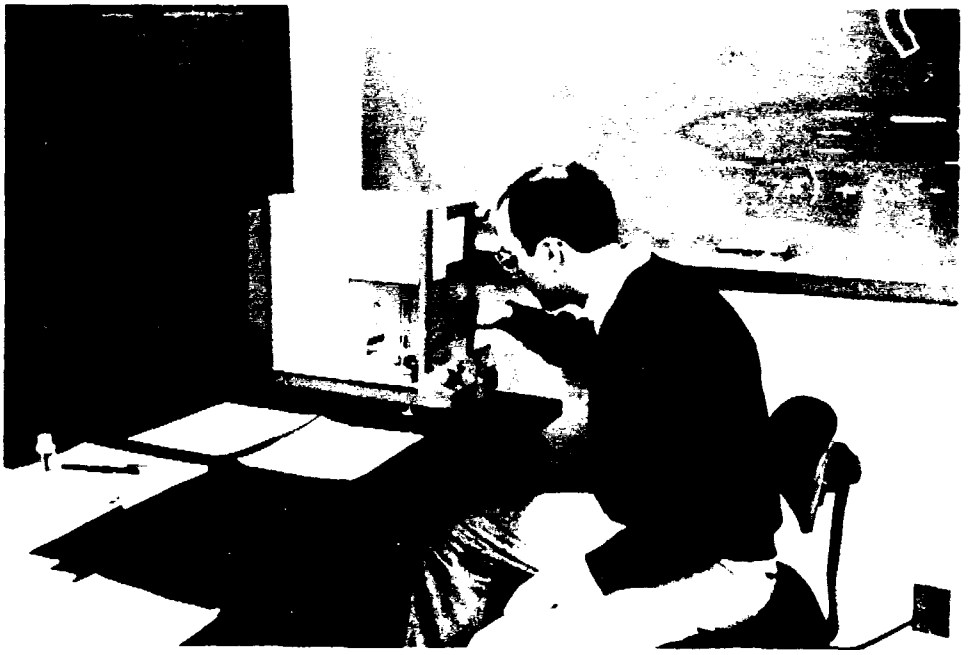

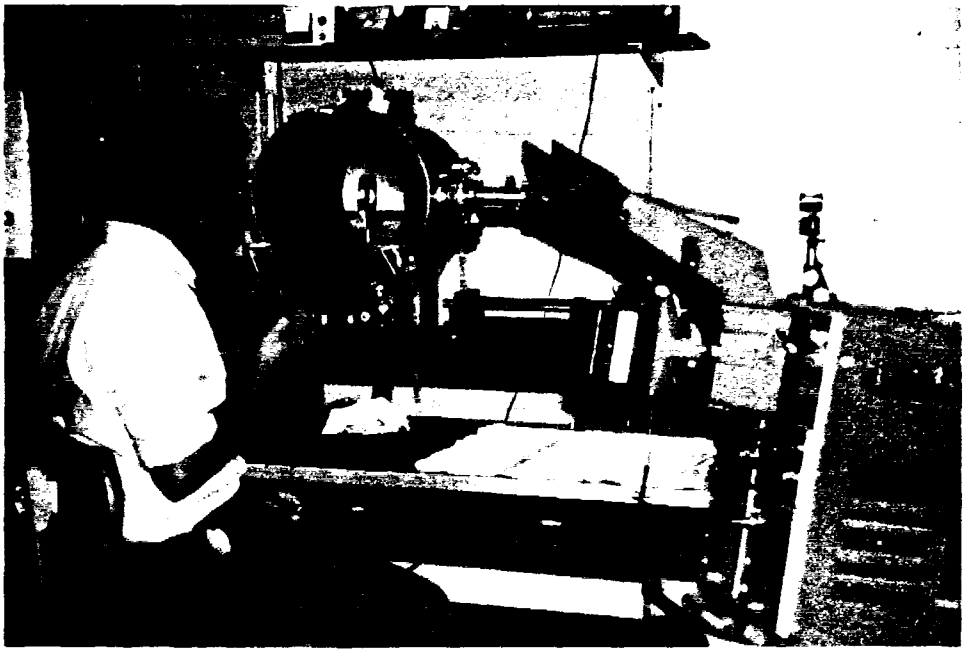

Figure A11. Lab assistant firing the laser.

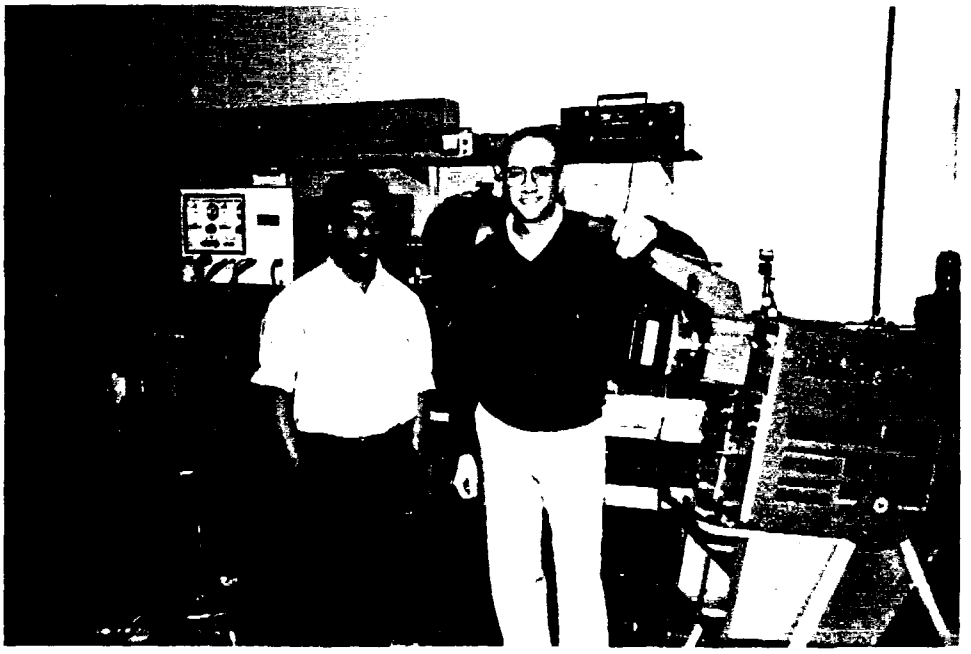

Figure A12. Lab assistant, Dulip Welipitiya, and author.

APPENDIX 3

FIRING THE LASER

1. OPEN VALVE (CCW) ON TOP OF DRY AIR BOTTLE (yellow) until handle turns no further.

2. CHECK PRESSURE on front gauge (line pressure) at 30 psig. If not at 30 psig, adjust green knob on side of valve until achieved.

3. OPEN VALVE (CCW) ON TOP OF MIXED GAS BOTTLE (blue) until handle turns no further.

4. CHECK PRESSURE on front gauge (line pressure) at 30 psig. If not at 30 psig, adjust green knob on side of valve until achieved.

5. Ensure STANDBY/OPERATE KEYSWITCH on remote panel is in STANDBY.

6. Ensure AUTO/MANUAL KEYSWITCH on remote panel is in AUTO.

   [NOTE: Turning this switch to MANUAL ON charges the HIGH VOLTAGE components and allows the mixed gas to flow.]

7. TURN MAIN AC POWER KEYSWITCH ON. (1/8 turn CCW)

   [ON (amber) light above MAIN AC POWER Keyswitch, STANDBY (white) light on remote panel, and EMISSION INDICATOR (red) light on remote panel all come on.]

8. WAIT until warm-up period is over.

   [This will be indicated by a loud clicking inside the main LASER cabinet and by the MIXED GAS flow and PRESSURE indicators dropping to zero.]

9. ADJUST SPARK GAP PRESSURE to 18 psig and FLOW to 0.6 scfh by the following procedure (if not at those settings after turn on):

   a. Turn flow knob full CW.
   b. Turn pressure knob full CCW. This may require loosening Philips screw first.
   c. Open flow knob ¼ turn CCW. (Pressure and flow go to zero)
   d. Turn pressure knob CW until 18 psig is reached.
   e. Turn flow knob slightly CW until 0.6 scfh is reached. (Turning flow knob too far CCW will cause it to come off.)

10. TURN STANDBY/OPERATE KEYSWITCH to OPERATE. [STANDBY light goes out, READY (amber) light comes on.]

11. TURN AUTO/MANUAL ON KEYSWITCH to MANUAL ON. [Click is heard from within the main LASER cabinet, READY light goes out, and ON (green) light comes on.]

    [NOTE: Turning this switch to MANUAL ON charges the HIGH VOLTAGE components and allow the mixed gas to flow. In order to conserve the mix gas, this keyswitch should be left in the AUTO position to the maximum extent possible.]

12. ADJUST MIX PRESSURE to 10 psig and FLOW to 3 scfh by the following procedure, if not at those settings when MANUAL is selected:

    a. Turn flow knob full CW.
    b. Turn pressure knob full CCW. This may require loosening Philips screw first.
    c. Open flow knob ½ turn CCW.
    d. Turn pressure knob CW until 10 psig is reached.
    e. Turn flow knob slightly CW or CCW until 3 scfh is reached. (Turning flow knob too far CCW will cause it to come off.)

13. PUT ON EYE SAFETY EQUIPMENT (if not already on).

14. Ensure OPERATE/TEST SWITCH inside cover of remote panel is set to TEST.

15. CLEAR THE FIRING LINE.

16. WHEN READY TO FIRE THE LASER, PUSH the remote FIRING BUTTON (or TEST BUTTON inside cover of remote panel).

* This checklist was reproduced from reference [7] with minor updates.

LASER SHUTDOWN PROCEDURES

1. TURN AUTO/MANUAL ON KEYSWITCH to AUTO.
2. TURN STANDBY/OPERATE KEYSWITCH to STANDBY.
3. TURN MAIN AC POWER KEYSWITCH 1/8 turn CW to OFF.
4. CLOSE VALVE (CW) on top of MIXED GAS BOTTLE.
5. CLOSE VALVE (CW) on top of DRY AIR BOTTLE.
6. RETURN LASER KEYS secure place.

THE LASER IS SHUTDOWN

* This checklist was reproduced from reference [7] with minor updates.

SAFING THE LASER

[CAUTION: THIS CHECKLIST SHOULD BE ACCOMPLISHED BEFORE ANY WORK IS DONE AROUND THE LASER WITH THE COVER OFF!]

1. Ensure that the MAIN AC POWER KEYSWITCH is OFF.
2. WAIT a minimum of 5 MINUTES before any further action.
3. REMOVE LEFT MAIN CABINET COVER (side opposite beam exit hole).
4. REMOVE SMALL GRAY COVER from mid section of main cabinet by CAREFULLY lifting the cover up and out. [DO NOT place fingers behind the cover when you lift it off.]
5. REMOVE PLASTIC BAG (if on) FROM SHORTING BAR.
6. With the shorting bar, SHORT THE FOLLOWING points in the given order:

[CAUTION: ENSURE GROUND END OF GROUNDING CORD IS ATTACHED TO CABINET BEFORE GROUNDING IS ATTEMPTED.]

   a. Dome nut on spark gap mid-plane terminal. (silver)
   b. Spark gap high voltage terminal. (copper)
   c. Top terminal of main discharge capacitor. (copper)
   d. Bottom terminal of blocking capacitor. (copper)

THE LASER IS SAFE

* This checklist was reproduced from reference [7] with minor updates.

REFERENCES

[1] Siegman, Anthony E., LASERS, University Science Books, 1986.

[2] Hecht, Eugene, OPTICS, Second Edition, Addison-Wesley Publishing Company, Inc., 1987.

[3] Duley, W.W., CO_2 Lasers: Effects and Applications, Academic Press, Inc., 1976.

[4] Yariv, Amnon, OPTICAL ELECTRONICS, Third Edition, CBS College Publishing, 1985.

[5] OPERATOR'S INSTRUCTION MANUAL FOR LASERMARK SYSTEM MODEL 901, Lumonics Inc., 1981.

[6] PRECISION OPTICS and COMPONENTS, Janos Technology Inc., 1984.

[7] Huston, Edward S., DIAGNOSTICS OF IONIZATION IN AIR PRODUCED BY INFRARED RADIATION FROM A PULSED CO_2 LASER, Creighton University, Omaha, Nebraska, 1984.

[8] Ronk, Robert M., BEAM DIAGNOSTICS OF A PULSED (TEA) CARBON DIOXIDE LASER, Creighton University, Omaha, Nebraska, 1985.

[9] Bartlett, John, Familiar Quotations, Fifteenth Edition, Little, Brown and Company, Inc., 1980.